MARION VILLACAMPA

CARBON SEQUESTRATION: MATHEMATICAL MODEL OF THE BRAZILIAN ATLANTIC FOREST

São Paulo

2016

MARION VILLACAMPA

CARBON SEQUESTRATION: MATHEMATICAL MODEL OF THE BRAZILIAN ATLANTIC FOREST

Tese apresentada à Escola Politécnica da Universidade de São Paulo para a obtenção do título de Doutor em Ciências

São Paulo

2016

Este exemplar foi revisado e corrigido em relação à versão original, sob responsabilidade única do autor e com a anuência de seu orientador.

São Paulo, 10 de outubro de 2016

Assinatura do autor: _____

Assinatura do orientador: _____

Catalogação-na-publicação

Villacampa, Marion
CARBON SEQUESTRATION: MATHEMATICAL MODEL OF THE BRAZILIAN ATLANTIC FOREST / M. Villacampa -- versão corr. -- São Paulo, 2016.
140 p.

Tese (Doutorado) - Escola Politécnica da Universidade de São Paulo. Departamento de Engenharia Química.

1.MODELOS MATEMÁTICOS 2.BIOMASSA I.Universidade de São Paulo. Escola Politécnica. Departamento de Engenharia Química II.t.

MARION VILLACAMPA

CARBON SEQUESTRATION: MATHEMATICAL MODEL OF THE BRAZILIAN ATLANTIC FOREST

Tese apresentada à Escola Politécnica da Universidade de São Paulo para a obtenção do título de Doutor em Ciências

Área de concentração: Engenharia Química

Orientador: Prof. Dr. Claudio Augusto Oller do Nacimento

São Paulo

2016

ACKNOWLEDGEMENTS (in Portuguese)

Ao professor Claudio Oller por ter me dado a oportunidade de trabalhar neste projeto, pela atenção e pela competência na orientação desta tese.

Ao Bruno Capron sem o qual não teria sido possível fazer esse doutorado. Obrigada pela disponibilidade, pela paciência e pelo senso de humor no que diz respeito às minhas habilidades em programação.

Aos amigos da turminha francesa, Vincent, Mickael, Bel, Rémi, Robin, Karina, Igor, Julia, Dani e Xavier pela felicidade que vocês me trouxeram durante esses 5 anos.

Aos amigos do NELE, Marina, Ilan, Francesco, Tita, Denis e Candida pelas saídas culturais, e pela alegria que vocês me proprocionam.

Á minha familia e meus amigos na França que sempre me apoiaram, mesmo sendo longe.

Estendo meus agradecimentos aos funcionarios da EQ-USP que me ajudaram quando eu precisava.

Á agência de fomento CNPq (Processo 140385/2013-4) pelo apoio financeiro.

RESUMO

A Mata Atlântica é um dos 34 hotspots mundiais e provavelmente uma das florestas tropicais mais ameaçadas. Entender o seqüestro do carbono e construir uma representação válida da dinâmica a longo prazo da floresta é primordial. Restaurar um ecossistema implica conhecer a complexidade dos fenômenos que se desenvolvem nestas formações, compreender os processos que levam à estruturação e manutenção destes ecossistemas ao longo do tempo e, finalmente, utilizar estas informações para a implantação de projetos de restauração. O objetivo desse projeto é buscar conhecimento sobre o crescimento da Mata Atlântica em meio ao comportamento antropogênico extrativista, buscando ações rumo à sustentabilidade e sua importância no processo de seqüestro e estocagem de carbono. Desenvolver um modelo de crescimento da floresta adaptado ao local de estudo, que toma em consideração as atividades humanas, nos ajudará a determinar ações rumo à sua sustentabilidade.

Na primeira parte da tese, é desenvolvido um modelo matemático que gera um sistema de equações diferenciais ordinárias não lineares. As características do Parque Estadual da Serra do Mar, no estado de São Paulo, são incluídas nesse modelo, que representa várias espécies de árvores agrupadas em nove grupos em função de sua altura máxima e de seu comportamento em relação à sombra.

Em seguida, a tese trata do impacto de várias formas de desmatamento na dinâmica da floresta e na estrutura e no sequestro de carbono. Os resultados mostram que o modelo offshore inland minimiza o impacto do desmatamento em termos de quantidade de biomassa perdida ou do impacto na biodiversidade.

No final, com o objetivo de restaurar a Mata Atlântica, vários cenários de regeneração são abordados/considerados. O modelo determina em quantos anos a floresta estará restaurada e mostra a importância da contribuição externa de sementes.

O desempenho desse modelo traz bons resultados em comparação com outros estudos, e pode ajudar a tomar decisões para a concretização de um futuro sustentável.

ABSTRACT

The Brazilian Atlantic Forest is one of the world's biodiversity hotspots and probably one of the most highly threatened tropical forests. Understanding the forest, the carbon sequestration and develop a valid representation of the long-term dynamics of natural tropical forest are essential. Building a local forest growth model including anthropogenic activities will lead us to a better understanding in order to take sustainable actions.

In the first part of the thesis a model of the floristic and ecological interaction in plant communities in the Parque Estadual da Serra do Mar, state of São Paulo, Brazil is built. The model is a multi-species model which contains nine functionally different species, each depicting a component of the canopy layer that it can reach and a shade tolerance.

In a second part, the thesis explores the impact of different patterns of non forest areas due to human colonization on the Brazilian Atlantic Forest. The long-term structure, the dynamics and the carbon sequestration of the forest is then analyzed. The results suggest that an offshore inland colonization minimizes ecological impact on the forest composition and on the quantity of carbon stored in the forest biomass.

Finally this project aims to understand the forest regeneration under different scenarios. The thesis determines how long it takes for the forest to recover after a clear out, and what are the impacts of external seed input playing during the regeneration of the forest.

The proposed model gives satisfactory results and can be use as a decision support tool in order to take sustainable actions.

LIST OF FIGURES

LIST OF TABLES

GLOSSARY

BAF:	Brazilian Atlantic Forest
CO_2:	Carbon dioxide
dbh:	Diameter at breast height
FAO:	Food and Agriculture Organization of the United Nations
IBM:	Individual-based models
LAI:	Leaf Area Index
Mg:	Megagram (10^6 gram)
PESM:	Parque Estadual da Serra do Mar (State Park Serra do Mar)
PFT:	Plant Functional Type
t_{ODM}/ha	Ton of Organic Dry Matter per hectare

CONTENTS

1. Introduction

1.1. Background

The Brazilian Atlantic Forest (hereafter abbreviated to BAF) was a huge forest of evergreen and seasonally-dry forests covering almost 1,5 million km² of over 3300km of the Brazilian coast (Tabarelli et al., 2010). Of the original area, only 7,6% remains (see figure 1) (Instituto Florestal do estado de São Paulo, 2008). The deforestation has accompanied economic development (FAO, 2012).

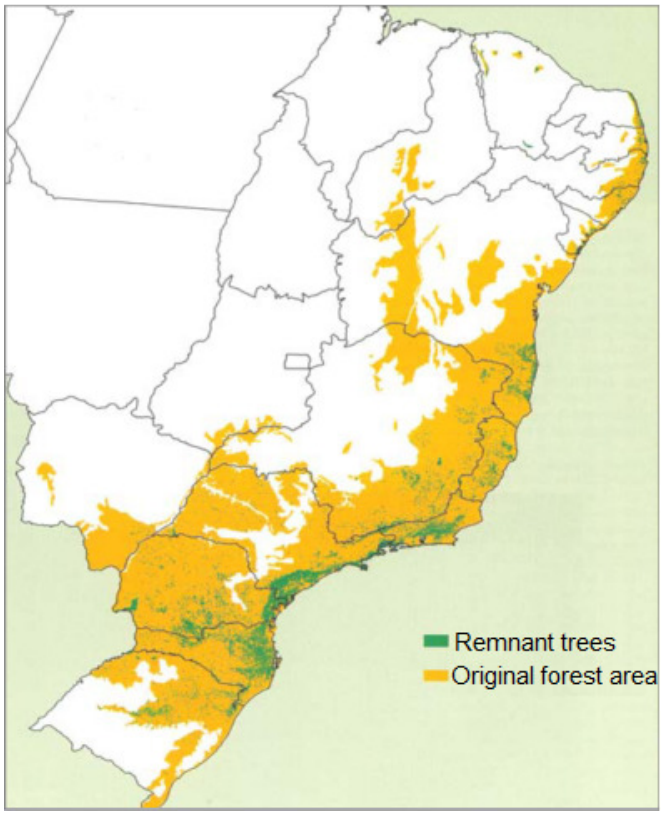

Sources : Fundação SOS Mata Atlântica, Instituto Nacional de Pesquisas Espaciais, Instituto Socioambiental

Figure 1: Original and remnant area of the Brazilian Atlantic Forest

The BAF is one of the 25 biodiversity hotspots (see figure 2), i.e. a biogeographic region with a significant reservoir of biodiversity that is under human threats such as agriculture, pasture, hunting, logging and fire. It is one of the richest in terms of number of endemic trees and at the same time, it features some of the most depleted habitats (Myers et al., 2000).

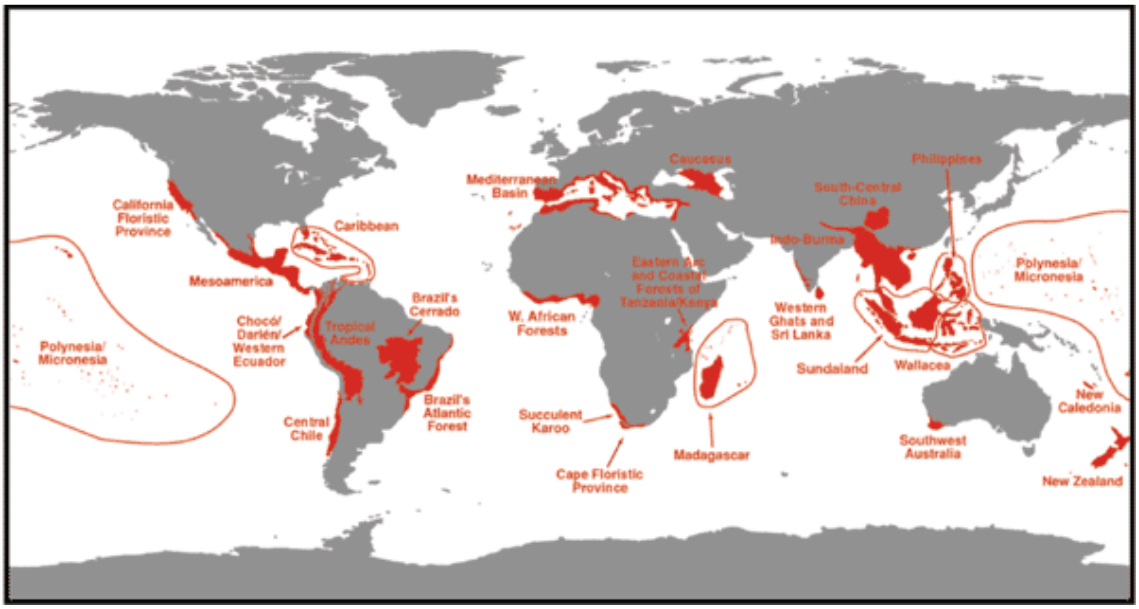

Sources : (Myers et al., 2000)

Figure 2: The 25 hotspots included the Brazilian Atlantic Forest

In the BAF, a lot of remnants compose conservation units which are propitious to action and long-term conservation investments. One of the main goals is to create larger habitat corridors establishing links between remnant patches. As explained by Boyle (2014) a biological corridor is a continuous geographic extent of habitat linking ecosystems, either spatially or functionally; such a link restores or conserves the connection between habitats that are fragmented. Biological corridors are primordial in the preservation of species richness and biodiversity because they provide connections for species through fragmented landscapes such as the BAF.

The largest biological corridor of BAF in Brazil is the Serra do Mar State Park (Parque Estadual da Serra do Mar - PESM) and it spans over one of the most

developed state of the country: the São Paulo state (Instituto Florestal do estado de São Paulo, 2008). The park was created in August 1977 and expanded in 2010 from 315 000 hectares to almost 332 000 hectares. It is managed by the Forest Institute (Instituto Florestal), an environmental agency of the São Paulo state (Secretaria do Meio Ambiente do Estado de São Paulo). The PESM is located in the West part of the São Paulo state (see figure 3) over 25 cities. It spreads on the hillsides along the coast and on the Atlantic plateau.

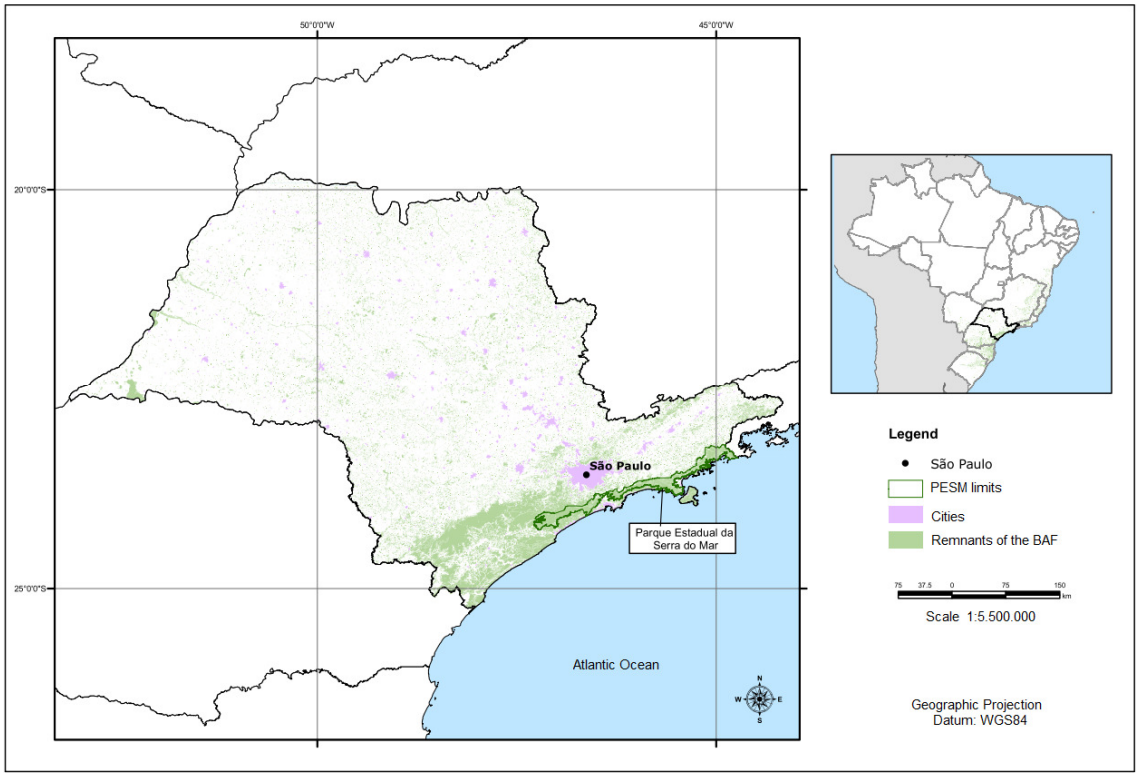

Sources : 1. IBGE digital cartographic database (http://www.ibge.gov.br/home/);
2. Forest Institute (http://fflorestal.sp.gov.br/files/2012/01/2-Volume-Principal-Completo_com-mapas-parte1-01a52.pdf)

Figure 3: Serra do Mar State Park

The PESM is divided into 8 subdivisions according to the soil use and the management program developed or potential (see Table 1).

Table 1: Municipalities in the subdivisions

Subdivision	City
Cunha	Cunha
Santa Virginia	São Luiz do Paraitinga, Natividade da Serra
Picinguaba	Ubatuba
Caraguatatuba	Caraguatatuba, Paraibuna, Natividade da Serra
São Sebastião	São Sebastião, Salesópolis
Itutinga-Pilões	Biritiba Mirim, Mogi das Cruzes, São Bernardo do Campo, Santo André, São Paulo, Bertigoa, Cubatão, Santos, Praia Grande
Curucutu	Juquitiba, São Paulo, Itanhaém, Mongaguá
Pedro de Toledo	Peruíbe, Pedro de Toledo, Juquitiba

Sources : (Instituto Florestal do estado de São Paulo, 2008)

Based on the Brazilian Institute of Geography and Statistic (Instituto Brasilieiro de Geografia e Estatística - IBGE) phytogeography classification (Instituto Brasileiro de Geografia e Estatística, 2012; Pimenta Veloso et al., 1991), the BAF in the area is a tropical moist forest and includes the following vegetation types: lowland forest, sub-montane forest and montane forest. According to the National Institute of Meteorology (Instituto National de Meteorologia - INMET), the mean annual rainfall in the PESM is 2600 mm, and the monthly average temperature ranges from 17,6 °C to 24,7 °C depending on the altitude (Scaranello et al., 2012). Intensive local rainfall can reach 100mm in 24 hours, which can cause landslides in this steep terrain area (Instituto Florestal do estado de São Paulo, 2008).

In comparison with the Atlantic plateau, the forest on the hillside is perennial with a higher relative humidity and more rainfalls. The area is characterized by a

thin to deep clay soil. In these environmental conditions, trees can grow over 15 to 32 meters in height.

Since the Portuguese colonization, the BAF has been degraded due to Pau Brazil wood extraction, sugar cane and coffee plantations and mineral extractions. More recently, the strong urban density peculiar to this region, the implementation of basic infrastructures (roads, harbors, and industries), the disordered growth of tourism, extractive activities and hunting are some examples of pressure the PESM is under.

Furthermore, cities play an important role in encouraging mass tourism and massive development. This cannot be done without considerable damages to the PESM biodiversity (Morellato and Haddad, 2000). As reported by the non-governmental organization SOS Mata Atlântica, even nowadays, the BAF continues to be under severe anthropogenic pressure.

According to IBAMA (Instituto Brasileiro do Meio Ambiente e dos Recursos Naturais Renováveis – Brazilian environmental and renewable natural resources institute) 1361 animal species and 20 thousand types of plants were documented on site.

Beyond that, PSEM is important to reduce climate change, to help stabilize soil and to conserve slopes. This is primordial in a hilly landscape containing dense inhabited areas such as in the PSEM to avoid ecological and human catastrophes.

The importance of the PESM no longer needs to be demonstrated. To protect remnant trees and preserve the PESM it is primordial to understand the dynamics of the forest. These are the reasons why it is chosen in this thesis to develop a model of the carbon sequestration and develop a valid representation of the long-term dynamics of natural tropical rainforest.

As was seen before, the BAF suffered extremely from deforestation. Deforestation takes many different patterns, depending upon the origin of the forest clearing. When one cuts a clearing in a forest for wood extraction, mining exploration, housing construction, or road construction, the forest is exposed to the conditions of a different ecosystem, i.e. an edge effect. Edge effects are the result of abrupt transition between two adjacent ecosystems (Murcia, 1995) and deeply impact the forest composition. Another objective of this thesis will then be to understand the impact of different deforestation patterns on the dynamics of the forest of the PESM and determine which kind of colonization has less impact.

With the reduction of forested areas, regeneration of damaged ecosystems is a growing activity (Vieira and Gandolfi, 2006). The study aims at providing a better understanding of the dynamics of the regeneration, in relation to clearing sizes and seed influence.

In summary, the objective of this thesis is presenting a model of the floristic and ecological interaction in plant communities in the PESM, state of São Paulo, Brazil. Building a local forest growth model including anthropogenic activities will lead us to a better understanding in order to take sustainable actions.

1.2. Outline of the thesis

This thesis entails to explore questions related to forest biomass stocks and scenarios of human interaction. Therefore, this will allow us to understand the carbon capture and storage of the BAF for finely build a tool to support BAF management sustainable decisions.

The main steps of this thesis are:

- To design a model of the natural dynamics of the BAF
- To study the impacts of different colonizations on the forest structure
- To understand the forest regeneration under different scenarios

1.3. Base mathematical model

The base mathematical model developed hereafter was adapted from the FORMIND model and it were implemented in MATLAB 2010. The computer used is a HP Z600 Workstation with 12 GB of RAM. In the base case, 8 hours are necessary to run the simulation.

1.4. Publications

1.4.1. Submitted papers

Villacampa, M., Oller do Nascimento, C.A., Modeling scenarios of human interactions on Brazilian Atlantic Forest submitted to the Forest Ecology and Management journal.

1.4.2. Participation at conferences

Villacampa, M., Oller do Nascimento, C.A. Carbon Sequestration: Mathematical Model of the Brazilian Atlantic Forest. 2013 AIChE Annual meeting. San Francisco. November 3-8 2013.

Honorable Mention at the "CAST Directors' Award," for the best poster presentations at the 2013 AIChE Annual Meeting, San Francisco, CA (http://www.castdiv.org/spring2014newsletter/index.html)

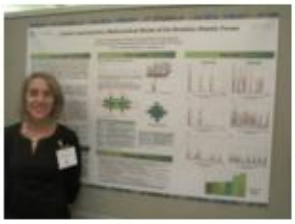

Honorable Mention

Marion Villacampa, Universidade de Sao Paulo, 200f
Carbon sequestration: mathematical model of the Brazilian Atlantic forest

2013 Poster and Presentation Awards

2. Bibliographical review

2.1. What is a model?

As defined by Byl (2003), a model is an abstraction, or a simplified representation, of some aspect of reality in order to obtain description and/or calculation. The purpose of the model drives how one simplifies the reality, what one represents, which property is relevant or not.

According to the Natural Sciences and Engineering Research Council of Canada (2003) a good model should meet the following expectations:

- ✓ It should give an explanation of certain patterns and properties from the reality it represents.
- ✓ It should link several observations in order to obtain a structured interpretation from the reality it represents.
- ✓ To a certain extent, it should foresee new events or new states.
- ✓ In the light of new observations, it should be possible to improve the model.

Mathematical models play a large role in science. They are sets of equation, using symbolic representations of quantitative variables in simplified systems (Barbour, 1974). Their chief role is prediction. It is useful to distinguish between models for prediction, and models for understanding (Bunnell, 1989).

The expression "forest growth model" usually refers to an abstraction of the natural dynamics of a forest stand. A mathematical forest growth model is a system of equations which can predict the growth and yield of a forest stand. It generally takes into account growth, mortality, and other changes in stand composition and structure (Vanclay, 1994).

The term "growth" implies the increase in dimensions (volume in m^3) of one or more trees in a forest stand over a given period of time.

The components of a fully implemented growth model are the estimates of growth and mortality (catastrophic and non-catastrophic), the regeneration and the display of relevant results (Marshall, 2005).

To deal with series of non-linear differential equations and all the numerical values, this kind of model is always implemented on a computer.

Then it is necessary to understand the specificities of the tropical forest to be able to build the mathematical model.

2.2. Specificities of a tropical forest

A tropical forest is a peculiar ecosystem type which has a high level of biodiversity. It is a high and dense tree formation with a warm and wet climate. Tropical forests are seriously threatened by large-scale fragmentation due to human activity and its total area is reducing. The rate of deforestation is only slowing down and remains alarming in many countries. Globally, around 13 million hectares of forests were lost through natural causes or converted to other uses each year between 2000 and 2010 as compared to around 16 million hectares per year during the 1990s (FAO, 2010).

As reported by Bourgeron (1983), tropical forest structures are characterized by different strata, or layers, with vegetation organized into a vertical pattern from the top of the soil to the canopy. The different strata of a tropical forest are shown in figure 4.

Each stratum is a unique biotic community containing different plants adapted for this particular layer. The height of the layer can vary from a region to another.

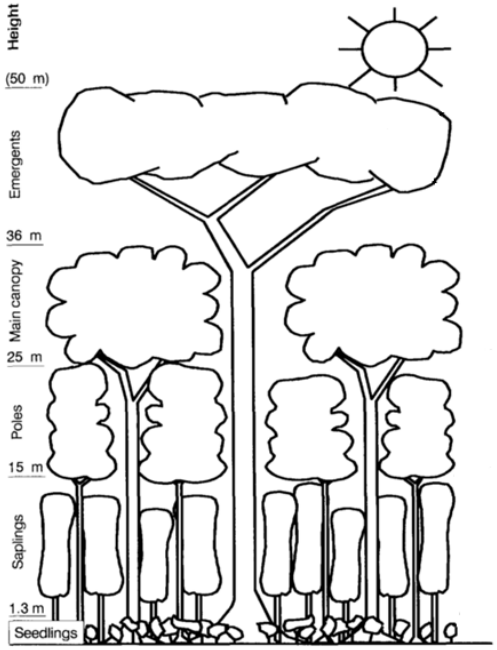

Source : (Bossel and Krieger, 1991)

Figure 4: Schematic representation of the vertical structure of a tropical forest

As in any ecological community, a tropical forest observes a natural process of change in the species structure over time (Hamilton, 2002). Forest succession generally means replacement of tree species or tree associations.

As explained by Martin and Gower (1996a), each stage of the succession creates the conditions for the next stage and some of the existing plants are replaced by more stable plant communities. The established species impact their own environment creating new environmental conditions. The original environment was optimal for the first species of plant, but the new environment may be optimal for some others. With this environmental change, the previously dominant species may disappear and another species may become ascendant (Hamilton, 2002).

Underneath a leaf canopy, light availability is highly reduced (Gommers et al., 2013). Tree species that tolerate shade are called shade tolerant species; those that require full sunlight and limited competition are called shade intolerant or light demanding species (Martin and Gower, 1996b). In other words, in ecology, shade tolerance refers to a plant's ability to compete for survival under shaded conditions (Snyder, 2010). According to Snyder (2010) the shade tolerance is a tree trait, a functional adaptation that varies among species. Forest successional stages are closely linked to the shade tolerance of the tree species. Succession basically progresses from very shade intolerant species to the very shade tolerant species over time (Martin and Gower, 1996b).

The complete sequence of forest successional stages is represented in figure 5.

Source : (Martin and Gower, 1996a)

Figure 5: Process of forest succession

At the very beginning or after a strong disturbance, the grass and shrubs monopolize the site. Then trees appear and begin to dominate. Light demanding species grow faster than the shade tolerant ones, and start to overshadow the other plants. As the shade intolerant species are growing rapidly and the shade tolerant are appearing, there is a tree-to-tree competition. At this stage, if a shade intolerant tree dies, a shade tolerant tree occupies the gap. In a mature forest intolerant and tolerant trees may share the main canopy. At climax stage the shade tolerant trees dominate the site and the

environmental conditions are not favorable for shade intolerant trees to reproduce.

In tropical forests, there is a particular process: the big trees fall and create canopy gaps. Trees grow in a cycle of succession in these gaps and the pioneers strongly depend on these gaps. Pioneers are species whose seeds can only germinate in full sunlight at ground level for at least part of the day. As a consequence pioneer seedlings are found in openings in the forest and are never found under a closed forest canopy (Swaine and Whitmore, 1988). Pioneers are commonly found in regrowth after a major disturbance.

The model structure for tropical and non-tropical forests is different. In the latter case, monospecific even-aged forests are often the object of research (Bossel and Krieger, 1994).

As tropical forests are peculiar ecosystems, modelers face a lot of difficulties in designing a growth model for this kind of forest (Vanclay, 1995):

- ✓ There is a small number of models available.
- ✓ There are many tree species (up to 500 species per hectare), and a corollary to this high diversity is that a lot of the tree species are locally rare (Clark and Clark, 1999).
- ✓ The lifetime of many species is very long (some hundred years).
- ✓ The tree age is usually unknown and difficult to measure.
- ✓ There is a lack of long-term field data, observation periods are generally smaller than 30 years.

As the FAO (Food and Agriculture Organization of the United Nations) explains (FAO, 2001), developing simulation models for tropical forests faces a greatest obstacle: suitable data are not easily available. This point represents a challenge for who wants to parameterize and test forest growth models.

2.3. Tropical forest growth model overview

Forest growth models are grouped into different families. Each group of models is characterized by a key design paradigm, which helps choosing the most suitable model for a specific situation. At the end, the choice of a modeling paradigm is made mainly in function of the objectives for which the model is to be built, and the potentially or currently available data (Alder, 1995). Vanclay (1994) explained that there is no perfect method for forest growth models. However, he notes that tropical forests pose a peculiar problem because there may be hundreds of species and a huge diversity of tree sizes and growth patterns.

According to Porté et Bartelink (2002), in the literature several and sometimes contradicting classification schemes are found. The large amount of growth models in existence difficult the examination of the methodology used in each (Seo, 2005). Not all models were built to serve the same purpose, consequently not all models are suitable for all applications (Porté and Bartelink, 2002).

In agreement with Weiskittel (2012) a forest growth model can be qualitative or quantitative, as shown in figure 6.

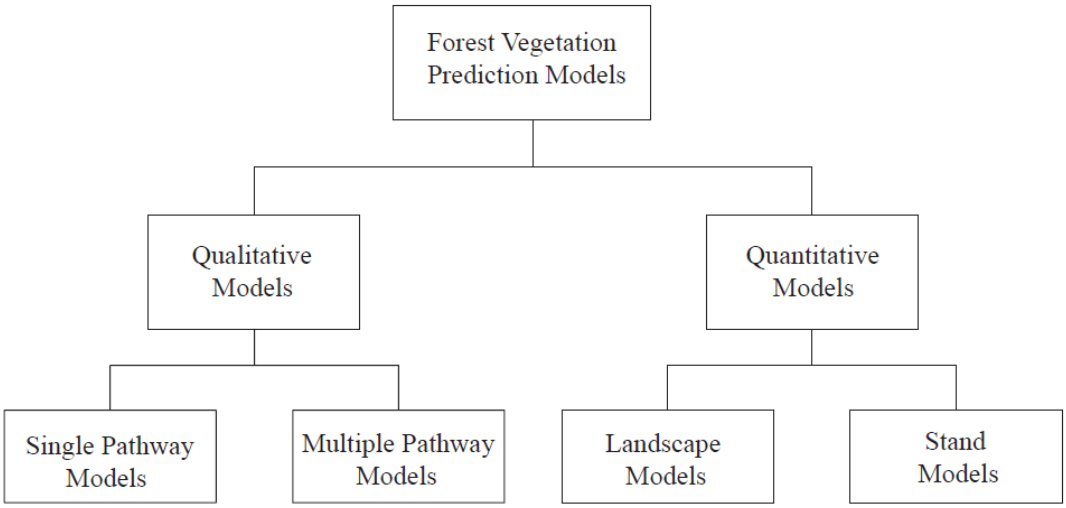

Figure 6: Different types of forest vegetation prediction models according to Weiskittel (2012)

In this study, a quantitative model focused on a small forest would be considered more appropriated in relation with the study site size.

An easy way to classify models is the level of details they provide. According to Vanclay (1994) a model is for prediction or for understanding, then it may represent a whole stand, a size class or a single tree. At a smaller level, models are grouped in relation with the approach used to calculate the evolution of the system. This approach can be based on equations, matrices, tables, etc.

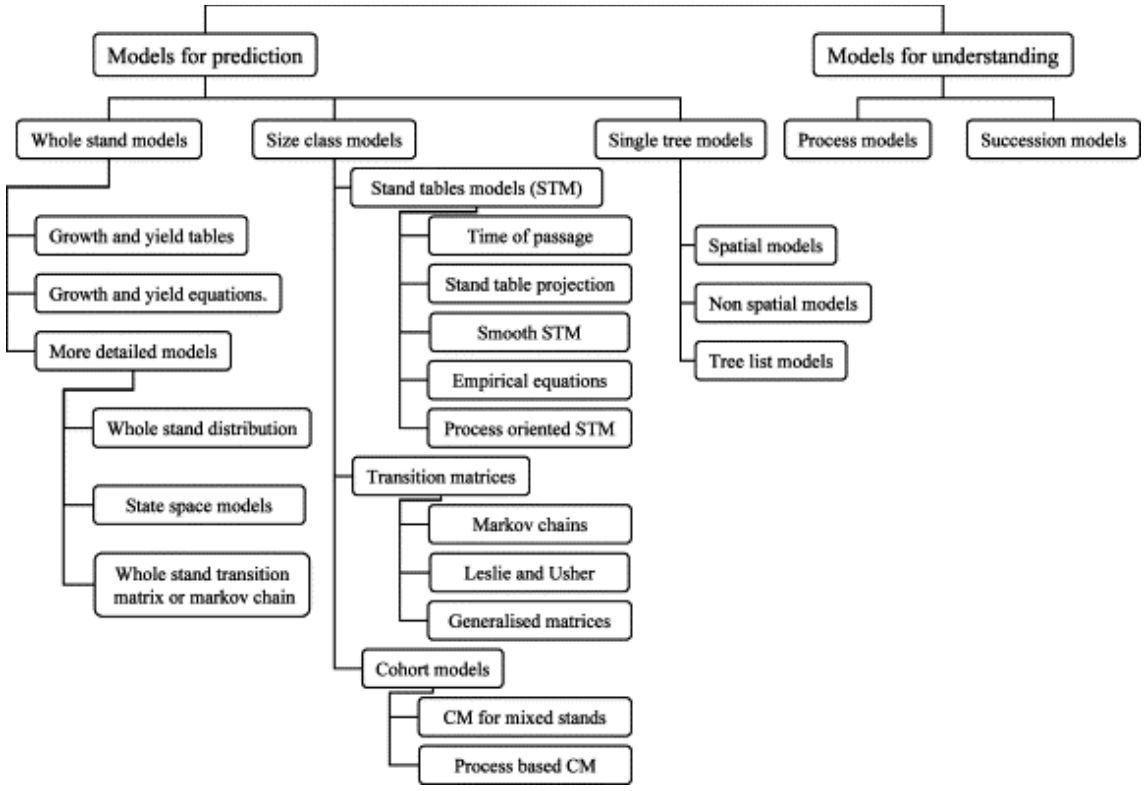

Figure 7: Classification of forest growth models according to Vanclay (1984)

Vanclay (1994) gives the most detailed classification but in that approach a model might belong to more than one class at the same time (Porté and Bartelink, 2002). Because of the lack of data, some model of the figure 7, are unusable, such as models based on transition matrices, markov chain, or stand tables.

Another possibility involves the classification of Liu and Ashton (1995) with two alternative categories (see figure 8): stand models and individual-based models (size class and single tree models are grouped into one classification).

The whole stand models are principally built for timber projection and have drawbacks for species diversity studies (Liu and Ashton, 1998). In the stand-level model, no individual trees are described and the canopy is represented by horizontally homogeneous leaf layers (Porté and Bartelink, 2002). As reported by the same authors, stand-level models are unable to represent different planting patterns in mixtures, or to take crown dynamics into account. Indeed in complex systems like mixed forests, a tree-level model will be required to

represent competition effects. The different characteristics of the species and the spatial distribution of the trees have a different impact on stand development (Porté and Bartelink, 2002). As a result, whole stand models will not suit the purposes of this project.

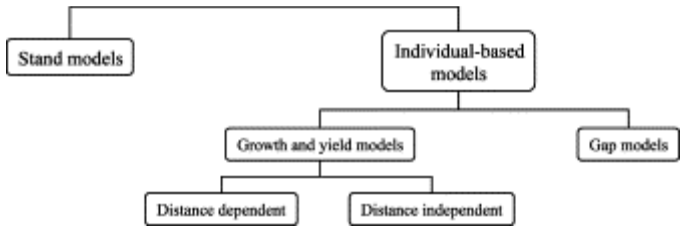

Figure 8: Classification of tree level forest growth models according to Liu and Ashton (1998)

In agreement with Liu and Ashton (1998), another classification is proposed; there are two categories of model, the stand models and the individual-based models (IBM).

Classical models attempt to describe all individuals in an environment with only one variable (Huston et al., 1988), which implicates that individuals do not vary in their physiology or behavior. On the other hand, according to Reynolds (1987), IBM are simulations based on the global consequences of local interactions of members of a population. IBM aim to treat individuals as unique and discrete entities (Grimm, 1999).

According to Carlotti et al. (2000), in an IBM, one has to treat populations as collections of individuals. Each individual is represented by a set of variables that stores its "*i*-state" (i.e. age, height, diameter...). Then the *i*-state of an individual evolves depending on its current *i*-state, the state of the local environment and the interaction with others individuals.

According to figure 8, the second criterion divides each of these two groups in growth and yield model or gap model.

The gap model is built on ecological theory and interpretation of species dynamics. It is generally used to predict long-term forest succession (Weiskittel et al., 2011). Conforming to Porté and Bartelink (2002) in gap model, the forest is simulated as a group of patches or gaps, each being characterised by a list of individual trees. Moreover, the gap size has to be set so that the environmental conditions inside the gap can be considered horizontally homogeneous. Inside each cell, forest dynamics are modelled with a description of recruitment, growth and mortality at the individual tree level. Generally, the location of the patch is not made spatially explicit: therefore patches behave independently from one another. However, a few exceptions exist (Porté and Bartelink, 2002).

Gap models are developed in section 2.4.

As reported by Porté and Bartelink (2002) a logical way of discriminating between forest growth models is to look at the description of the stand structure. They chose three criteria: the first corresponds to the smallest unit identified (i.e. a tree, a stand) in the model; the second criterion is spatial dependence; and the third criterion describes whether or not forest heterogeneity is taken into account see figure 9.

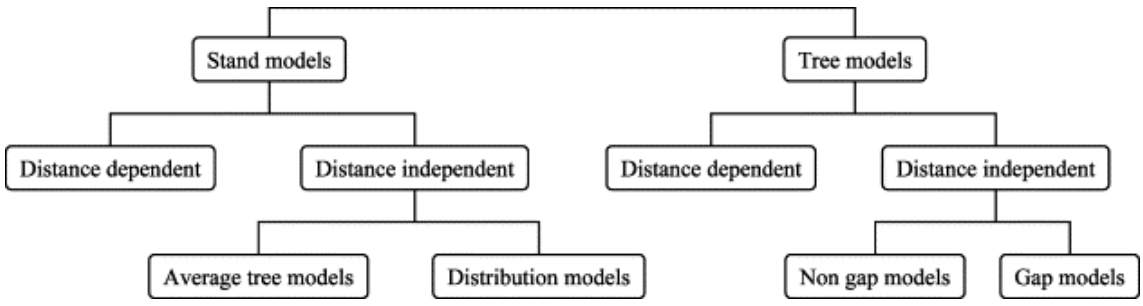

Figure 9: Classification of forest growth models according to Porté and Bartelink (2002)

A model may also consider individual tree position (position dependent model) or not (position independent model), and a model may be considered a dynamic model or a static model (Lee and Fishwick, 1996).

Then to represent the dynamic of the forest various possible approaches are used in the models.

According to Seo (2005) process model approach uses key plant physiological processes to estimate growth at tree or stand level. Another possibility is to use transition probabilities to model the forest growth, but a disadvantage may be the difficulty to set certain parameters without long-term data.

Within a given subcategory, models differ in their resolution, i.e. the basic unit of space and time for predictions (Weiskittel et al., 2011). As seen, for the spatial resolution, it goes from a whole-stand forest to a individual based approach. The temporal resolution is usually a one year time step, but some process models have shorter steps (one hour, one day) and some statistical models longer steps (1 to 10 years).

According to the purposes of the thesis, the model developed here belongs to the IBM group, more specifically to the gap model family because according to Porté and Bartelink (2002) gap models are mostly used to describe forest dynamics and succession.

In the next part a review of forest gap model is addressed.

2.4. Forest gap models

Bugmann (2001) explains that forest gap models are individual-tree based models first conceived in 1969. At the beginning, in the first, now classic, JOBAWA model (Botkin et al., 1972), four simplifications were made in order to consider mixed-species and mixed-age forests, complex forests:

- ✓ The forest is represented as a grid of many small patches, and each patch can have trees at different ages and different successional stages.
- ✓ The position of a tree in a patch is not considered, i.e. a patch is horizontally homogeneous.
- ✓ The leaves of the trees are represented as a cylinder at the top of the stem.
- ✓ Patches do not interact one with another.

Since then, the simplifications and equations have been analyzed, tested and sometimes replaced by other formulations in specific gap models. Therefore, there are now a lot of gap models, most of which sharing many features. The principal differences among gap models are the functions, routines and/or parameters that have to be set to study site forests, climate or purposes (Porté and Bartelink, 2002).

Variations in the formulation can be grouped in five points:

- ✓ Choice of state variables.
- ✓ Plant production (diameter increment-based, assimilation and respiration-based,...).
- ✓ Allocation of biomass in tree compartments.
- ✓ Competition (Competition for different resources; water, nutriment, space, light,...).

- ✓ Environmental influences (seasonal variation of environmental factors such as soil moisture, CO_2 concentration, degree-days,...).

It is important to note that light availability plays a major role in the regeneration and tree growth processes of all gap models (Porté and Bartelink, 2002).

To quantify the biomass in the BAF, a model with at least the biomass and the number of tree as state variables is selected. Then, the models FORET (Shugart and West, 1977), BRIND (Shugart and Noble, 1981), FORTNITE (Aber, 1982), FORICO (Doyle, 1981), CLIMACS (Dale et al., 1984), SILVA (Kercher and Axelrod, 1984), FIRESUM (Keane et al., 1990) nor JABOWAII (Botkin, 1993) could be considered.

To simplify the simulations, yearly climatic variations are not considered, so that the LINKAGES model (Pastor and Post, 1985) will not be useful. The FORSKA model family approach (Leemans and Prentice, 1989), which is based on daily mean temperature (Bugmann, 2001) would be excessively computational time consuming for our objectives.

The problem of increasing physiological details in a model is to find sufficient data to actually parameterize the functions. Consequently, models such as the FORECE model (Kienast, 1985) are avoided here.

The FORMIX family model designed by Bossel and Krieger (1991), which seems to be adequate to our objectives, our available data, and our study site, was then considered for our project.

On the basis of FORMIX, FORMIX2, FORMIX3-Q, FORMIND and FORMIND2.0 (Bossel and Krieger, 1991, 1994; Ditzer et al., 2000; Groeneveld et al., 2009; Köhler and Huth, 1998), a multi-species model which contains nine

functionally different species, each depicting a component of the canopy layer that it can reach and a shade tolerance, was therefore developed. In the following chapters, the model will be described.

3. Description of the model

In this chapter, a model to understand the long-term dynamics of uneven-aged and very rich species forest stands after natural or anthropogenic disturbances (i.e. logging, landslides, etc.) is presented.

The model is an individual-oriented based model and its aim is to represent growth dynamics in mixed tropical forest. The growth processes and parameters of the model are adapted to the BAF specific conditions.

3.1. Basic structure of model

3.1.1. Plant Functional Type grouping

The BAF is very rich in tree species. Let us remind that, for instance, 20 thousand types of plants were documented on site. It is important to represent the complex interactions (tree size distribution, species composition) between the species in order to reproduce forest dynamics (Köhler and Huth, 1998). Having said that, modeling high complexity increases time to find the parameters and possible errors from the lack of empirical data for a lot of species may occur (Fischer et al., 2016).

To improve computing efficiency, the model has a cohort approach, i.e. trees are packed together into groups.

The dynamic processes of tropical forest produce over time an arrangement of great heterogeneities. The classification of species into groups is particularly necessary in the BAF because many species are represented by only a few individuals (Swaine and Whitmore, 1988). Even if the classification implies a degree of simplification that diminishes information content, it allows general patterns and consequently helps to predict the plant community response to environmental changes without demanding precise information from each species (Reich et al., 2003; Souza et al., 2010).

Grouping by genus or family is not useful because some families contain species that have a large range of maximum diameters and growth rates (Phillips et al., 2002).

Canopies are organized in size from one to various tree crowns in depth, and at the same time, drilled of holes by falling trees (Lieberman et al., 1995). This structural complexity gives to the system a large heterogeneity in light environments. Therefore, it is assumed that the responses of the tree species to these light variations are important.

According to field studies, species generally have comparable attributes (seed production rates, growth rate, mortality rates) making it possible to organize similar tree species of extremely rich BAF into species group (Fischer et al., 2016). In the light of this knowledge, trees are grouped according to their light regeneration strategies and their potential maximum height. These two physiological attributes are presumed to be independent from each other (Fischer et al., 2016). Each group is a Plant Functional Type or PFT (Whitmore, 1998).

These group species have different behaviors. Light demanding species grow faster than shade tolerant species (Poorter, 1999). Leaves of shade tolerant species often have lower net photosynthesis rate (Koike et al., 2001).

Light demanding trees overshadow and outcompete shade tolerant species, attain a position at the top of the re-growing gap vegetation, and achieve fast growth (Poorter, 2009). According to Poorter (2009), a lot of light demanding species have minute seeds and on the other hand shade tolerant species are more large seeded. In addition, light demanding species have a better growth rates in the light because of a higher maximum photosynthetic rate. However, they have a higher respiration rate than most shade tolerant species (Okuda et al., 2013; Poorter, 2009). Also, light demanding species have lower survivorship rates and a higher minimum light requirement for growth than shade tolerant species (Okuda et al., 2013). Finally, light demanding species often show low-density wood (King et al., 2006).

Intermediate shade tolerant species characteristics spread out between shade tolerant and light demanding species (Pütz et al., 2011).

Table 2 shows the classification of species into PFT in function of the maximum tree height at maturity and shade tolerance (or light requirement).

Table 2: Plant Functional Type

Potential height (m)	Shade tolerance	PFT
15	Light demanding species	1
25	Light demanding species	2
32	Light demanding species	3
15	Intermediate shade tolerant species	4
25	Intermediate shade tolerant species	5
32	Intermediate shade tolerant species	6
15	Shade tolerant species	7
25	Shade tolerant species	8
32	Shade tolerant species	9

Here, a cohort is a group of trees of same PFT, with the same age and in a specific localization. In a cohort, all trees are considered equal they have the same height and the same diameter, and tree growth is simulated for a representative individual, which interacts through functional relationships with trees of its own cohort and of the cohorts around. Trees with a diameter higher than 40 cm are generally simulated individually. Actually it is then assumed that all other trees of its cohort are dead because of the space competition and mortality (Köhler et al., 2001).

3.1.2. Spatial resolution

The simulation area is represented as a quadratic grid of cells, regularly ordered.

Each cell has a 400m² size (20m x 20m) because it is assumed that the size of a patch is equal to the size of the crown of the largest mature trees.

A four hectares model is simulated in order to have a compromise between an acceptable computational time and sufficient fragment size. Consequently the simulation area is a grid of 10 columns and 10 lines as can be seen in figure 10.

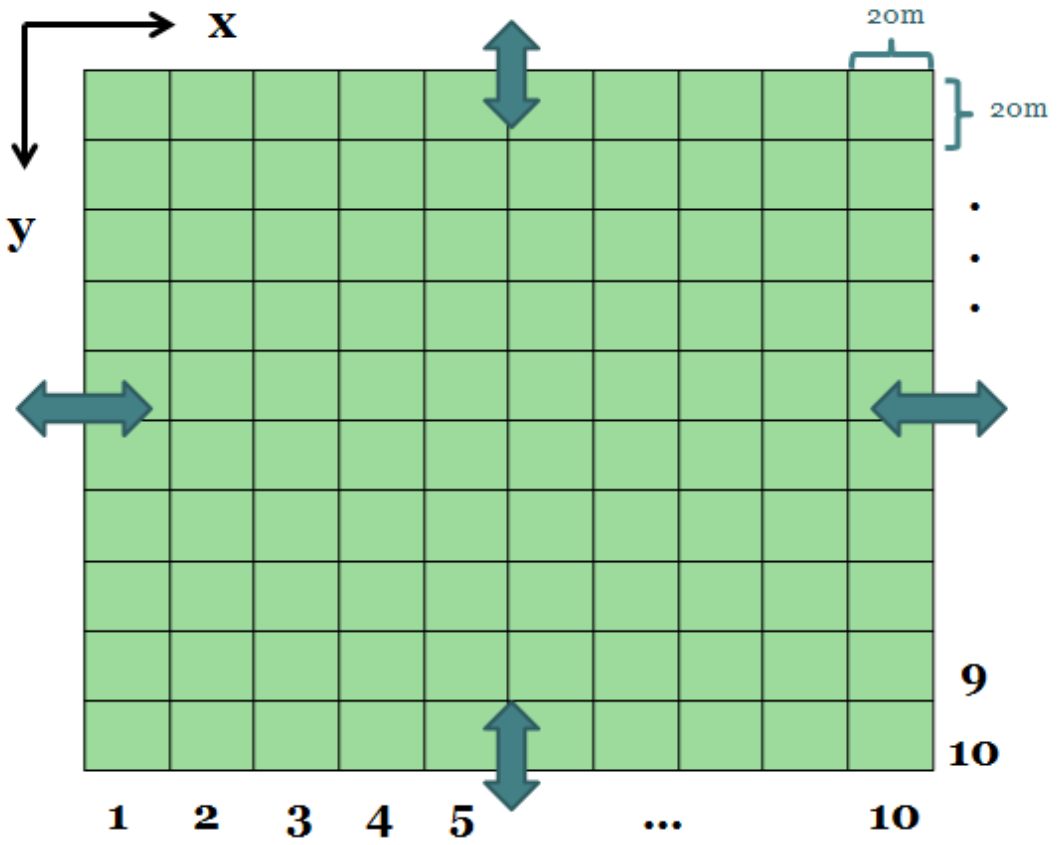

Figure 10: Simulation area mapping

In a cell, trees do not have explicit positions in order to save computational time. All the trees of a patch compete for space and light. There are interactions with the trees of the patches around due to falling trees and seed dispersal.

The forest is simulated in periodic boundary conditions, in other words, processes (seed dispersal, tree falling) leaving one side of the simulation area map reenter the area from the opposite side.

3.1.3. Temporal resolution

The temporal resolution is set to one year.

The daily or seasonal variations are not simulated to save computational time. Annual average values are used. Besides, according to the INMET (Instituto Nacional de Meteologogia - Brazilian National Institute of Meteorology), the day length does not change a lot in a year in the BAF area, so that it is not too simplistic to focus more in long term variations than in annual ones.

3.2. Description of the submodels

3.2.1. Overview

Figure 11 shows a schematization of the interactions between cohorts and the principal variables of a cohort, i.e. the biomass B and the number of trees N.

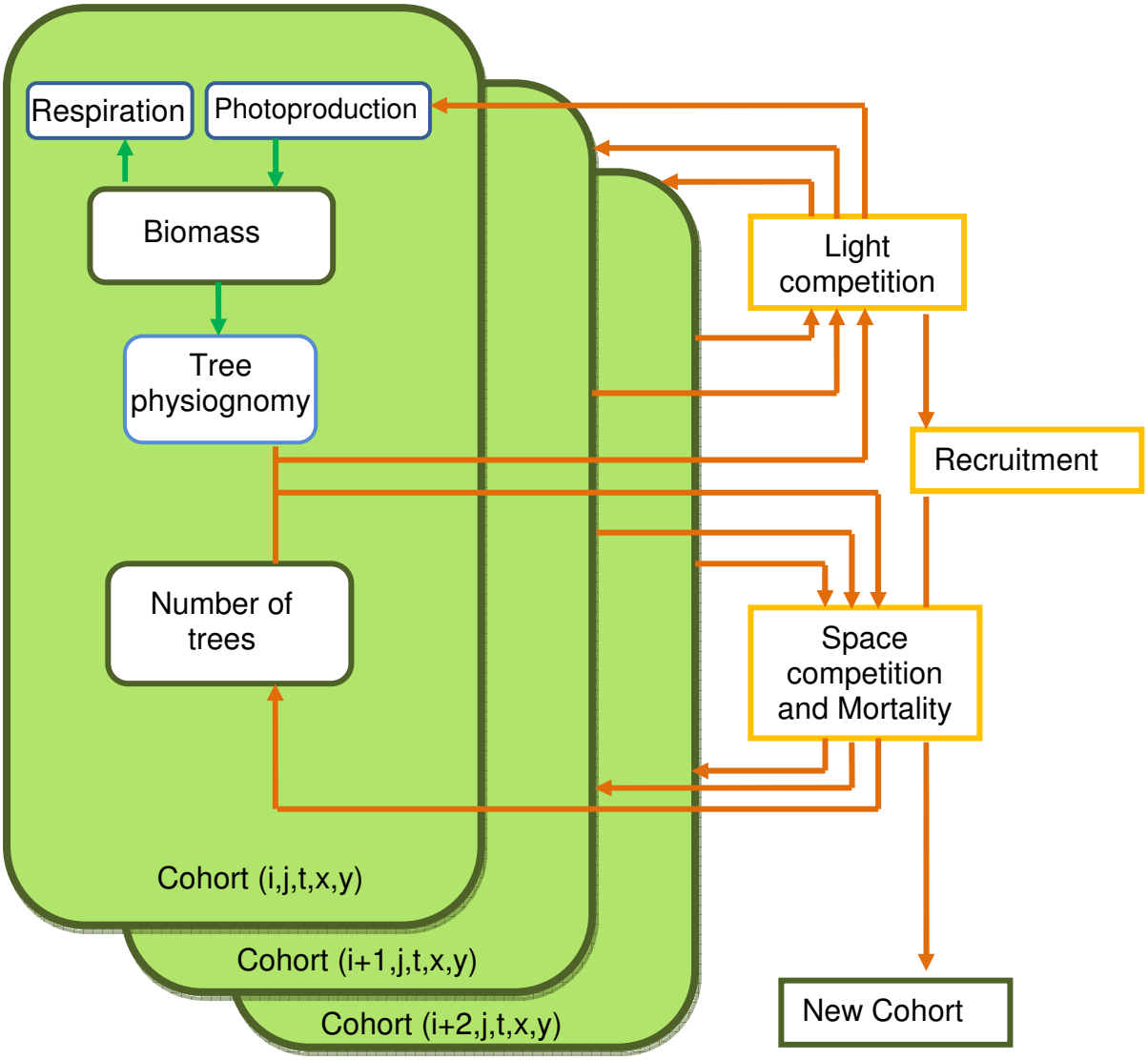

(from (Köhler, 2000))

Figure 11: Overview of interactions in the layer *j*, at time *t* and in the cell (*x,y*)
where *i* is the type of PFT, *j* the layer of the vertical discretization, *t* the time, and (*x,y*) are the coordinates of the cohort

Each tree of a cohort is characterized by the following indexes:

- ✓ ***i*** : type of PFT (1 to 9).
- ✓ ***j*** : layer in which the crown of the cohort is (1 to 64). The vertical structure of the forest is discretized into 64 layers of Δh (0,5m) each in order to simulate the space competition
- ✓ ***t*** : time step
- ✓ ***x,y*** : coordinates of the cohort in the grid (1 to 10, 1 to 10). The forest simulated is represented as a ten columns and ten lines grid.

The annual biomass augmentation is the difference between the biomass produced from photoproduction and the one lost from the trees respiration and it is calculated for a cohort. Then, from the biomass production, tree physiognomic assumptions allow calculating other variables such as diameter, tree height, leaf area, crown diameter, etc. (Ditzer et al., 2000).

Light competition affects trees of the same and different cohorts, it impacts directly on the photoproduction of the trees. Also, this competition changes the available light at the forest floor, which directly affects the recruitment of new trees.

It is assumed that the ambient temperature is constant and that water and nutrient supplies are unlimited. Also, it is also postulated that light availability is the main driving force for individual tree growth and forest succession. That is why, following the gap model approach (Bossel and Krieger, 1991), all trees compete for light and space. Obviously, the physical laws of energy and mass conservation are considered to model the forest growth.

In each canopy layer, the cohort growth is described by two differential equations representing the temporal development of wood biomass *B* [t_{ODM}/ha] and stem number *N* in that particular layer.

Growth respiration refers to the biosynthesis process within a growing organ and the phloem transport associated. That includes the carbon cost of creating new tissues.

Maintenance respiration is the CO_2 produced during basal rate of metabolism.

The light conditions in the canopy depend on incident solar radiation, on light attenuation in the canopy, and on the photoproduction of the leaves of the species considered (light response curve). The light conditions are calculated via the Beer-Lambert law, which relates the absorption of light to the properties of the material through which the light is traveling. The leaves absorbs the available light, as a consequence tropical forests are characterized by a strong vertical light gradient (Duz et al., 2004).

Light interception is one of the most important factors driving the carbon assimilation and growth of plants(Hilbert and Messier, 1996). The light availability along the understorey canopy gradient of a tropical forest may originate several strategies in space occupation and resource allocation to photosynthetic area among tree species that differ in their maximum size attained.

Thus, the light availability is calculated for each layer of the canopy for every cohort and, as trees present different photoproduction rates, different growth potentials are therefore obtained.

The photosynthesis converts light energy into chemical energy. The trees use this energy to form chemical compounds, for maintenance respiration, and for the formation of temporary or permanent biomass (leaves, wood losses, etc.).

In a given patch, due to shading, the annual growth rates of trees are deduced from the light competition between the trees. The recruitment depends on the light conditions at the forest floor. Once the establishment of seedlings is realized, the growth and the global mortality of the trees in a given patch are calculated from the current tree assemblage of this patch (dependant on the number of tree, the size and the PFT). The global mortality is the sum of various types of mortality (regular mortality, self-thinning, gap creation and edge effect). Regular mortality is a time step regular mortality, self-thinning is due to overcrowded patch, gap creation results of falling trees, and the edge effect increases tree mortality. The mortality submodel is developed in section 3.2.7.

For now, the model does not represent any adaptive traits at tree level nor forest level. Diameter and height growth strategies of an individual tree are fixed and do not change over time. No mechanism aiming to evaluate the future fitness consequences of different growth scenarios is considered.

As far as possible, data from studies carried out in the São Paulo State Park of Serra do Mar were used. However, as the model requires very specific data (unfortunately unavailable at the time of the study), some parameter values have been used from former model parameterizations by Bossel and Krieger (1991, 1994), Ditzer et al. (2000), Köhler (2000), from the Malaysian tropical Sabah forest.

3.2.2. Initialization

In order to study the long term dynamics of the BAF, a treeless area is considered at t=0 year. In this way, all trees have the chance to establish. During the first year, all the PFTs establish randomly in all patches using seeds from the seed bank, all with a diameter of 1 cm. Smaller trees are not taken into account because of:

- ✓ the high stochasticity and the lack of knowledge on growth and mortality of seedlings and saplings
- ✓ the high computational time that implies the consideration of smaller trees, knowing that the vast majority will not survive.

As a result, the model does not allow considering the interactions between all life forms (between herbs and trees for instance).

It is assumed that the environmental conditions are homogeneous, i.e. that there is no seasonal fluctuation of solar radiation. Also, it is presumed that there is no degradation of the site quality nor lack of nutriment and any drought effect is neglected.

At t=0 year, 12 seedlings of PFT1, 13 of PFT2, 10 of PFT3, 10 of PFT4, 9 of PFT5, 7 of PFT6, 3 of PFT7, 4 of PFT8 and 5 of PFT9 establish in each patch. These values were randomly determined, but it is assumed that there would be more pioneer seeds than intermediate shade tolerant because of the pioneer group characteristics. Indeed, pioneers species produce copiously and more-or-less continuously small seeds (Swaine and Whitmore, 1988). Moreover it is assumed that there would be more intermediate shade tolerant seeds than shade tolerant seeds, since, generally, shade tolerant trees produce bigger seeds in smaller quantities.

3.2.3. Submodels

The main processes of the forest growth model are described in the flowchart of the figure 12 and in table 3

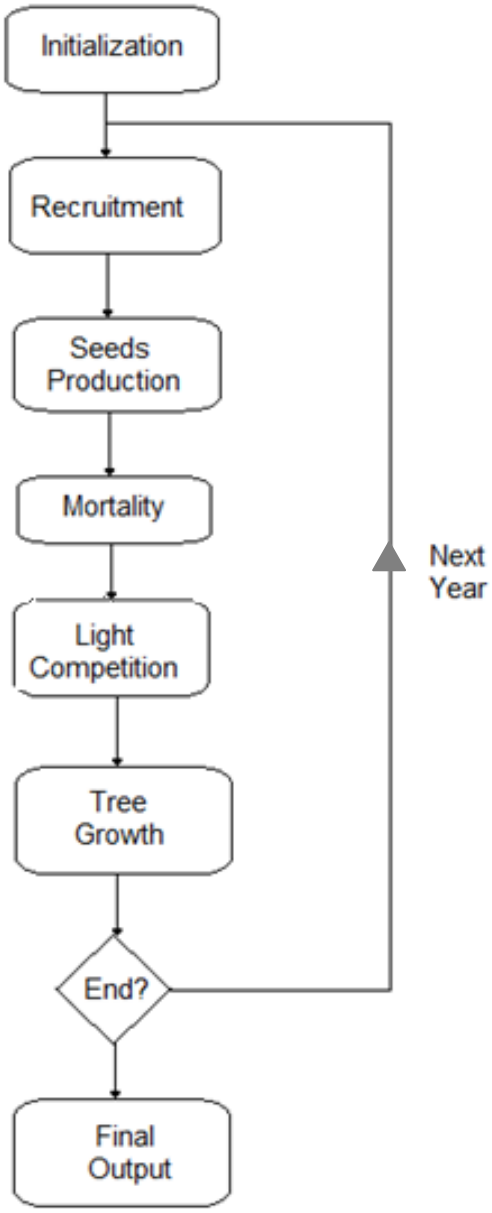

,

Figure 12: Flowchart of the main processes of the forest growth model

Table 3: Main processes of the forest model

Main processes	Comments
Species grouping	Functional groups (maximum growth height, shade tolerance)
Spatial structure	Plots of 400m² (20m x 20m - gap concept)
Tree geometry	Empirical relations between tree biomass, stem diameter, height and crown diameter
Light	Lambert-Beer law of light attenuation
Growth of tree	Carbon balance for tree growth: photosynthetic production of leaves, losses (respiration and litter fall)
Mortality	Normal and crowding, stochastic mortality of large trees, gap dynamics
Recruitment	Seedling input rates depending on light climate
Competition	Competition for light and space

The submodels corresponding to these processes are described in the following sections. The units of the variables are given in table 5 and the list of the model parameters in table 6.

3.2.4. Tree physiognomy

Thereafter, simulation time is at t, and the aim is to calculate the variables at t+1. The simulation always starts with the biomass per tree and the number of trees values.

To calculate the tree physiognomy, the variables stem diameter $D_{(i,j,t,x,y)}$ [m] and height of the tree $H_{(i,j,t,x,y)}$ [m] are crucial.

From one step to the next one, the stem diameter and the height of a tree are calculated from the new aboveground biomass. The biomass per tree $B_{t_{(i,j,t,x,y)}}$ [t_{ODM}] is defined as follows:

$$B_{t(i,j,t,x,y)} = \frac{\pi}{4} * D_{(i,j,t,x,y)}{}^{2} * H_{(i,j,t,x,y)} * \frac{f*\sigma_{(i)}}{TR} \quad \textbf{(1)}$$

Where $D_{(i,j,t,x,y)}$ is the stem diameter, $H_{(i,j,t,x,y)}$ is the height of the tree, *f* is a form factor [unitless], $\sigma_{(i)}$is the wood density [t_{ODM}/m^3] PFT dependant and *TR* is the proportion of stem biomass in the total aboveground biomass [unitless].

Then, the aboveground biomass of a cohort $B_{(i,j,t,x,y)}$ [t_{ODM}] is given by:

$$B_{(i,j,t,x,y)} = B_{t(i,j,t,x,y)} * N_{(i,j,t,x,y)} \quad \textbf{(2)}$$

The relationship between tree height $H_{(i,j,t,x,y)}$ and stem diameter $D_{(i,j,t,x,y)}$ is expressed as:

$$H_{(i,j,t,x,y)} = \frac{D_{(i,j,t,x,y)}}{\frac{1}{h_{0_{(i)}}} + \frac{D_{(i,j,t,x,y)}}{h_{1_{(i)}}}} \quad \textbf{(3)}$$

Where $h_{0_{(i)}}$ [m/m] and $h_{1_{(i)}}$[m] are PFT specific parameters.

Figure 13 shows that the saturation approach of relation height to diameter depends on the potential height of the tree

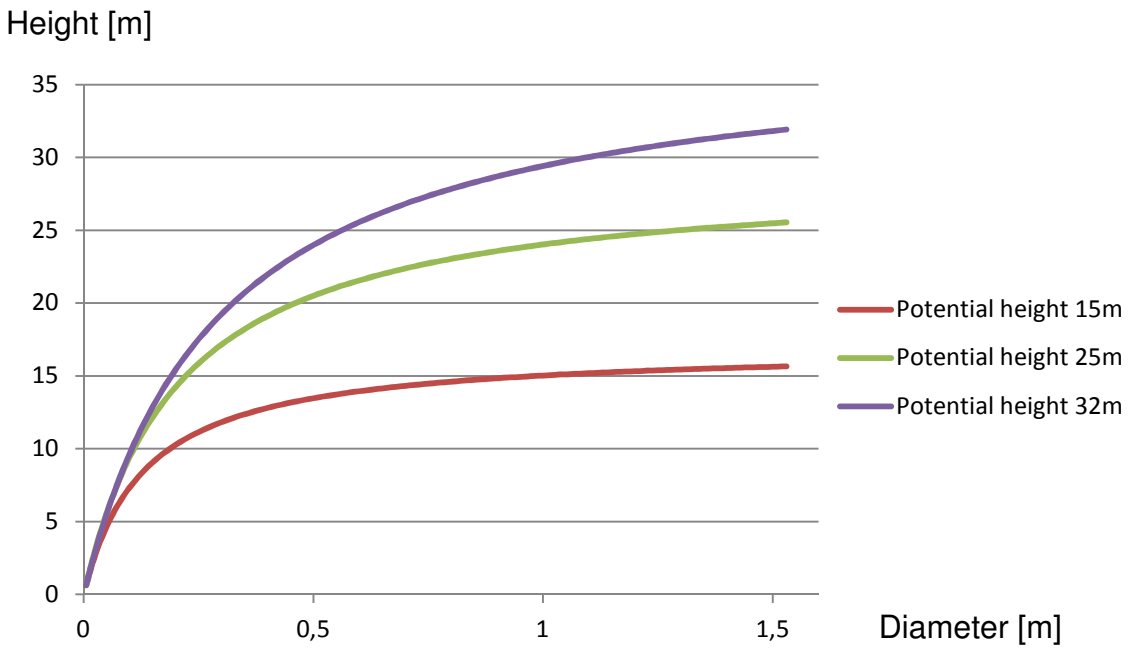

Figure 13: Relation Height – Diameter in function of the potential height

The form factor is a PFT specific form factor, which accounts for deviations of the stem from a cylindrical shape. The form factor changes during the growth of a tree with respect to its diameter $D_{(i,j,j,x,y)}$ through the following relationship

$$f = f_0 * exp^{f_1 * D_{(i,j,t,x,y)}^{f_2}} \quad \textbf{(4)}$$

Where f_0, f_1 and f_2 are unitless type specific parameters.

The crown length $CL_{(i,j,j,x,y)}$ [m] is proportional to the height of the tree as it can be seen in figure 14:

$$CL_{(i,j,t,x,y)} = c * H_{(i,j,t,x,y)} \quad \textbf{(5)}$$

where c represents the crown depth proportion of tree height [unitless].

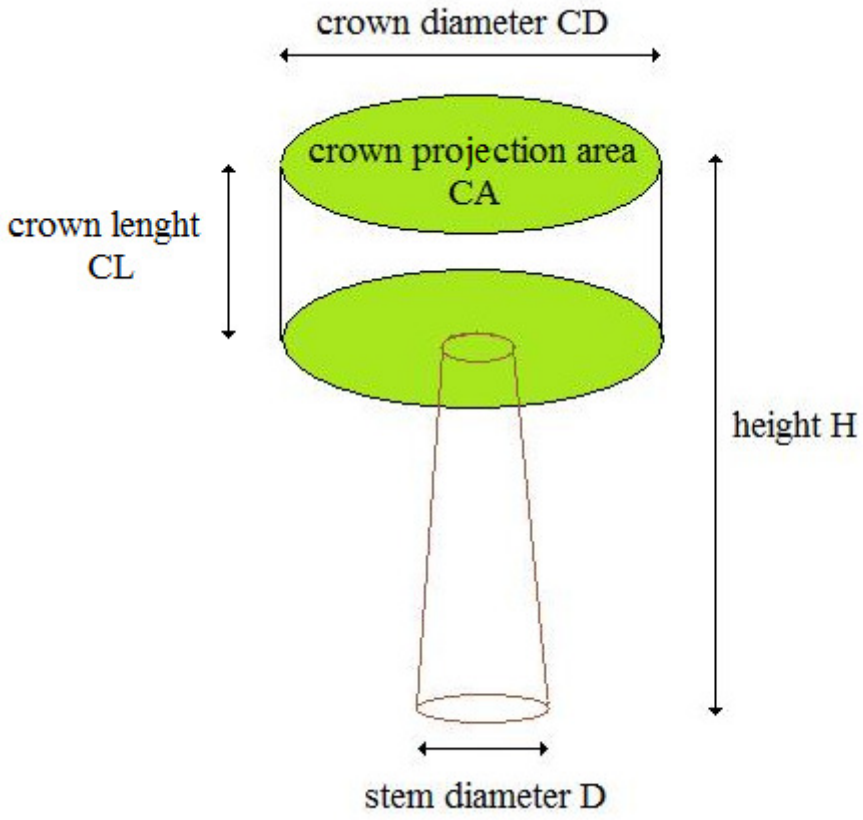

Figure 14: Tree geometry

The crown diameter $CD_{(i,j,t,x,y)}$ [m] is proportional to the diameter of the tree (see figure 14)

$$CD_{(i,j,t,x,y)} = cd * D_{(i,j,t,x,y)} \quad (6)$$

Where *cd* represents the crown diameter / steam diameter relationship [unitless]. The crown is limited to the cell and cannot invade other neighbor cell except when falling.

As a tree has a cylindrical crown shape in our model, the crown projection area $CA_{(i,j,t,x,y)}$ [m²] depends on the diameter of the tree:

$$CA_{(i,j,t,x,y)} = \frac{\pi}{4} CD_{(i,j,t,x,y)}^{2} \quad (7)$$

3.2.5. Light competition

The average daytime solar radiation depends on the position of the cell.

According to Gobron (2008), the Leaf Area Index (LAI) represents the amount of leaf material in an ecosystem and is geometrically defined as the total one-sided area of photosynthetic tissue per unit of ground surface area. LAI is a major characteristic of forest ecosystems because green leaves are involved in many biological and physical processes. Moreover, LAI controls the amount of light that reaches the forest floor, playing a part in understorey development. The LAI is dimensionless and usually ranges from 0 (bare ground) to 10 (very dense forest) (Olivas et al., 2013).

For each tree, the total leaf area $L_{(i,j,t,x,y)}$ [m²] is calculated as a function of the stem diameter $D_{(i,j,t,x,y)}$ [m] through the following relationship:

$$L_{(i,j,t,x,y)} = \max\begin{Bmatrix} l_0 * D_{(i,j,t,x,y)} + l_1 * D^2_{(i,j,t,x,y)} + l_2 * D^3_{(i,j,t,x,y)} \\ LAI_{max} * CA_{(i,j,t,x,y)} \end{Bmatrix} \quad \textbf{(8)}$$

Where l_0, l_1 and l_2 are type specific parameters and $CA_{(i,j,t,x,y)}$ [m²] is the crown projection area of a tree (see equation (7)). The value of $L_{(i,j,t,x,y)}$ [m²] is bounded by $LAI_{max} * CA_{(i,j,t,x,y)}$, where the maximum Leaf Area Index (LAI_{max}) is fixed to 4, in order to avoid unrealistic high values. Groeneveld et al. (2009) set LAI_{max} to 3, however Paula and Lemos Filho (2001) found value up to 4,9, so in this study LAI_{max} is fixed to 4 as an average of these two values.

Then the leaf area index $LAI_{(i,j,t,x,y)}$ [unitless] of an individual tree is obtained from the total leaf area divided by the crown projection area of the tree:

$$LAI_{(i,j,t,x,y)} = \frac{L_{(i,j,t,x,y)}}{CA_{(i,j,t,x,y)}} \quad \textbf{(9)}$$

If there is only one tree in a cell, it will receive full incoming radiation. But with many trees of different heights in a cell, some trees will be shaded by other ones. In that case, the light availability decreases from higher to smaller heights within the canopy because the radiation is progressively attenuated. This vertical distribution of light availability within a cell is named “light climate” (Fischer et al., 2015).

For each height layer of each cell, the leaf area accumulated by all trees belonging to this height layer is added up. If the crown of a tree belongs to various height layers, it will contribute to all those height layers. The maximum and minimum layers occupied by the crown are calculated as follows:

$$layermax_{(i,j,t,x,y)} = \frac{H_{(i,j,t,x,y)}}{\Delta h} \quad \textbf{(10)}$$

$$layermin_{(i,j,t,x,y)} = \frac{H_{(i,j,t,x,y)} - CL_{(i,j,t,x,y)}}{\Delta h} \quad \textbf{(11)}$$

The number of layers occupied by a crown is then:

$$NBlayer_{(i,j,t,x,y)} = layermax_{(i,j,t,x,y)} - layermin_{(i,j,t,x,y)} \quad \textbf{(12)}$$

For an individual crown in layer *j* (with *j* between $layermax_{(i,j,t,x,y)}$ and $layermin_{(i,j,t,x,y)}$) the contribution of a tree to the total leaf area of this very same layer is:

$$LAI\_layer_{(i,j,t,x,y)} = \frac{LAI_{(i,j,t,x,y)} * CA_{(i,j,t,x,y)}}{NBlayer_{(i,j,t,x,y)}} \quad \textbf{(13)}$$

Then adding up the contributions of all the trees' leaf area of a specific layer, the cell-based leaf area index $LAI\_pb_{(j,t,x,y)}$ [unitless] is expressed as follows:

$$LAI\_pb_{(j,t,x,y)} = \sum_{i=1}^{Nb\_PFT} \frac{LAI\_layer_{(i,j,t,x,y)} * N_{(i,j,t,x,y)}}{A\_patch} \quad \textbf{(14)}$$

With A_patch the area of a cell [m].

The distribution of light within the forest canopy is the major determinant of the forest ecosystem functioning (Baudry et al., 2014). Then, finally the radiation each tree is able to intercept is determined. The light attenuation within the canopy of the BAF can be approximated by the Monsi-Saeki formulation of exponential attenuation (Bossel and Krieger, 1991). The incoming radiation $I_{(j,t,x,y)}$ [W/m²] on top of a crown (i.e. at $layermax_{(i,j,t,x,y)}$ height layer) is calculated as follows:

(15)

$$I_{(j,t,x,y)} = I_0 * \exp^{(-k * \sum_{jj=j}^{Nb\_layer} LAI\_pb_{(i,jj,t,x,y)})}$$

where I_0 is the incoming radiation above the canopy [W/m²], k is the light attenuation factor in the forest canopy set here to 0,6 [m^2_{ground}/m^2_{leaf}], and $LAI\_pb_{(i,j,t,x,y)}$ is the cell-based leaf area index (see equation (14)).

The figure 15 shows a schematization of the light climate in a cell. On the right side of the figure, grey rectangles represent the available light in function of the layers. When tree 1 intercepts light, there is less light available for smaller trees, here tree 2.

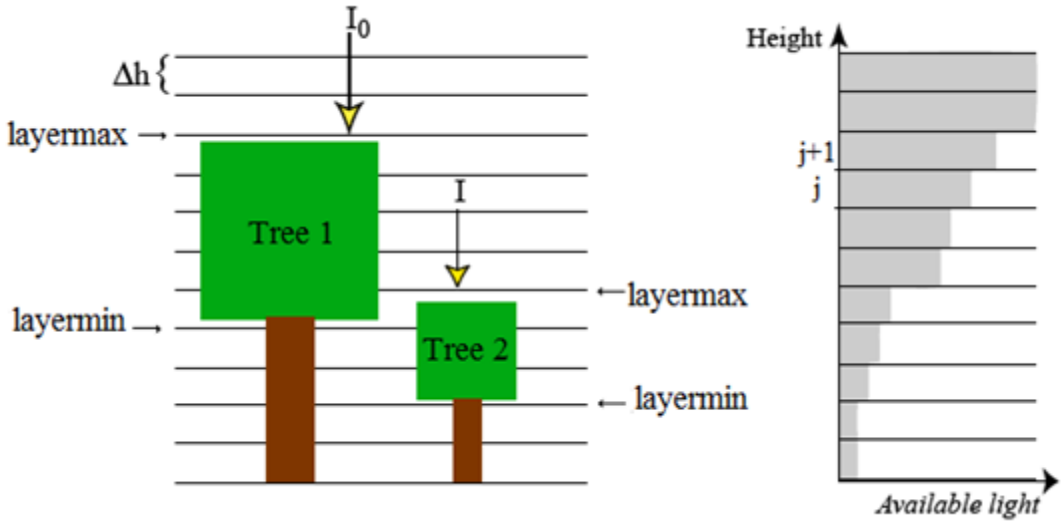

Sources: (Fischer et al., 2015)

Figure 15: Illustration of the light climate

3.2.6. Growth of a tree

To calculate the changes in biomass from one time step to the next, the photosynthetic production and then the respiration of the trees are determined.

Due to the incoming irradiance on top of the crown, a tree produces organic dry matter via gross photosynthesis. Let us remind that there are neither water limitations nor temperature effects.

The photosynthetic production is modeled using the model given by Kira (1978). This model is based on an exponential light distribution within the crown. The light response of the leaves is a saturation type curve represented by the following Michaelis-Menten equation:

$$P = \frac{m*I}{1+\frac{m}{P_{max}}*I} \quad \textbf{(16)}$$

Where P_{max} [$\mu mol_{(CO2)}/m^2/s$] is the light response at light saturation (i.e. the maximum gross photosynthesis), *m* is the dimensionless initial production which increases with increasing radiation (i.e. the slope of the curve), and *I* the photoactive solar radiation [W/m^2]. Normally, the parameters *m* and P_{max} are determined by experimental data and are PFT dependent. Here, values from Groeneveld (2009) are taken.

According to the FORMIND handbook (2015) the photosynthesis of a tree per year without reduction due to limited soil water availability nor temperature effects is:

$$P_{(i,j,t,x,y)} = \frac{Pmax_{(i)}}{k} \ln \left(\frac{\propto_i * k * I_{(j,t,x,y)} + Pmax_{(i)} * (1-m)}{\propto_i * k * I_{(j,t,x,y)} * exp^{-k*LAI_{(i,j,t,x,y)}} + Pmax_{(i)} * (1-m)} \right) \quad \textbf{(17)}$$

Where *k* is the light extinction coefficient [m^2_{ground}/m^2_{leaf}], $Pmax_{(i)}$ is the maximum gross photosynthesis per PFT [$\mu mol_{(CO2)}/m^2/s$] and $\propto_i$ is the initial production per PFT [unitless].

Now, the actual gross photoproduction for a cohort is calculated as follows:

$$PB_{(i,j,t,x,y)} = codm * P_{(i,j,t,x,y)} * CA_{(i,j,t,x,y)} * Day * H\_Sun \quad \textbf{(18)}$$

Where $codm$ is a conversion factor [g_{ODM}/g_{CO2}] (it includes the molar mass of CO_2), Day is the number of days per year [day] and H_Sun is the length of photoactive day time [h/day].

Respiration leads to the following biomass losses: root decay, litter-fall and respiration of tree organs and leaves.

In agreement with Pretzsch in *Forest Dynamics, Growth and Yield: From Measurement to Model* (Pretzsch, 2009), biomass losses due to respiration r_g are about 40% of the gross photoproduction. On the other hand there is a $r_{l_{(i)}}$

loss of biomass due to dead wood, leaf losses, etc. proportional to the current woody biomass (Groeneveld et al., 2009). Then $r_{l_{(i)}}$ varies in function of the PFT. Finally the biomass losses of the trees *R* is defined as:

$$R_{(i,j,t,x,y)} = r_g * PB_{(i,j,t,x,y)} + r_{l_{(i)}} * Bt_{(i,j,t,x,y)} \quad \textbf{(19)}$$

3.2.7. Mortality

There are 4 kinds of tree mortality considered sequentially: the regular mortality, the mortality due to crowded layer, the mortality to the falling trees effects and the mortality due to edge effect. The total mortality in the forest is the sum of the different kinds of mortality.

1. Regular mortality: a mortality rate per tree $Ma_{(i,j,t,x,y)}$ [year^{-1}] is activated at each time step. This mortality is the sum of the background mortality per PFT $Mb_{(i)}$ [year^{-1}] which is a type-specific constant input parameter, and of the diameter dependent mortality $Md_{(i,j,t,x,y)}$[year^{-1}] which represents a higher mortality for small trees. As a matter of fact, younger trees (with a smaller stem diameter) have a higher mortality rate than older trees (Nowak et al., 2004).

$$Ma_{(i,j,t,x,y)} = Mb_{(i)} + Md_{(i,j,t,x,y)} \quad \textbf{(20)}$$

With

$$Md_{(i,j,t,x,y)} = \begin{cases} 0 & if D_{(i,j,t,x,y)} > D_m \\ M_{max} - M_{max} * \frac{D_{(i,j,t,x,y)}}{D_{mort}} & else \end{cases} \quad \textbf{(21)}$$

Where M_{max} [unitless] is the maximum size-dependent mortality of small trees and D_{mort} [m] is the stem diameter up to which mortality is increased.

When there are few trees per cohort, a stochastic approach is applied to calculate the number of trees dying (Fischer et al., 2015). In other words, we compare a random number from a uniform distribution in the range of [0;1] with the mortality rate $Ma_{(i,j,t,x,y)}$ [year^{-1}] which represents the probability of a tree to die. Let us define *numAleat* as a random number from a uniform distribution in the range of [0;1].

Then *numAleat* is compared to the mortality rate $Ma_{(i,j,t,x,y)}$. If *numAleat* is smaller than $Ma_{(i,j,t,x,y)}$ then $\delta_{(i,j,t,x,y)}$ is equal to zero, in the contrary if *numAleat* is bigger, then $\delta_{(i,j,t,x,y)}$ is equal to one:

$$\delta_{(i,j,t,x,y)} = \begin{cases} 0 & if numAleat < Ma_{(i,j,t,x,y)} \\ 1 & if numAleat \geq Ma_{(i,j,t,x,y)} \end{cases} \quad \textbf{(22)}$$

By adding all the $\delta_{(i,j,t,x,y)}$, the number of dead trees due to regular mortality per cohort at each time step $Na_{(i,j,t,x,y)}$ is calculated:

$$Na_{(i,j,t,x,y)} = \sum \delta_{(i,j,t,x,y)} \quad \textbf{(23)}$$

2. Mortality due to crowded layer: it is considered that a layer is crowded when the cumulative crown area $CCA_{(j,t,x,y)}$ of all trees in a cell exceeds $A_{\_patch}$. The cumulative crown area of a layer *j* is the sum of all the crown areas that belong to this very same layer within a cell.

$$CCA_{(j,t,x,y)} = \frac{1}{A_{\_patch}} \sum_{i=1}^{9} \sum_{jj=1}^{64} CA_{(i,jj,t,x,y)} * N_{(i,jj,t,x,y)} \quad \textbf{(24)}$$

With *j* and *jj* a layer of the discretization of the vertical structure, and it is assumed that j is between $layermax_{(i,jj,t,x,y)}$ and $layermin_{(i,jj,t,x,y)}$of a tree.

Where $A_{\_patch}$ is the area total of a cell [m²].

On the left side of figure 16, the crown of each tree is delimited by *layermax* and *layermin*. On the right side of the figure, the sum of the crown projection areas of all the trees present in the layers is represented. When the patch is crowded, the sum of the crown area of all the tress is equal to the cell size. There is no more space left. Consequently the cumulative crown area is equal to 1, and some random trees need to be removed from the patch.

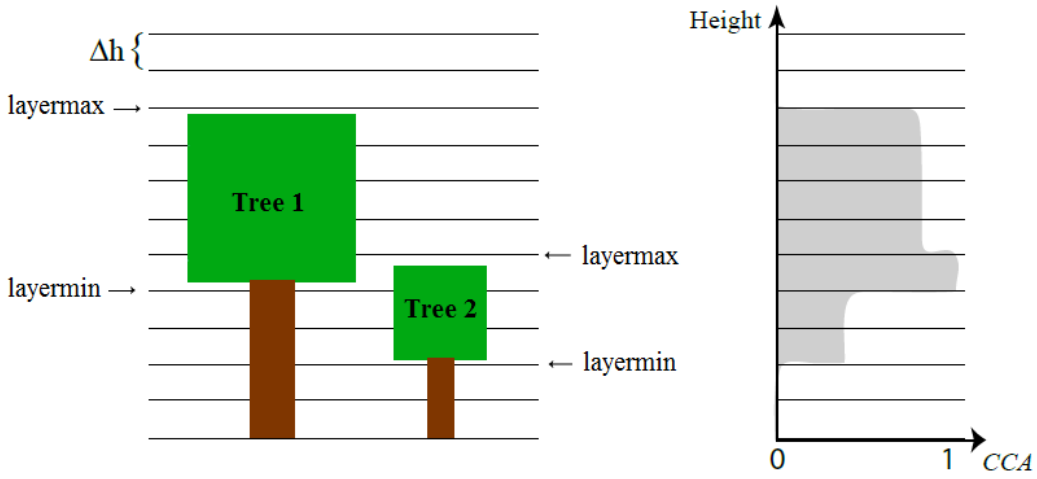

Sources: (Fischer et al., 2015)

Figure 16: Illustration of crowding

Then we calculate the crowding reduction factor $R_{c(j,t,x,y)}$[unitless], which represents the inverse of the maximum cumulative crown area of a tree between its individual limits *layermin* and *layermax*:

(25)

$$R_{c_{(j,t,x,y)}} = \frac{1}{\max\left(CCA_{(layermin:layermax)}\right)}$$

When the cumulative crown area of a cell exceeds 1, i.e. when the patch is crowded, the crowding reduction factor $R_{c_{(j,t,x,y)}}$ drops below the threshold of 1. As a consequence, $N_{c_{(i,j,t,x,y)}}$ trees of the cohort die:

$$N_{c_{(i,j,t,x,y)}} = \left(1 - R_{c_{(j,t,x,y)}}\right) * N_{(i,j,t,x,y)} \quad \textbf{(26)}$$

3. Mortality due to adjacent fallen trees: when a tree dies, it has been assumed that it has a probability p_{fall} [unitless] to fall upon other trees of the patch or of the patches around. At each step time, the number of falling trees $N_{fall_{(i,j,t,x,y)}}$ is then given by:

$$N_{fall_{(i,j,t,x,y)}} = p_{fall} * (N_{c_{(i,j,t,x,y)}} + N_{a_{(i,j,t,x,y)}}) \quad \textbf{(27)}$$

The damages caused by the fallen trees depend on the falling direction and on the tree heights. The falling direction DIR is chosen randomly in a uniform distribution in the range of [0°, 360°]. Then, the coordinates of the patch target are given by:

$$x_{fall} = x_{tree} + H_{(i,j,t,x,y)} * \sin\left(2\pi \frac{DIR}{360}\right) \quad \textbf{(28)}$$

$$y_{fall} = y_{tree} + H_{(i,j,t,x,y)} * \cos\left(2\pi \frac{DIR}{360}\right) \quad \textbf{(29)}$$

where (x_{tree}, y_{tree}) are the coordinates of the fallien tree, DIR is a random number and $H_{(i,j,t,x,y)}$is the height of the mother tree.

Fallen tree can only cause damages to smaller trees. Let us now define the probability for one of these smaller trees to die $Mdam_{(i,j,t,x,y)}$:

$$Mdam_{(i,j,t,x,y)} = \frac{CA_{(i,j,t,x,y)}}{A\_patch} \quad \textbf{(30)}$$

Where $CA_{(i,j,t,x,y)}$ [m²] is the crown area of the fallen tree and A_patch [m²] the patch area.

As previously, we deal with a small number of individuals per cohort, we apply a stochastic approach to calculate the number of trees dying (Department of Ecological Modelling of the Helmholtz Centre for Environmental Research – UFZ, 2014; Fischer et al., 2015). To put it another way, we compare a random number *numAleat* from a uniform distribution in the range of [0;1] with the mortality rate $Mdam_{(i,j,t,x,y)}$ which represents the probability of a tree to die.

Then we compare *numAleat* to the mortality rate $Ma_{(i,j,t,x,y)}$. If *numAleat* is smaller than $Mdam_{(i,j,t,x,y)}$ then $\delta_{(i,j,t,x,y)}$ is equal to zero, in the contrary if *numAleat* bigger then $\delta_{(i,j,t,x,y)}$ is equal to one:

$$\delta_{(i,j,t,x,y)} = \begin{cases} 0 \; if numAleat < Mdam_{(i,j,t,x,y)} \\ 1 \; if numAleat \geq Mdam_{(i,j,t,x,y)} \end{cases} \quad \textbf{(31)}$$

Finally by adding up all the $\delta_{(i,j,t,x,y)}$, the number of dead tree per cohort due to fallen tree at each time step $Ndeadbyfallentree_{(i,j,t,x,y)}$ is calculated:

$$Ndeadbyfallentree_{(i,j,t,x,y)} = \sum \delta_{(i,j,t,x,y)} \quad \textbf{(32)}$$

4. Mortality due to edge effect: it is assumed that mortality is higher at the edges of a fragment. Consequently this reality is represented by multiplying the basic mortality $Mb_{(i)}$ by a factor '*a'* and an extra mortality is added for large trees, i.e. trees with a stem diameter superior than 60 cm. The parameters '*a'* and extra mortality for large tree depend on the distance from the forest edge.

Therefore factor '*a'* [unitless] is determined within the first 20 m of the forest edge as *a* = 2,5 and within 20-40 m from the edge *a* = 1,75 (Groeneveld et al., 2009)

In addition, all large trees suffer an additional mortality with a=5 within the first 20m of the forest edge and within 20-40m from the edge an additional mortality with a=2,5.

If the distance from the forest edge is larger than 40m, it is assumed that the mortality is not affected by edge effects.

The edge effect is not always simulated, it depends on the simulated scenario. When a continuous forest is simulated, i.e. a forest without edge, there is no edge effect.

Finally the total number of trees dying per time step is the sum of all the dead trees whatever the cause:

$$Ndead_{(i,j,t,x,y)} = Ndeadbyfallentree_{(i,j,t,x,y)} + N_{c(i,j,t,x,y)} + N_{a(i,j,t,x,y)} \quad \textbf{(33)}$$

3.2.8. Recruitment of seedlings

Two seed dispersal modes are represented: the local dispersal (seeds from trees within the simulated area) and the external seed rain (seeds transported by wind, water or animals). Both dispersal modes fill a per patch seed bank.

In the BAF, it has been proved that seeds found down to 2,5 cm deep in the soil represented between 56,9% and 67,4% of all viable seeds (Baider et al., 2001). According to the same study, as the forest becomes older, a decrease in the density of viable seeds of herbaceous species, and then an increase in the density of viable seeds of woody plant species are observed. So it is assumed that there is a constant seed bank in the forest ground.

It is assumed that each tree of a cohort is able to produce a PFT dependent number of seeds $N_{rr(i)}$ if it reaches a determined diameter $D_{r(i)}$, leading to a production of $N_{r(i,t,x,y)}$seeds in a cohort:

$$N_{r(i,t,x,y)} = \begin{cases} 0 & if D_{(i,j,t,x,y)} < D_{r(i)} \\ N_{rr(i)} * N_{(i,j,t,x,y)} & if D_{(i,j,t,x,y)} \geq D_{r(i)} \end{cases} \quad \textbf{(34)}$$

The seeds are then dispersed in the patches around the mother tree cell. Dispersal agents are not differentiated; for instance, whether the seeds are spread out due to wind or animals.

Following Groeneveld et al. (2009), and Pütz et al. (2011), the seed dispersal is a function of a determined dispersal kernel, of the crown diameter $CD_{(i,j,t,x,y)}$ of the mother plant and of a PFT dependent dispersal distance *DIST*. The dispersal kernel is approximated by a Weibull distribution with a shape parameter of 2 and a scale parameter of $(DIST + \frac{CD_{(i,j,t,x,y)}}{2})^2$.

The probability that a seed is dispersed at a distance '*r*' from the mother plant is determined as:

$$f_{disp}(r) = \frac{2r}{(DIST + \frac{CD_{(i,j,t,x,y)}}{2})^2} e^{\frac{-2r}{(DIST + \frac{CD_{(i,j,t,x,y)}}{2})^2}} \quad \textbf{(35)}$$

The coordinates of the patch that receives the seed (see APPENDIX A - Seed dispersal function) are :

$$x_{seed} = x_{mother} + rsin(2\pi \frac{DIR}{360}) \quad \textbf{(36)}$$

$$y_{seed} = y_{mother} + rcos(2\pi \frac{DIR}{360})$$

Where (x_{mother}, y_{mother}) are the coordinates of the mother tree, *DIR* a number chosen randomly in a uniform distribution in the range of [0°, 360°] and '*r*' the distance from the mother tree.

Then, all the seeds received in a patch are added up and these seeds go to the seed bank of the cell. Next time step, seeds may be able to germinate and establish if the conditions allow it.

In table 4 the probabilities for a seed produced by a mother tree to reach the patches in the neighborhood from a mother tree in (3,3) are presented. For example, looking at the PFT1 table of table 4, a seed produced in the cell (3;3), has a probability p=0,0123 to stay in the same cell, and a probability p=0,0091 to arrive in the cell (5,1).

Table 4: Seed dispersal probability matrix
For a mother tree in (3,3) grey cell

PFT1

y \ x	1	2	3	4	5
1	0.0093	0.0100	0.0112	0.0114	0.0091
2	0.0096	0.0106	0.0109	0.0099	0.0113
3	0.0113	0.0119	0.0123	0.0114	0.0105
4	0.0091	0.0111	0.0104	0.0127	0.0118
5	0.0099	0.0103	0.0097	0.0090	0.0093

PFT2

y \ x	1	2	3	4	5
1	0.0080	0.0105	0.0103	0.0111	0.0081
2	0.0103	0.0114	0.0142	0.0098	0.0108
3	0.0105	0.0128	0.0124	0.0106	0.0111
4	0.0103	0.0111	0.0128	0.0121	0.0111
5	0.0089	0.0095	0.0111	0.0116	0.0086

PFT3

y \ x	1	2	3	4	5
1	0.0096	0.0109	0.0106	0.0117	0.0099
2	0.0096	0.0121	0.0123	0.0092	0.0095
3	0.0093	0.0115	0.0114	0.0101	0.0134
4	0.0111	0.0116	0.0116	0.0138	0.0091
5	0.0095	0.0096	0.0093	0.0106	0.0086

PFT4

y \ x	1	2	3	4	5
1	0.0124	0.0145	0.0177	0.0149	0.0134
2	0.0135	0.0197	0.0202	0.0204	0.0144
3	0.0157	0.0175	0.0224	0.0183	0.0162
4	0.0162	0.0203	0.0200	0.0197	0.0151
5	0.0121	0.0152	0.0156	0.0178	0.0132

PFT5

y \ x	1	2	3	4	5
1	0.0137	0.0142	0.0170	0.0173	0.0132
2	0.0135	0.0180	0.0199	0.0201	0.0159
3	0.0146	0.0206	0.0229	0.0193	0.0191
4	0.0137	0.0189	0.0207	0.0184	0.0153
5	0.0124	0.0173	0.0141	0.0174	0.0128

PFT6

y \ x	1	2	3	4	5
1	0.0151	0.0169	0.0157	0.0169	0.0131
2	0.0156	0.0209	0.0178	0.0188	0.0167
3	0.0163	0.0210	0.0213	0.0189	0.0149
4	0.0160	0.0188	0.0186	0.0173	0.0167
5	0.0125	0.0155	0.0169	0.0155	0.0120

PFT7

y \ x	1	2	3	4	5
1	0.0144	0.0207	0.0264	0.0235	0.0148
2	0.0228	0.0326	0.0413	0.0335	0.0253
3	0.0246	0.0395	0.0477	0.0384	0.0278
4	0.0250	0.0347	0.0417	0.0334	0.0254
5	0.0157	0.0197	0.0261	0.0217	0.0132

PFT8

y \ x	1	2	3	4	5
1	0.0156	0.0221	0.0278	0.0226	0.0124
2	0.0200	0.0384	0.0400	0.0363	0.0209
3	0.0235	0.0399	0.0484	0.0416	0.0251
4	0.0214	0.0350	0.0440	0.0348	0.0202
5	0.0153	0.0232	0.0269	0.0219	0.0151

PFT9

y \ x	1	2	3	4	5
1	0.0144	0.0238	0.0249	0.0212	0.0124
2	0.0207	0.0359	0.0402	0.0346	0.0224
3	0.0244	0.0425	0.0457	0.0436	0.0248
4	0.0208	0.0343	0.0390	0.0384	0.0247
5	0.0157	0.0206	0.0256	0.0207	0.0153

These matrices are calculated with the function presented in appendix A.

The seed pool is supplied by external seed rain $N_{S_{(i)}}$ and by the $N_{seed\_received_{(i,t,x,y)}}$ seeds produced by trees around received in the cell by seed dispersion. Each patch has its own seed pool.

The quantity of seeds in the seed pool depends on the remaining seeds from the previous time step and on the input of seeds, it is calculated as follow:

$$N_{pool_{(i,t,x,y)}} = N_{seed\_received_{(i,t,x,y)}} + N_{S_{(i)}} + N_{pool_{(i,t-1,x,y)}}$$

To obtain an input of seedlings, in other words, for a seed to germinate and establish, it's necessary to have:

- ✓ A free space for the crown of the seedlings at forest floor
- ✓ A minimum light intensity $Imin_{(i)}$ at forest floor:

$$Imin_{(i)} \leq I_{(1,t,x,y)} \quad \textbf{(37)}$$

If the conditions are met at a particular time step, a new cohort $N_{(i,1,t,x,y)}$ of trees from the seed bank appears with a corresponding biomass $Bs_{(i,1,t,x,y)}$ [t_{ODM}/ha]

$$N_{(i,1,t,x,y)} = \begin{matrix} Nseedling_{(i,t,x,y)} if I_{(1,t,x,y)} > Imin_{(i)} \; and \; CCA_{(1,t,x,y)} < 1 \\ 0 \qquad\qquad\qquad\qquad if I_{(1,t,x,y)} \leq Imin_{(i)} \; or \; CCA_{(1,t,x,y)} \geq 1 \end{matrix} \quad \textbf{(38)}$$

With $Nseedling_{(i,t,x,y)}$ the quantity of new trees at forest floor.

The remaining seeds of the seed bank have a probability $m_{seed\ (i)}$ PFT dependant to die during the time step.

3.2.9. Changes in biomass.

The biomass of a tree at *t+1* depends on its biomass at *t* plus the photoproduction $PB_{(i,j,t,x,y)}$ and less the losses $R_{(i,j,t,x,y)}$ due to respiration and dead wood, dead leaves:

$$Bt_{(i,j,t+1,x,y)} = Bt_{(i,j,t,x,y)} + PB_{(i,j,t,x,y)} - R_{(i,j,t,x,y)} \quad \textbf{(39)}$$

3.2.10. Changes in number of trees.

The number of trees at *t+1* depends on the number of trees at *t* and the number of trees that died during the time step. The equation (40) shows the changes in number of trees throughout time:

$$N_{(i,j,t+1,x,y)} = N_{(i,j,t,x,y)} - Ndead_{(i,j,t,x,y)} \quad \textbf{(40)}$$

With $Ndead_{(i,j,t,x,y)}$ calculated in the equation (33).

Table 5: Variables of the model

Variable	Description	Unit
B	Biomass of a cohort	[t_{ODM}]
Bt	Biomass per tree	[t_{ODM}]
CA	Crown projection area of a single tree	[m^2]
CCA	Cumulative crown area of all trees	[m^2]
CD	Crown diameter of a single tree	[m]
CL	Crown length of a single tree	[m]
D	Diameter of a tree	[m]
f	Form factor	[-]
H	Height of a tree	[m]
I	Solar radiation on tree crown	[W/m^2]
L	Total leaf area of one tree	[m^2]
LAI	Individual leaf area index of a tree	[-]
LAI_layer	Contribution of a tree's leaf area to the layer	[m^2]
LAI_pb	Patch-based leaf area index	[-]
Layermax	Maximum layer occupied by the crown	[-]
Layermin	Minimum layer occupied by the crown	[-]
M_a	Regular mortality	[-]
M_d	Diameter dependent mortality	[-]
M_{dam}	Probability to die because of a fallen tree	[-]
N	Number of trees	[-]
N_a	Number of tree dying due to basic mortality	[-]
N_c	Number of tree dying due to crowding	[-]
NBlayer	Number of layer that a crown of a tree occupies	[-]
N_{dead}	Total number of trees dying per step	[-]
$N_{deadbyfallentree}$	Number of tree dying due to fallen trees	[-]
N_{fall}	Number of fallen trees	[-]
N_{pool}	Seed quantity in the seed pool	[$patch^{-1}$]
N_{seed}	Seed production per tree	[$year^{-1}$]
$N_{seedling}$	Quantity of new seedlings at forest floor	[-]

$\mathbf{N_{seed\_received}}$	Quantity of seeds received in a patch	[-]
P	Interim gross photosynthetic rate of a tree	[µmol(CO_2)/m^2/s]
PB	Biomass production by photosynthesis	[t_{ODM}]
R	Biomass looses from respiration and dead wood looses	[-]
$\mathbf{R_c}$	Crowding reduction factor	[-]

Table 6: Parameters of the model

Symbol	Description	PFT1	PFT2	PFT3	PFT4	PFT5	PFT6	PFT7	PFT8	PFT9	Unit
A_patch	Area of a cell					400					[m²]
alpha (α)	Light use efficiency	0,036	0,036	0,036	0,049	0,049	0,049	0,05	0,05	0,05	[-]
c	Crown depth fraction					0,2					[-]
cd	Parameter of diameter crown-diameter relationship					0,25					[-]
codm	parameter for conversion in organic dry matter					0,63					$[g_{(ODM)}/g_{(CO2)}]$
Δh	Width of layers of aboveground vertical space discretization					0,5					[m]
D_{fall}	Minimum diameter of falling trees					0,1					[m]
D_{mort}	Diameter up to which mortality is increased					0,1					[m]
D_r	Minimum stem diameter of mother trees for producing seeds	0,135	0,135	0,2	0,135	0,135	0,2	0,135	0,135	0,2	[m]

Day	Number of day in a time step					365					[day]
h_0	Height calculation parameter	1,3	1,4	1,3	1,3	1,4	1,3	1,3	1,4	1,3	[cm/m]
h_1	Height calculation parameter	17	29	38	17	29	38	17	29	38	[m]
H_sun	Hour of sun per day					12					[h/day]
f_0	Form factor parameter					2,5					[-]
f_1	Form factor parameter					-1,4					[-]
f_2	Form factor parameter					0,04					[-]
I_{min}	Minimum light intensity (% of full light above canopy) required for establishment of seeds)	0,2	0,2	0,2	0,08	0,08	0,08	0,01	0,01	0,01	[-]
I_0	Average irradiance above canopy					600					[W/m²]
k	Light extinction coefficient					0,6					[m^2_{ground}/m^2_{leaf}]
l_0	Total leaf area of a tree parameter					3,2					[-]
l_1	Total leaf area of a tree parameter					0,07					[-]

l_2	Total leaf area of a tree parameter					-0,0004					[-]
LAI_{max}	Upper threshold of LAI					4					[-]
m	Transmission coefficient of leaves					0,1					[-]
m_{seed}	Mortality rate of seeds remaining in the seed pool	0,1	0,1	0,1	0,5	0,5	0,5	1	1	1	[-]
M_b	Regular mortality	0,1	0,1	0,1	0,06	0,04	0,05	0,03	0,02	0,02	[-]
M_{max}	Maximum mortality of small trees					0,1					[-]
Nb_layer	Number of layer in the vertical discretisation					64					[-]
Nb_PFT	Number of PFT					9					[-]
N_{rr}	Local dispersal per mother trees	100	100	100	34	34	34	22	22	22	[-]
N_s	External seed rain	350	350	350	188	188	188	76	76	76	[-]
Nx	Number of column in the grid					10					[-]
Ny	Number of row in the grid					10					[-]

P_{fall}	Probability of dying trees to fall	0,4									[-]
P_{max}	Maximum rate of photosynthesis	19	19	19	12	12	12	7	7	7	[µmol(CO_2)/m²/s]
r_g	Parameter of growth respiration	0,4									[-]
r_l	Parameter of maintenance respiration	0,08	0,08	0,08	0,02	0,02	0,02	0,01	0,01	0,01	[-]
rho (σ)	wood density	0,37	0,37	0,37	0,55	0,55	0,55	0,75	0,75	0,75	[t_{ODM}/m^3]
TR	Stem wood fraction	0,825									[-]
Tsim	Simulation time	500 or 1000									[year]

4. SIMULATION RESULTS

In this part, first a base case will be developed. The base case represents the regular plain forest of the PESM without disturbance or anthropogenic activities. The results will be compared to existing studies to validate the model.

Then, clearings will be applied on the forest, and the base case will be used to compare and analyze the results of the scenario.

Finally, regeneration scenarios will be studied in the light of base case results.

4.1. **Base case**

The simulation is made using the model described in chapter 3 with the following assumptions:

- ✓ At t=0, there is no tree in the field.
- ✓ Patch size is set to 4 ha in periodic boundary conditions.
- ✓ Simulation time is set to 1000 years in order to see clearly when the forest reaches climax. The hypothesis that the forest reaches climax in less than 1000 years in this area is formulated.
- ✓ There are no edge effects, a continuous forest is simulated.
- ✓ There are no disturbances during the simulation time other than gap creation due to falling trees (i.e. no fire, no clearing, no landslide).
- ✓ There are no variations in the external environmental conditions such as solar radiation or number of hour of sun per day. Annual average values are used.
- ✓ The mathematical model representing the natural processes of the growing trees remain unchanged during the simulation (trees do not develop new strategy throughout simulation time).

The mathematical model was simulated using MATLAB 2010.

4.1.1. Biomass of the BAF

As shown in figure 17, the above ground biomass is increasing with forest age. Pioneer species biomass (PFT1, PFT2 and PFT3) increases rapidly to 65 t_{ODM}/ha and then decrease quickly. The intermediate shade tolerant species biomass (PFT4, PFT5 and PFT6) rises to a maximum; around 170 t_{ODM}/ha, and then decreases to around 90 t_{ODM}/ha. Finally the shade tolerant species biomass (PFT7, PFT8, PFT9) progresses until a plateau is reached between 160 and 180 t_{ODM}/ha. As expected, first the pioneer species appear, then the intermediate shade tolerant species and finally the shade tolerant species.

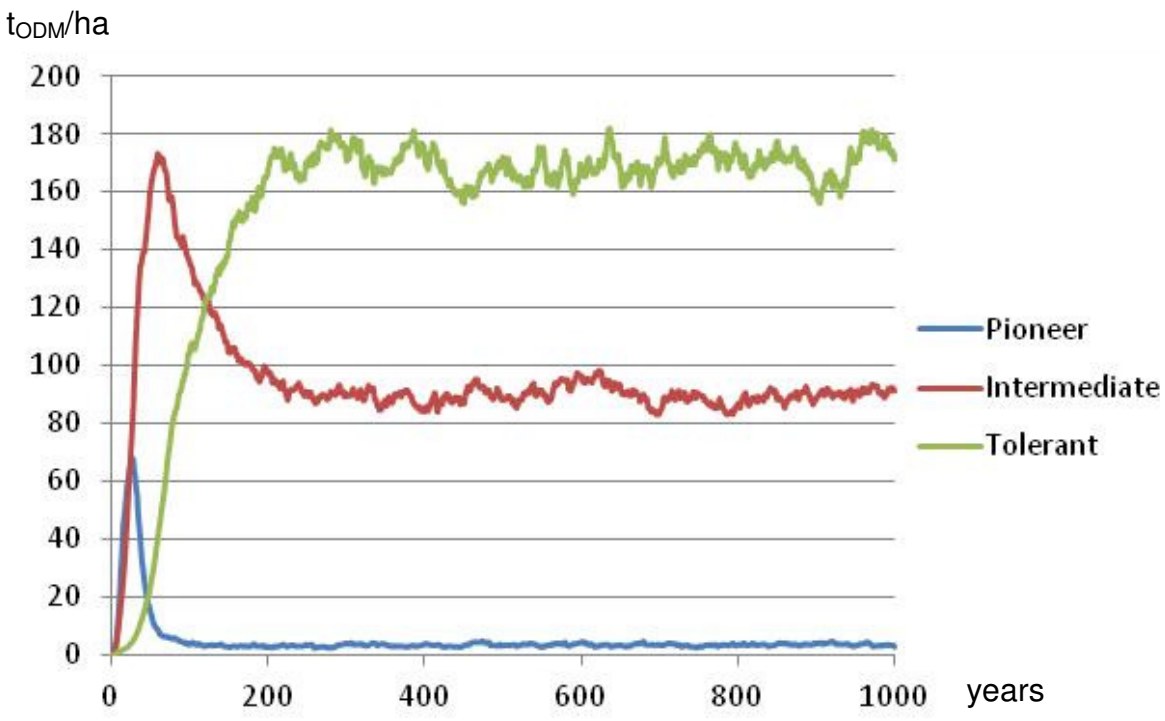

Figure 17: Base case biomass per shade tolerance

Figure 18 shows the relative group biomass in function of the forest age. In very young forest, pioneers represent more than 60% of the total biomass. After 50 years 80% of the biomass of the forest is due to intermediate shade tolerant trees. After 500 years, shade tolerant trees represent 66% of the forest total biomass, intermediate shade tolerant 33% and pioneers 1%.

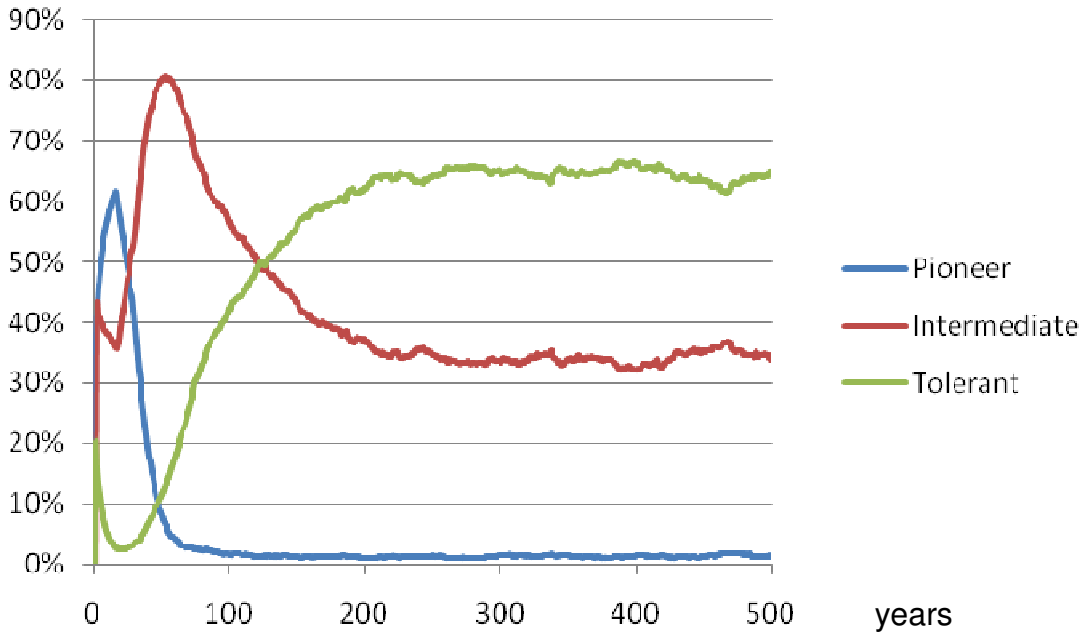

Figure 18: Relative group biomass in function of the forest age

Then, in figure 19 the detailed evolution of the biomass per PFT is exposed. PFT9 species (i.e. shade tolerant trees with a 32m maximum height) have a higher biomass than any other groups.

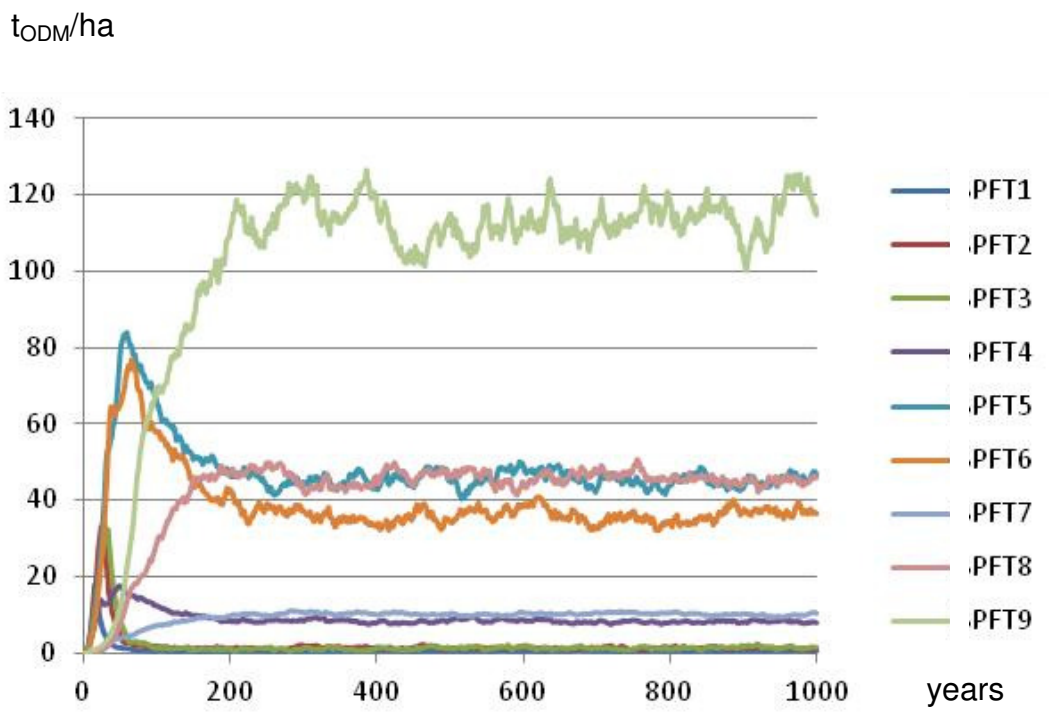

Figure 19: Base case biomass per PFT

Figure 20 presents the evolution of the number of trees per shade tolerance group. As exposed, first pioneer trees appear then intermediate shade tolerant trees and finally shade tolerant trees. It can be observed a slightly diminution of shade tolerant number of trees per hectare between t=16 and 22 years approximately. This phenomenon is the result of a constant number of new seedlings at each time step and a higher mortality due to crowding and fallen pioneer trees. This trend stops when shade tolerant trees start to produce seeds which increase the quantity of seedlings. Then the ratio of new seedlings - tree mortality results in an augmentation of the number of trees.

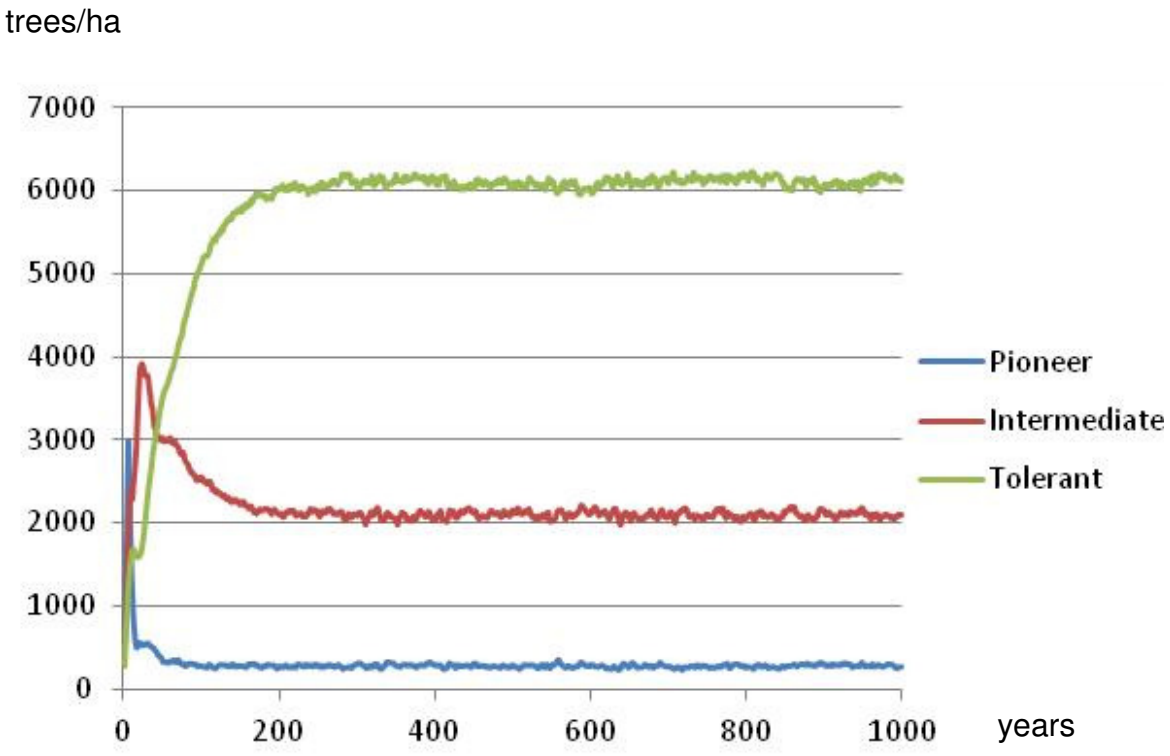

Figure 20: Base case number of trees per shade tolerance

Figure 21 shows the relative group abundance in function of the forest age. In a young forest pioneer trees represent almost half of the trees. Then after 25 years intermediate shade tolerant trees represent more than 60% of the trees. At climax stage, the model suggests that 72% of the trees are shade tolerant, 25% are intermediate shade tolerants and 3% are pioneers.

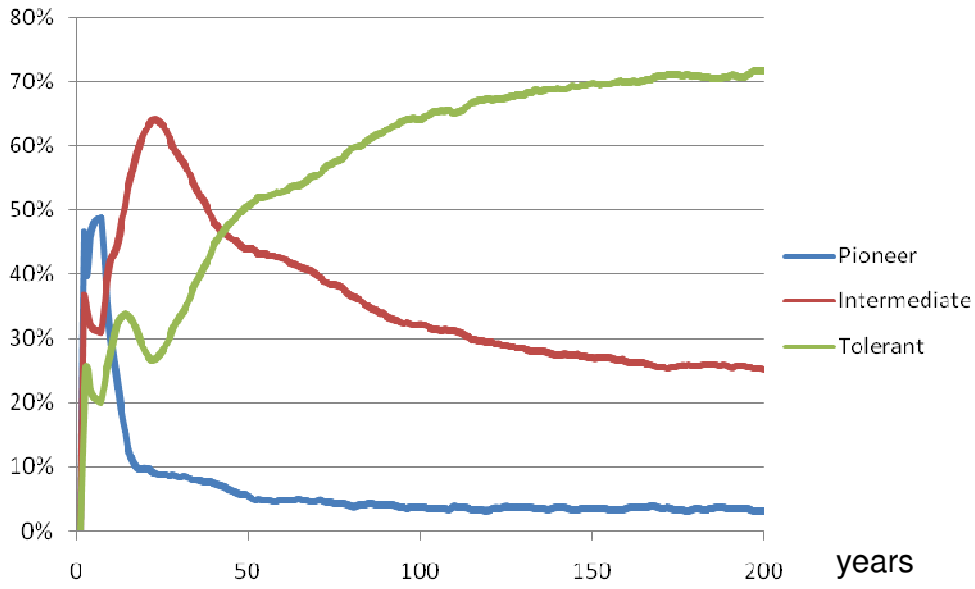

Figure 21: Relative group abundance in function of the forest age

Figure 22 presents the evolution of the base case number of trees per PFT. The figure shows that trees of the same shade tolerance group have the same dynamic, i.e., pioneers (PFT1, PFT2 and PFT3) have a similar dynamic, this is true for the intermediate shade tolerant species as well (PFT4, PFT5 and PFT6) and also for the shade tolerant species (PFT7, PFT8 and PFT9).

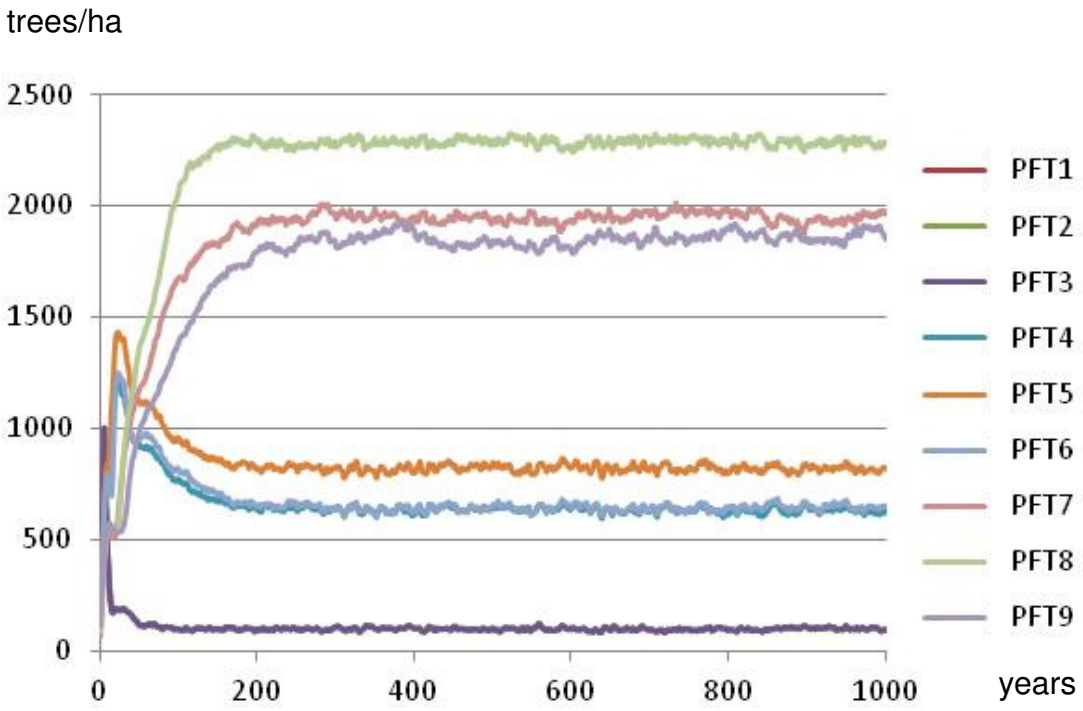

Figure 22: Evolution of the base case number of trees per PFT

4.1.2. Validation of the model

In the light of these results, the hypothesis is made that after 500 years the forest has reached climax. Therefore to estimate the climax biomass of each PFT, the average biomass values (in t_{ODM}/ha) of the last 500 years of the simulation (time= 500 to 1000 years) are calculated.

Simulated base case leads to a total biomass for stem diameters larger than 1cm of approximately 263 ± 5,8 t_{ODM}/ha, i.e. the average biomass of the last 500 years is 263 t_{ODM}/ha and the standard deviation is 5,88 t_{ODM}/ha.

In detail, at climax stage, the forest has the highest quantity of biomass mainly due to shade tolerant trees (169 t_{ODM}/ha). The intermediate shade tolerant species contribute with 90 t_{ODM}/ha and the pioneer species only contribute a small amount of the forest biomass with 3,6 t_{ODM}/ha.

With the same method, an average of the last 500 years, the total stem number at climax is 8487 ± 56 trees/ha. Of all these trees 6100 are shade tolerant, 2101 are intermediate shade tolerant and 286 are pioneer.

Most of the inventories for tropical forest do not include small trees (steam diameter below 5 cm). Consequently to compare the results of the simulation with existing data, it is important to consider only trees with a stem diameter larger than 5 cm.

From 2006 to 2007, 4 one-hectare permanent plots in the PESM were defined along an altitudinal transect to evaluate forest diversity and ecosystem function variation (Alves et al., 2010). All trees with a stem diameter higher than 4,8 cm were tagged. Alves et al. (2010) used an empirical model to predict the density of trees in function of height and diameters. They found a value of 1488 ± 60 individuals.

Using our mathematical model and taking into account only trees with a stem diameter higher than 4,8 cm, the stem number goes to 1563 ± 52 trees/ha. The model shows a number of trees 5% higher than the previous inventory.

Alves et al. (2010), from the same permanent plot and for a stem diameter larger than 4,8 cm, found a biomass of 247,7 ± 14,8 t_{ODM}/ha. Our mathematical model indicates a biomass of 252,1± 6,5 t_{ODM}/ha, i.e. a quantity of biomass 2% higher than the simulation of the Alves et al. (2010) empirical model.

With their mathematical model, Putz et al. (2011) in the Atlantic Plateau between the municipalities of Cotia and Ibaiúna, found a total stem number and biomass at a diameter higher than 5 cm approximately 1050 ± 120 individuals and 256,1 ± 10,2 t_{ODM}/ha. For trees with a stem diameter higher than 1cm, their simulation shows 11440 ± 42 trees/ha and for biomass 254 ± 2,2 t_{ODM}/ha. The total biomass calculated by our model was similar (263 ± 5,8 t_{ODM}). However the number of trees was different. This could be explained by the different model approaches used.

Vieira et al. (2008) compared five empirical models built for other forest, using data from the same four permanent plots in the Atlantic forest (see figure 23).

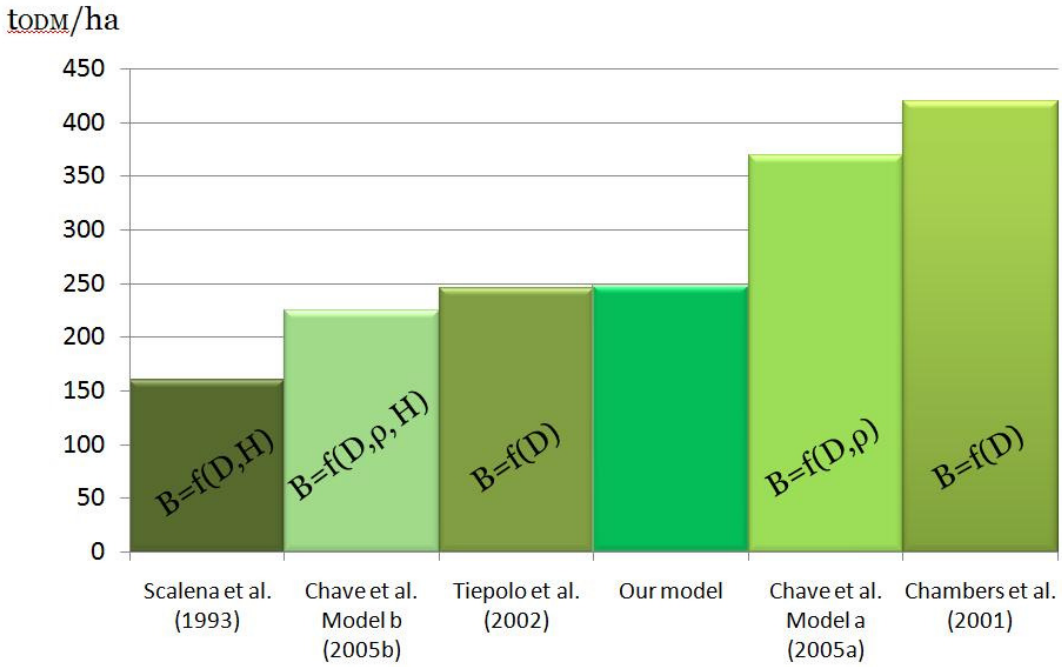

Sources: (Vieira et al., 2008)
With B for biomass, D for diameter, H for height and ρ for wood density

Figure 23: Above ground estimated biomass for BAF

They observed considerable variation among biomass. The biomass was estimated according to empirical models: using one variable, the diameter, (Chambers et al., 2001; Tiepolo et al., 2002); two variables, diameter and wood density (Chave et al., 2005) or diameter and height (Scatena et al., 1993); and finally three variables, diameter, wood density and height (Chave et al., 2005).

The model developed by Chambers et al. (2001) and model *a* from Chave et al. (2005) both give higher biomass values compared to the model from similar Atlantic Forest (Tiepolo et al., 2002). Biomass values found using model *b* of Chave et al. (2005) are similar to the site-specific model of Tiepolo et al. (2002) and with biomass values measured by Tiepolo et al. (2002) for two other areas in the Southeast Atlantic Forest (Vieira et al., 2008). By contrast, the model of Scatena et al. (1993) shows the lowest biomass compared to all of the other

models, maybe because it was developed for Puerto Rican submontane forests that suffer frequent hurricanes (Vieira et al., 2008).

According to Vieira et al. (2008) observations in the BAF suggest that model *b* of Chave el al. (2005) can be confidently used to estimate biomass. This model shows around 225 t_{ODM}/ha (±10) in the PESM, which is 10% less than in our study.

The model developed by Putz et al. (2011) is a phenomenological model, i.e. it describes the succession of the phenomena. On the other side, the study of Alves et al. (2010) is based on empirical observations.

Contrary to our model, models analyzed in Vieira et al. (2008) show a static mature forest, there is no biomass or number of trees evolutions among time. In addition, the forest is represented as a whole unlike our study where trees are grouped as Plant Functional Type. Moreover, another difference with our model is that Vieira et al. (2008) do not analyzed the dynamic of the forest along time.

In conclusion, compared to Putz et al. (2011), it can be said that using a different model approach, a similar quantity of biomass is found.

The biomass distribution for very small trees (diameter smaller than 5cm) and non-woody components is poorly known. Lianas, palm, tree ferns, bamboo and epiphytes can represent more than 10% of total biomass in the BAF (Vieira et al., 2008).

Our model does not take into account non-woody components. Nevertheless, comparing with other studies, our model gives a good estimation of biomass.

The simulation presented here can be view as an "ideal case"; according to the model hypothesis (see 4.1)

4.1.3. Climax state

To determine when the BAF attains climax, we focus on the data from 0 to 500 years of figure 19, and the curves are approximated with 6^{th} order polynomial trendlines. A good approximation of the time to reach climax is then the intersection point between the trendline and the biomass value at climax.

See table 7 for the equations, the R^2 and the time for PFT4 to 9 to reach climax. The time to reach climax for the pioneer species was not calculated as they are almost inexistent at climax state.

The coefficient of determination R^2, indicates how well a model fits fit data. With values from 0,9177 and 0,993 the polynomial trendlines approximate satisfactorily the simulation data points.

From table 7, it can be concluded that around 240 years are needed for the BAF to reach the climax stage.

No experimental information is available to confirm these values. The other studies available are for regeneration, and do not start with a whole matrix of non forested area.

Table 7: Trendline equations of the biomass variation for the control case
Calculated from 0 to 500 years

	Time to reach climax (years)	Trendline equation	R^2
PFT4	210	$y = -5E^{-13}x^6 + 7E^{-10}x5 - 4E^{-07}x^4 + 1E^{-4}x^3 - 0{,}0147x^2 + 0{,}8829x - 2{,}8777$	0,9584
PFT5	230	$y = -1E^{-12}x^6 + 2E^{-09}x^5 - 1E\text{-}06x^4 + 0{,}0003x^3 - 0{,}0532x^2 + 3{,}8747x - 27{,}814$	0,921
PFT6	220	$y = -7E^{-13}x^6 + 1E\text{-}^{09}x^5 - 8E^{-07}x^4 + 0{,}0003x^3 - 0{,}0475x^2 + 3{,}5227x - 25{,}426$	0,9177
PFT7	220	$y = 1E\text{-}^{13}x^6 - 1E^{-10}x^5 + 6E^{-08}x^4 - 1E^{-05}x^3 + 0{,}0009x^2 + 0{,}0599x - 0{,}4919$	0,993
PFT8	240	$y = 4E^{-13}x^6 - 6E^{-10}x^5 + 3E^{-07}x^4 - 1E^{-04}x^3 + 0{,}0123x^2 - 0{,}2801x + 1{,}4245$	0,9944
PFT9	230	$y = 2E^{-12}x^6 - 3E^{-09}x^5 + 1E^{-06}x^4 - 0{,}0003x^3 + 0{,}0366x^2 - 0{,}8863x + 4{,}1313$	0,9896

4.1.4. Sensitivity analysis of the model

The time step integration of the differential equations system is then set to 6 month in order to see if the climax is different and if there are numerical errors. Simulation time is set to 300 years because according to our results the climax is reached after approximately 240 years, and reducing the time step is more time consuming.

The dynamic of the forest during the first 300 years shows no differences with a time step of 6 month or 1 year.

As explained before, the maximum Leaf Area Index (LAI_{max}) was fixed to 4, as an average of Groeneveld et al. (2009) and Paula and Lemos Filho (2001) values. Using the hypothesis of section 4.1, LAI_{max} is set to 3 (Groeneveld et al. (2009) value), then to 3,5, next to 4,5 and finally to 5 (Lemos Filho (2001) value) afterwards.

Figure 24, figure 25 and figure 26 show the evolution along time of the quantity of biomass per hectare as a function of the LAI_{max}. It can be seen that the results are LAI_{max} value dependent.

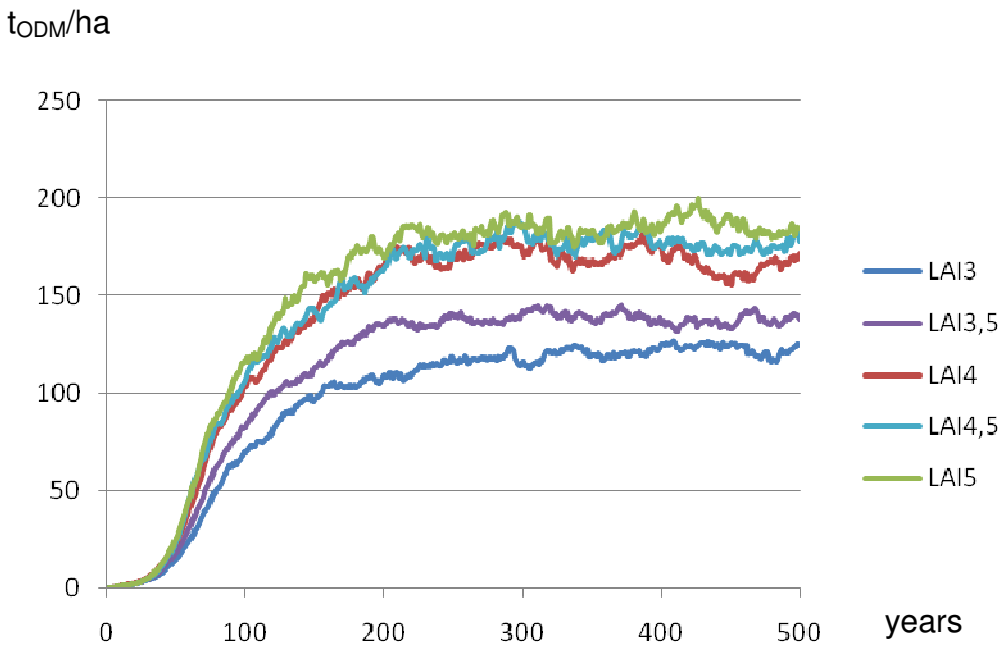

Figure 24: Quantity of biomass of shade tolerant trees per hectare in function of the parameter LAI_{max}.
The navy blue line represents the simulation result for LAI_{max} set to 3, the purple line for LAI_{max} set to 3,5 then the red line for LAI_{max} set to 4, the light blue line for LAI_{max} set to 4,5 and the green line for LAI_{max} set to 5.

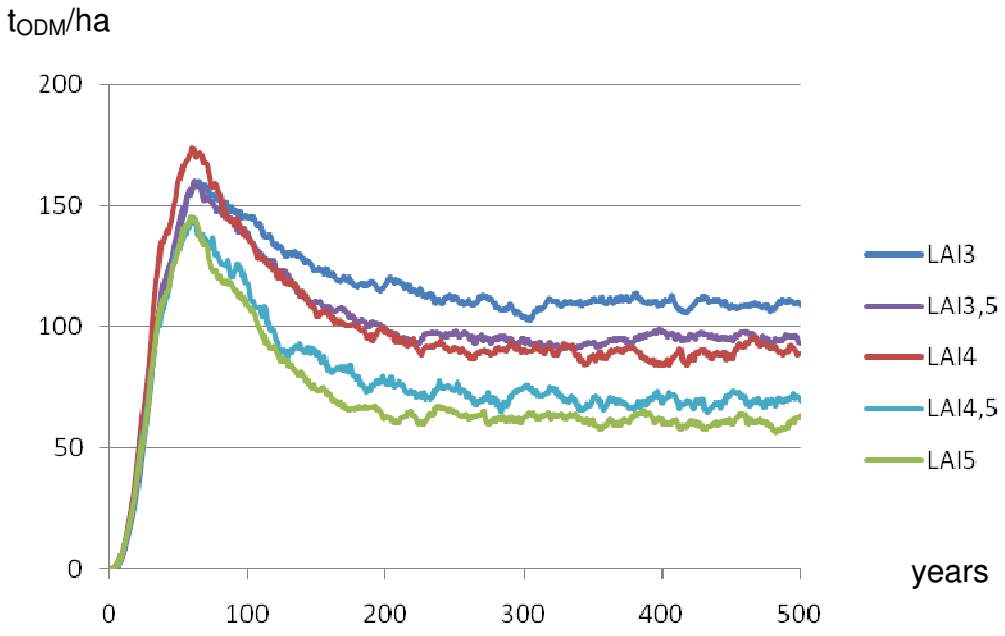

Figure 25: Quantity of biomass of intermediate shade tolerant trees per hectare in function of the parameter LAI_{max}.
The navy blue line represents the simulation result for LAI_{max} set to 3, the purple line for LAI_{max} set to 3,5 then the red line for LAI_{max} set to 4, the light blue line for LAI_{max} set to 4,5 and the green line for LAI_{max} set to 5.

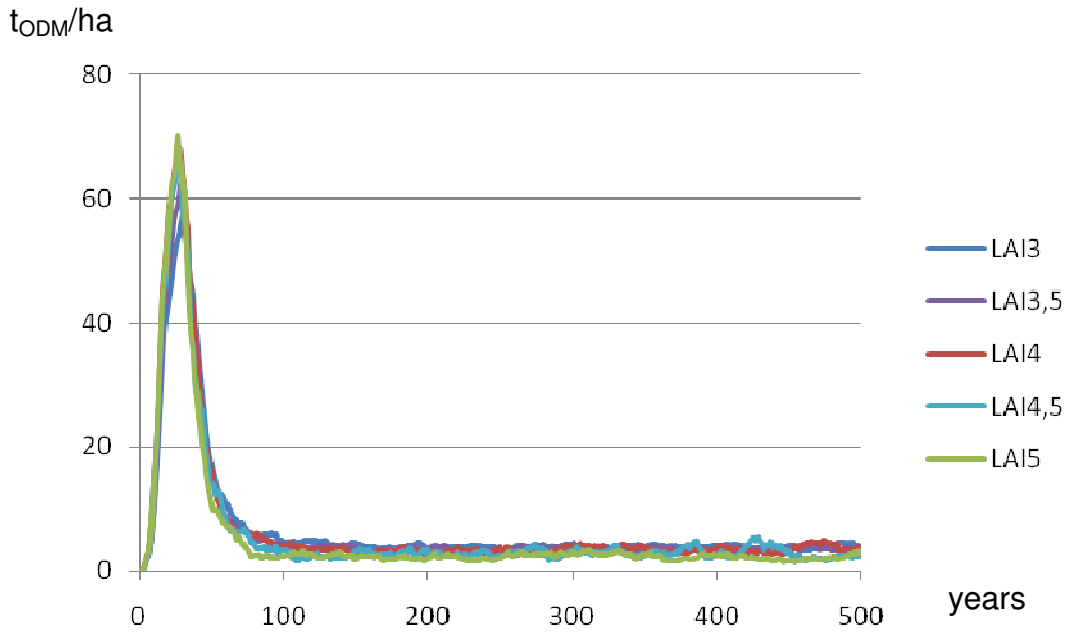

Figure 26: Quantity of biomass of shade intolerant trees per hectare in function of the parameter LAI_{max}.
The navy blue line represents the simulation result for LAI_{max} set to 3, the purple line for LAI_{max} set to 3,5 then the red line for LAI_{max} set to 4, the light blue line for LAI_{max} set to 4,5 and the green line for LAI_{max} set to 5.

To compare the value at climax, an average of the value from 300 to 500 is calculated. Table 8 compares the quantity of biomass at climax per shade tolerance and per LAI_{max} relatively to LAI_{max} 4 values

Table 8: Comparison of biomass quantity in function of the LAI_{max} parameter relative to LAI_{max} value 4

	Shade intolerant	Intermediate shade tolerant	Shade tolerant
LAImax 3	+10%	+23%	- 28%
LAImax 3,5	+4%	+6%	- 18%
LAImax 4,5	-17%	-22%	+5%
LAImax 5	- 36%	- 32%	+10%

A smaller LAI_{max} value, compared to LAI_{max}=4, leads to an increase of shade intolerant and intermediate shade tolerant biomass, and a decrease of shade tolerant biomass. On the contrary, a higher LAI_{max} value, compared to LAI_{max}=4,

leads to a decrease of shade intolerant and intermediate shade tolerant biomass and an increase of shade tolerant biomass.

Figure 27, figure 28 and figure 29 show the evolution along time of the quantity of number of trees per hectare in function of the LAI_{max}. It can be observed that the results are LAI_{max} value dependent

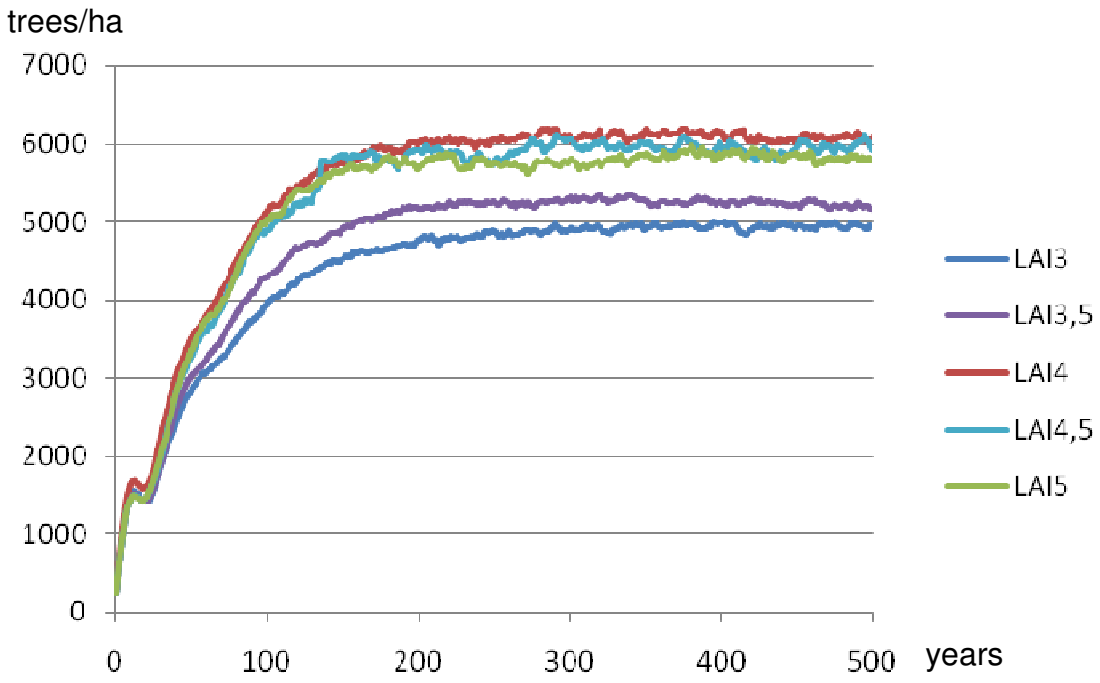

Figure 27: Number of shade tolerant trees per hectare in function of the parameter LAI_{max}
The navy blue line represents the simulation result for LAImax set to 3, the purple line for LAImax set to 3,5 then the red line for LAImax set to 4, the light blue line for LAImax set to 4,5 and the green line for LAImax set to 5.

Comparing figure 24 and figure 27, it is interesting to see that with LAI_{max} value set to 5 and 4,5 there are a little less shade tolerant trees (comparatively to LAI_{max} value set to 4) in the forest but there is more biomass per hectare. Indeed, with a LAI_{max} value set to 5 or 4,5 shade tolerant trees are a little larger, so the biomass per tree is higher than for LAI_{max} value set to 4. As the trees are larger, the space competition is stronger, resulting in a diminution of the number of trees.

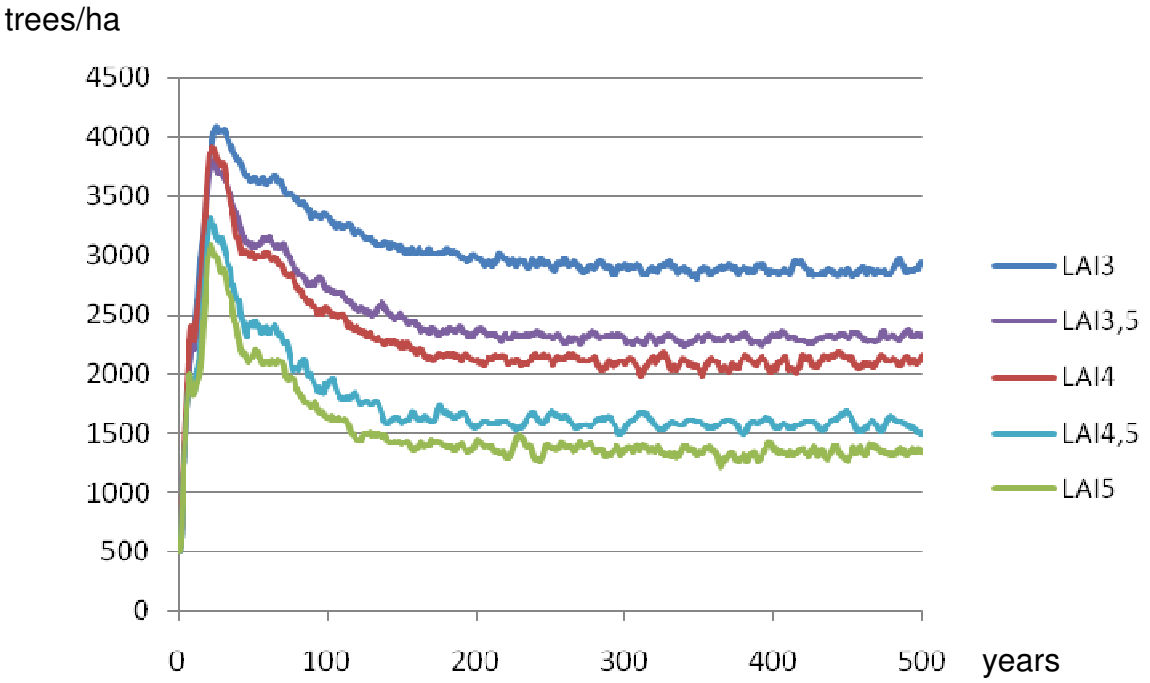

Figure 28: Number of Intermediate shade tolerant trees per hectare.
The navy blue line represents the simulation result for LAImax set to 3, the purple line for LAImax set to 3,5 then the red line for LAImax set to 4, the light blue line for LAImax set to 4,5 and the green line for LAImax set to 5.

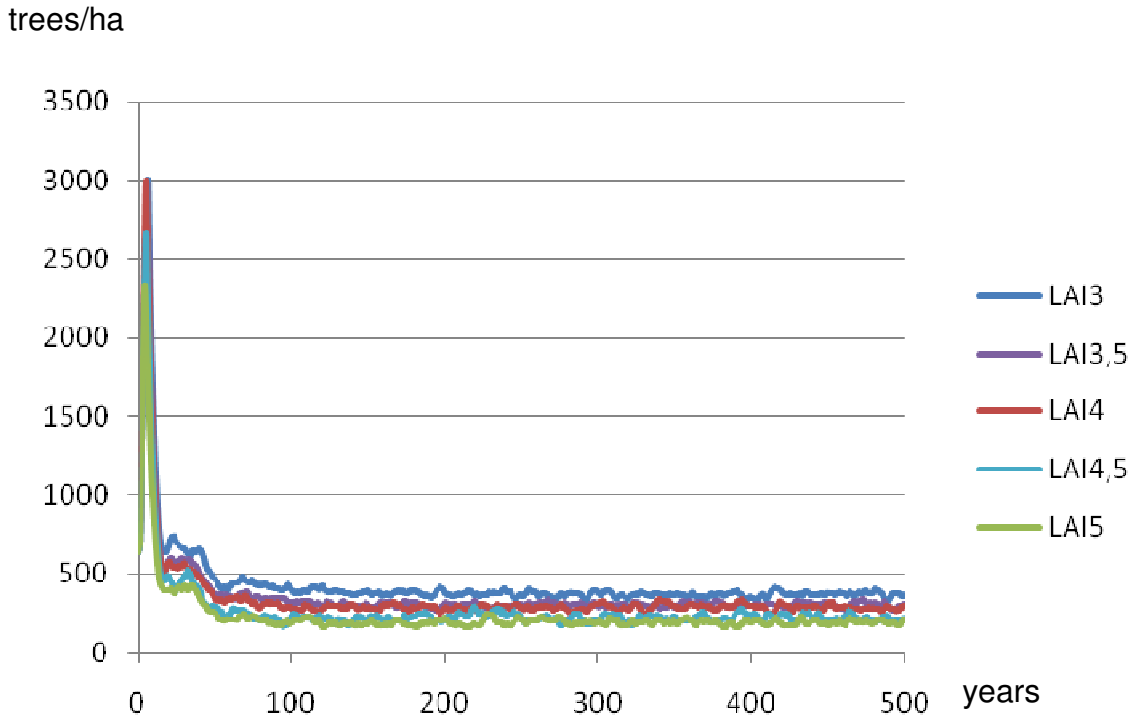

Figure 29: Number of shade intolerant trees per hectare.
The navy blue line represents the simulation result for LAImax set to 3, the purple line for LAImax set to 3,5 then the red line for LAImax set to 4, the light blue line for LAImax set to 4,5 and the green line for LAImax set to 5.

Table 9: Comparison of number of trees in function of the LAI_{max} parameter relative to LAI_{max} value 4

LAI_{max}	Shade intolerant	Intermediate shade tolerant	Shade tolerant
LAI_{max} 3	+27%	+37%	- 19%
LAI_{max} 3,5	+5%	+10%	-14%
LAI_{max} 4,5	-24%	-25%	-2%
LAI_{max} 5	- 34%	- 36%	- 4%

According to table 9, a LAI_{max} smaller than 4 leads to an increase of shade intolerant and intermediate shade tolerant number of trees and a decrease of shade tolerant number of trees. On the contrary, a higher value leads to a small decrease of all the trees of the forest comparing to results with a LAI_{max} value set to 4.

So the LAI, defined as the one sided green leaf area per unit ground area in broadleaf canopies (Scurlock et al., 2001), is a key parameter for modeling forest. A small value fosters shade intolerant species, and a high value is favorable to shade tolerant species. According to results from other studies, a LAI_{max} value set to 4 represents better the dynamic of the BAF.

4.2. Edge effects of different clearing patterns

As seen in the introduction, the BAF suffered extremely from deforestation.

According to Murcia (1995), there are three types of edge effects on the forest. First some changes in the environmental conditions appear at the edge; second, some changes in the abundance and distribution of species due to the new environmental conditions and species physiological tolerances to these conditions occur. Finally, these alterations imply modifications in species interactions, biotic pollination and seed dispersal.

When edges are created, forest experiments a fast and strong proliferation of pioneer trees along the edges triggered by elevated light availability (Tabarelli et al., 2008). This augmentation of pioneer species is done at the expenses of the old growth species, which aggravates the forest biomass collapse due to the increased mortality of large trees near the forest edges (Nascimento and Laurance, 2004)

Here, the impact of different patterns of non forested areas on the forest growth is simulated. 4 different shapes of 3600m^2 non forested area each are considered (9 cells).

The simulation is made using the model described in chapter 3, and with the following assumptions:

- ✓ At t=0, there is no tree in the forest.
- ✓ Patch size is set to 4 ha in periodic boundary conditions.
- ✓ Simulation time is set to 500 years.
- ✓ There is no edge effect from t=0 to 200 years.
- ✓ At t=200 years definitive clearings following one of the four patterns described in figure 30 are implemented.
- ✓ From t=200 years to the end of the simulation an edge effect is applied around the clearing as described in section 3.2.7.

- ✓ There are no variations in the external environmental conditions such as solar radiation or number of hour of sun per day since average values were adopted.
- ✓ The mathematical equations representing the natural processes of the growing trees remain unchanged during the simulation (trees do not develop new strategy throughout simulation time).

The mathematical model was simulated using MATLAB 2010.

4.2.1. The different clearing scenarios

Natural disturbances and anthropogenic activities combine to create richness in spatial pattern clearing. Figure 30 shows four possible patterns used in this study and it is expected that the response of the forest will vary with the type of pattern.

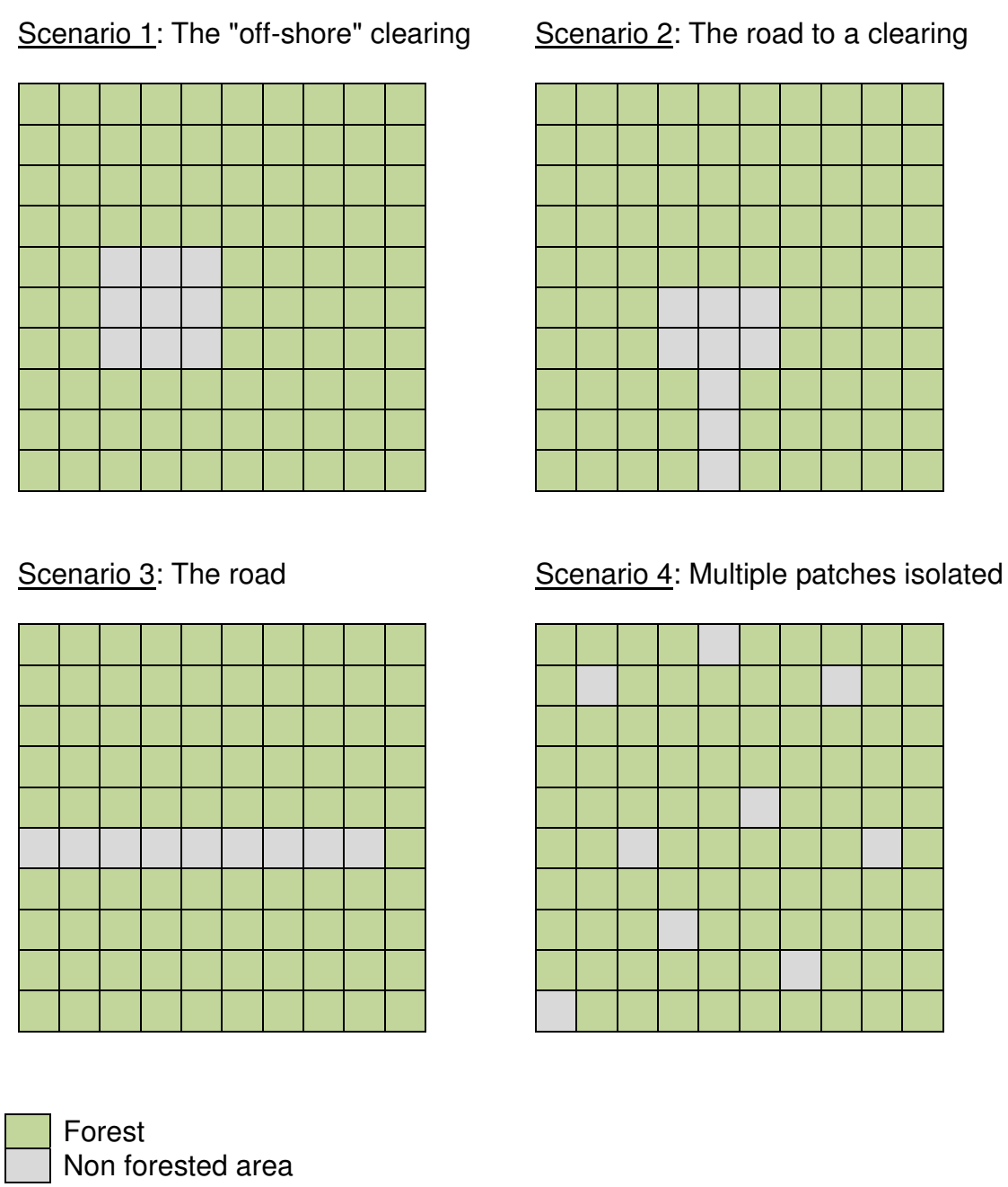

Figure 30: The different clearing scenarios

A common way to create a field in the depths of the forest is first to clear a road to the site, allowing access to equipment and personnel where it is needed. Nevertheless, roads contribute to deforestation; they cause direct damage to the forest, but they also make isolated regions accessible, thereby opening up previously primary forest to the possibilities of uncontrolled logging and hunting activities.

The scenario 1 tends to represent what is called “offshore-inland” by analogy to offshore platforms used to extract oil and gas from the oceans. The idea is to assure a development with minimal impact on the forest and on indigenous dwellers (Babbitt, 2015).

By contrast, scenario 2 represents the traditional way to establish a field in the forest: a road leading to an extraction center, cattle ranching projects or even to a village. This is the common way of forest colonization (Finer et al., 2015).

Scenario 3 aims to represent the impact of roads construction. Government programs to connect populations and areas of production, and private sector expansion for extraction of natural resources are two major reasons of road network development (Brandão and Souza, 2006; Perz et al., 2007). The construction of new roads increases the access to extractive industries and colonizers to the area, who further expand the road network by creating unofficial roads to transport their products. For example, in Amazon forest, Ahmed et al. (2013) found that on average, 17 000 km of new roads are added every year to the Brazilian Amazon road network.

Finally, scenario 4 represents an "anarchic" colonization of the forest with small clearings in a lot of places. This kind of forest fragmentation is more visible near cities. The inhabitants build their homes, cut down trees for construction, small-scale agriculture or small cattle ranch.

Keeping in mind that the major impact of a clearing on the forest trees is the environmental modifications associated to the creation of an edge, the different consequences of these different clearing patterns will be studied.

4.2.2. Impacts on shade tolerant trees

In figure 31 it can be observed that the creation of a clearing (at t=200 years) impacts deeply the shade tolerant tree biomass quantity. It can also be seen that the clearing shape has an influence.

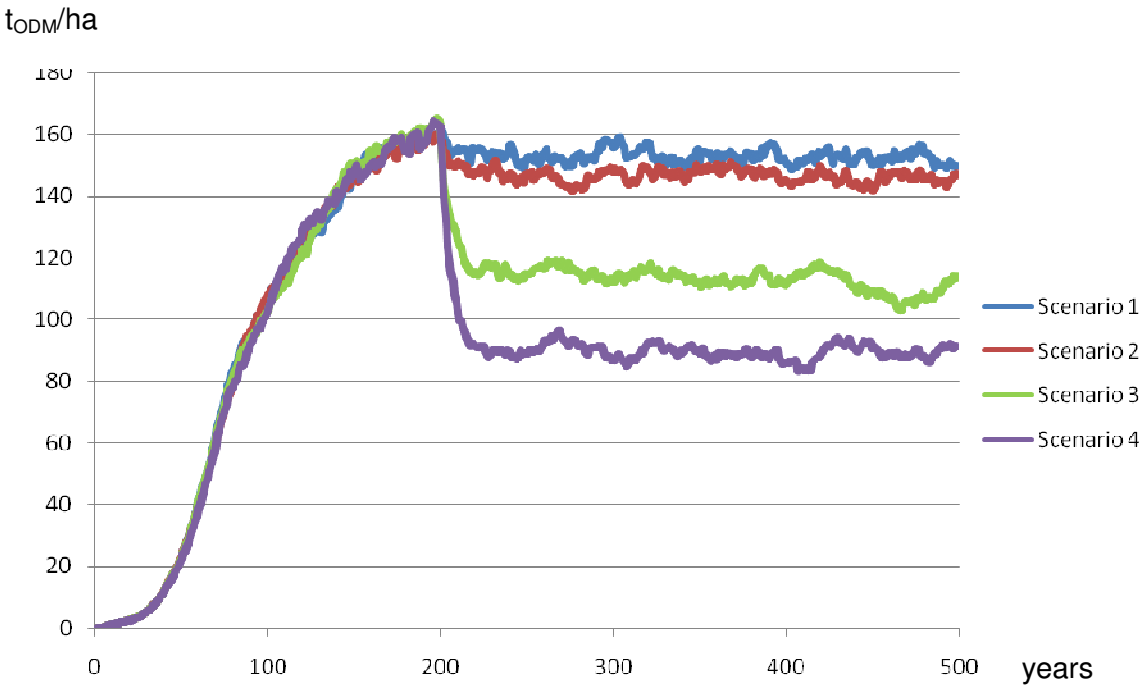

Figure 31: Evolution of shade tolerant trees biomass under different clearing shapes

Figure 32 shows the variation in relative abundance of shade tolerant trees depending on the scenarios. In control case, at climax there is 72% of shade tolerant trees, with scenario 1 there is 67%, with scenario 2 there is 66%, with scenario 3 there is 64% and finally with scenario 4 there is 58%. The clearing patter affects the relative abundance of shade tolerant trees.

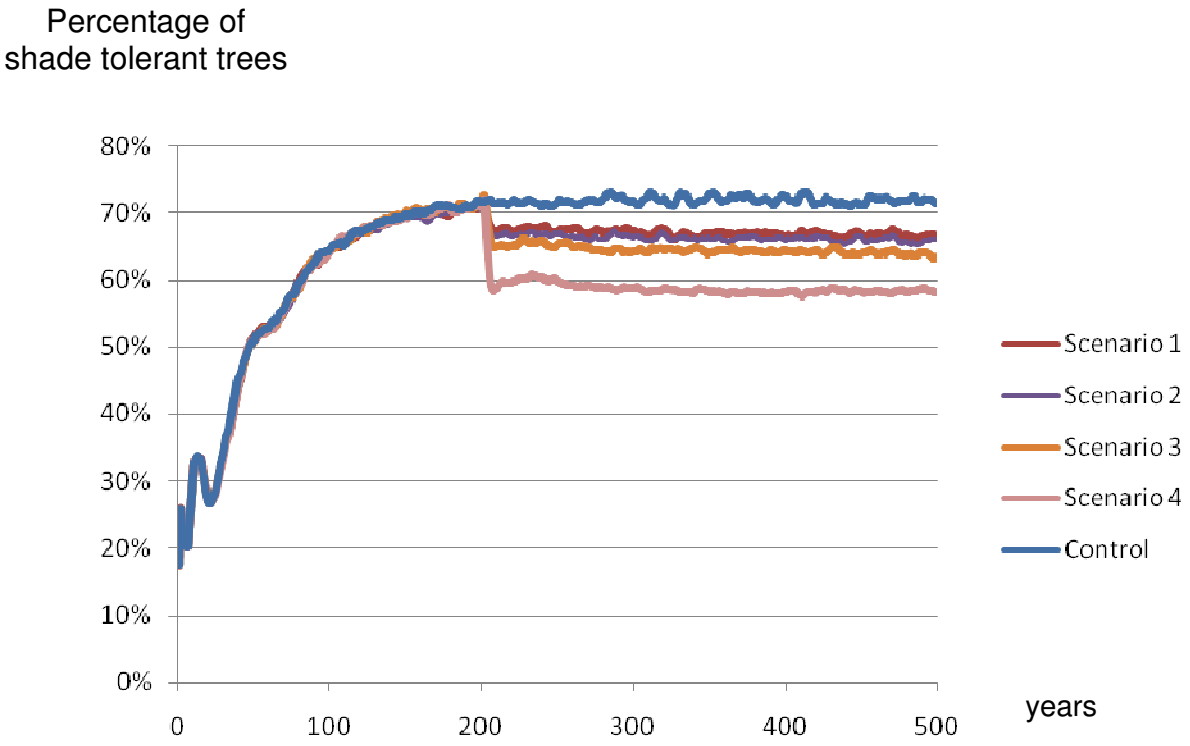

Figure 32: Relative abundance of shade tolerant trees in function of the clearing scenario

The new climax biomass and number of trees of the shade tolerant trees using the average value from t=300 to 500 years were determined (results in table 10).

Table 10: Loss of organic dry matter of shade tolerant trees per hectare and number of trees in relation to the control case

Edge effect scenario	Loss of biomass [t_{ODM}/ha]	Loss of trees [per ha]
Scenario 1	-9,7%	-19,5%
Scenario 2	-13,4%	-20,6%
Scenario 3	-32,8%	-26%
Scenario 4	-46,6%	-38,4%

In scenario 3 and 4 the loss of biomass is more important than the loss of tree. Actually large old trees stock more biomass than younger and smaller ones, but

also these trees are more sensible to edge effect. With a higher edge length in scenario 3 and 4, old trees are more impacted, that's why the loss of biomass is more important than the loss of trees.

It can be concluded that:

- ✓ A "offshore inland" clearing (scenario 1) has less impact on the quantity of biomass and on the number of trees of the forest.
- ✓ Comparatively, trees are smaller in scenario 3 and 4 because of the larger edge effect on the forest.
- ✓ An "erratic" deforestation, such as scenario 4, has a huge impact on the quantity of biomass of the forest

4.2.3. Impacts on intermediate shade tolerant trees

As shown in figure 33, it can also be seen that when the clearcuts are created at t=200 years, a drop of intermediate shade tolerant biomass is observed. As it was seen, at climax, the intermediate shade tolerant trees represent 90 t_{ODM}/ha in base case. Here however, it can be seen on figure 33 that there is less biomass than in control case after the clearings. The loss of biomass is more important in scenario 4 than in scenario 3, and in scenario 3 than in scenarios 1 and 2.

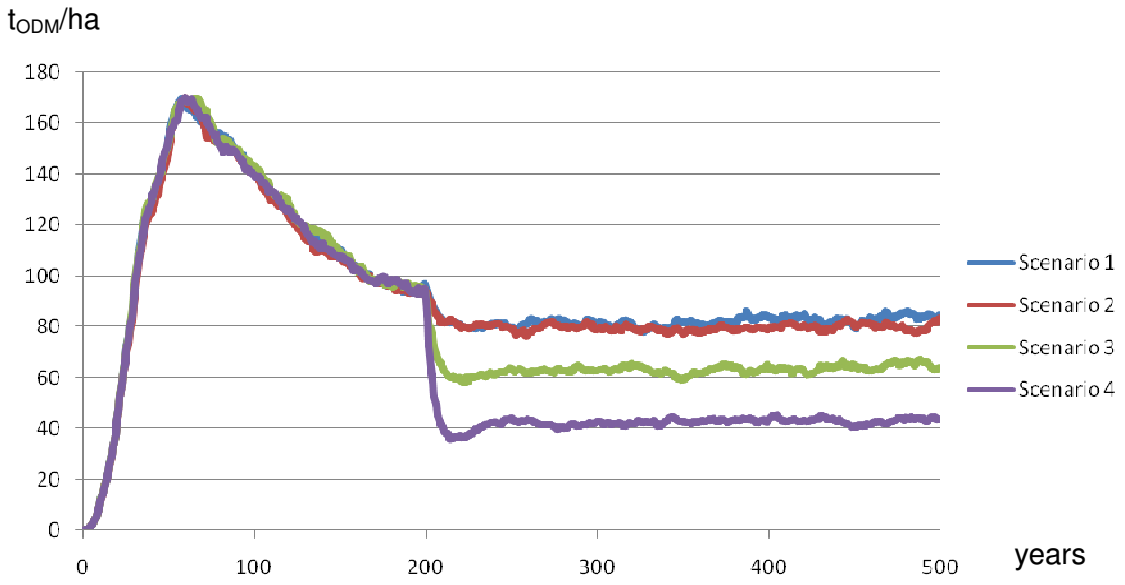

Figure 33: Evolution of intermediate shade tolerant trees biomass under different clearing shapes

Figure 34 shows the relative abundance of intermediate shade tolerant trees depending on the scenario. In control case, at climax there is 25% of intermediate shade tolerant trees, with scenario 1 there is 29%, with scenario 2 there is 30%, with scenario 3 there is 32% and finally with scenario 4 there is 37%. It can be said that with a clearing pattern accompanied by a high edge effect, the forest has more intermediate shade tolerant trees and less shade tolerant trees than in base case.

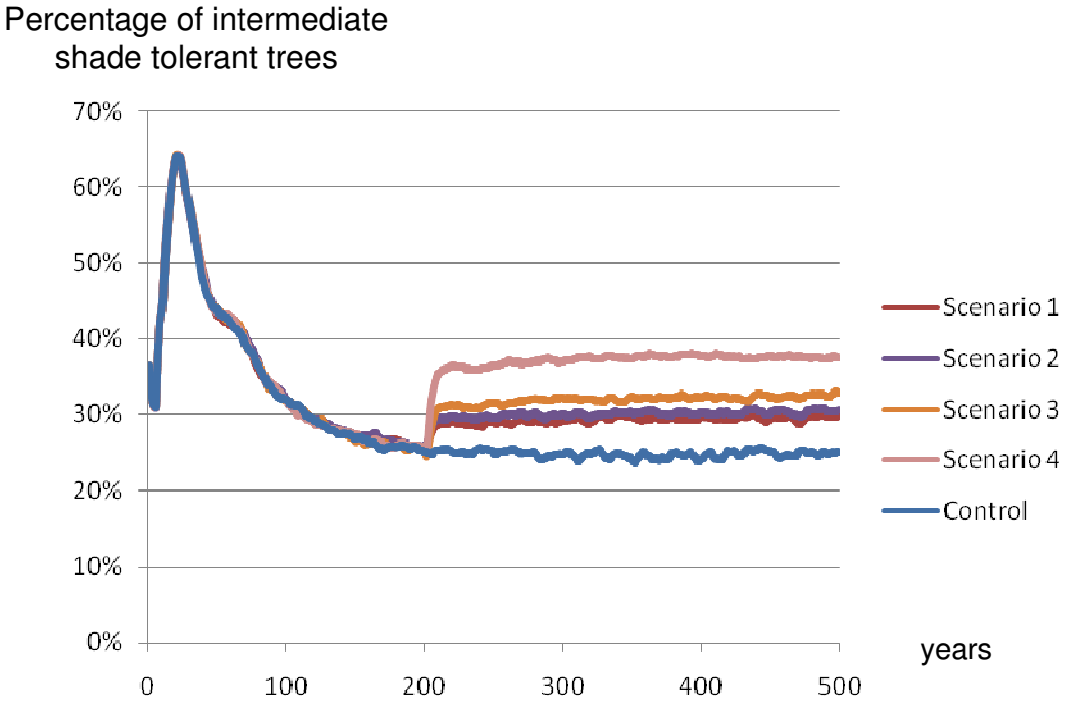

Figure 34: Relative abundance of intermediate shade tolerant trees in function of the scenario

By applying the same climax calculation method as in section 4.2.2 we determined the loss of biomass and the gain of trees as presented in table 11.

Table 11: Loss of organic dry matter per hectare and number of trees of intermediate shade tolerant trees in relation with base case

Edge effect scenario	Loss of biomass [t_{ODM}/ha]	Gain of trees [per ha]
Scenario 1	-8,9%	+2,3%
Scenario 2	-11,3%	+4,5%
Scenario 3	-29,8%	+6,3%
Scenario 4	-52,8%	+13,2%

All these clearings induce a loss of biomass by changing the forest composition.

Table 11 points out that all the clearing patterns induce a gain of trees per hectare in the forest, however a loss of biomass is observed.

Big trees are more sensible to edge effect than small ones. With the death of big trees, space is created for smaller trees. As each small tree has less biomass than bigger one, even with an augmentation of the number of trees, clearings lead to a loss of biomass comparatively to base case.

As a conclusion it can be said that:

- ✓ For intermediate shade tolerant trees too, an offshore inland clearing (scenario 1) has less impact on the loss of biomass than the other scenarios.
- ✓ All the clearing patterns lead to an increase of the quantity of trees, but trees are smaller and new conditions do not allow them to live enough to get big.
- ✓ Scenario 4 generates a drastic decrease of the quantity of biomass of the forest.

4.2.4. Impacts on pioneer trees

In figure 35, the evolution of pioneer trees biomass once the different scenarios of clearing are applied can be seen. As at clearing time (at t=200years), the quantity of pioneer trees per hectare is already quite low, there is no strong effect on the pioneer biomass. As in base case, at climax, the pioneer species biomass is only 3,6t_{ODM}/ha, clearings do not lead to a huge drop of biomass.

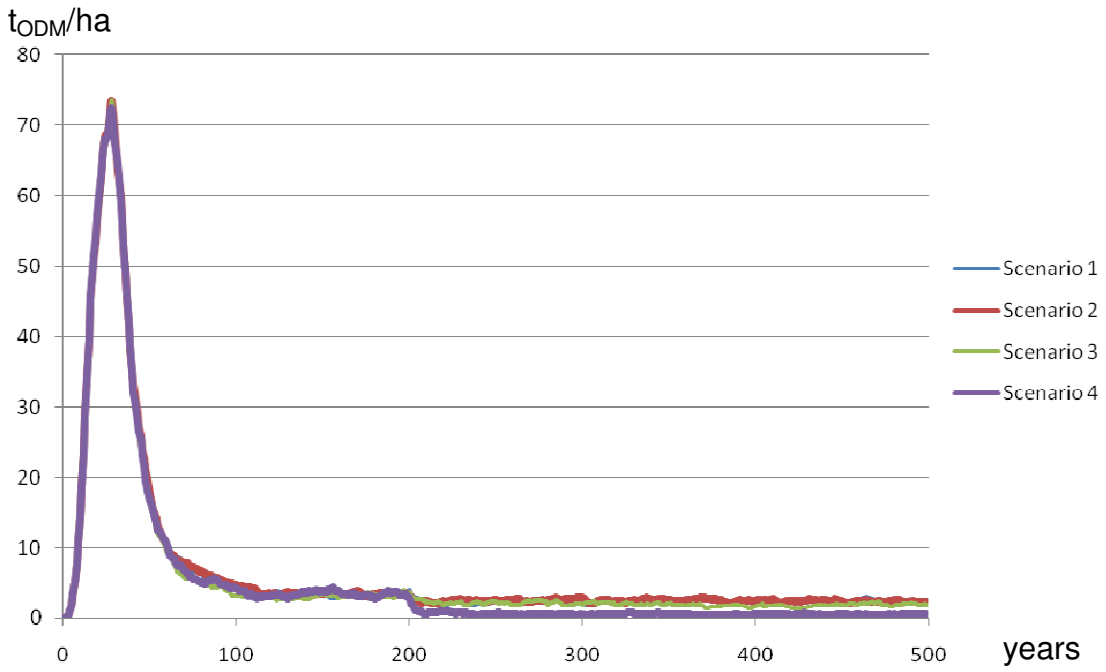

Figure 35: Evolution of the biomass of pioneer trees under different clearing shapes

In table 12, it can be seen that the loss of biomass varies from 33% to 84% and the loss of trees from 4 to 12%. In this case the loss of biomass is important in percentage but not in absolute value. The creation of clearings results in a diminution of pioneer trees leading to a loss of biomass.

Table 12: Loss of organic dry matter per hectare and number of pioneer trees in relation with the control case (t > 300years)

Edge effect scenario	Loss of biomass [t_{ODM}/ha]	Variation of number of trees [per ha]
Scenario 1	-34,1%	-1%
Scenario 2	-32,8%	-1,5%
Scenario 3	-45,8%	+0,8%
Scenario 4	-84,4%	+2,1%

From table 12 it can be said that the clearing pattern of scenario 4 is more impacting for big trees because a loss of 6% of the number of trees per hectare leads to a loss of 84% of biomass.

The values of biomass and number of trees seen above are for the forest as a whole. Hereafter the composition at the edge will be study.

4.2.5. Forest composition at the edge

An augmentation of pioneer species is expected at the edge as shown in a fragment of a tropical submontane forest, in Bahia state (Brazil) by (Rigueira et al., 2012). Looking at the composition at forest edge, this model suggests that at 0 to 20 meters of the edge there is an augmentation of 9% of pioneer trees stem number, an increase of 13% of intermediate shade tolerant trees stem number and a decrease of 44% of the shade tolerant trees stem number, comparing with untouched forest composition at climax. At 20 to 40m from the edge, there is an increase of 11% of the number of pioneer trees, an augmentation of 32% of intermediate shade tolerant trees and a reduction of 35% of shade tolerant trees.

In terms of relative abundance at climax, at 0 to 40m from the edge, there are 5% of pioneers, 39% of intermediate shade tolerants and 56 % of shade tolerant trees. By comparison, at climax in the middle of an untouched forest (i.e. base case) there are 3% of pioneers, 25% of intermediate shade tolerants and 72 % of shade tolerant trees.

Edge effect may vary depending on several factors such as fragment age, size, matrix management and edge orientation (Murcia, 1995) but these aspects were not considered in the present study.

4.2.6. Deforestation pattern general impacts

The results obtained are similar to the ones of Zipperer (1993) who showed that forest edge and interior dynamics were related to the type of deforestation pattern.

With the same "amount" of deforestation, different clearing patterns create different quantity of edges between deforested areas and intact forest. These edge areas, between deforestation and remaining forest, are much more exposed to wind damage, desiccation and are more susceptible to fire (Van der Pluijm, 2010).

The "offshore inland" deforestation has the least impact on forest (whether on biomass or number of trees) than any other scenarios. On the contrary, the multi-patches colonization is the worst scenario to preserve trees and biomass, and consequently habitat and biodiversity. In figure 36 the evolution of the total biomass of the forest after clearings is exposed.

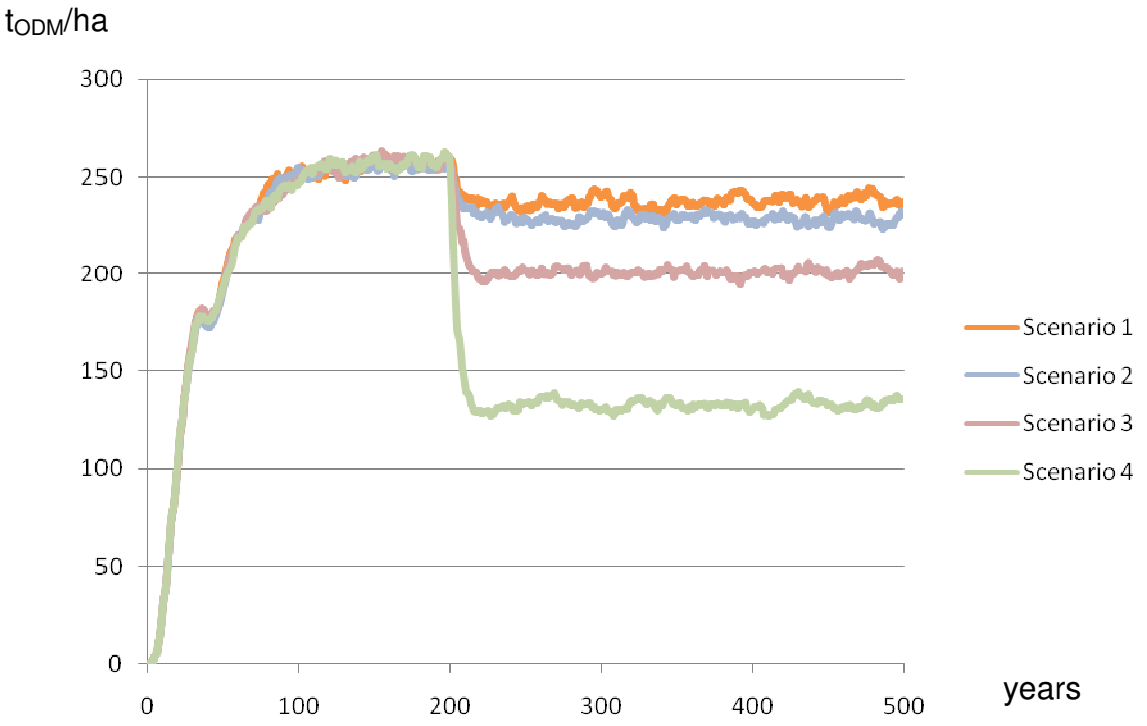

Figure 36: Loss of total biomass in function of deforestation patterns

In our study, applying scenario 1 to the BAF, implies a biomass reduction of about 9,3% compared to the base case. In comparison, scenario 2 leads to a reduction of 12,6% of the total biomass, scenario 3 a decrease of 23,1% and finally scenario 4 a loss of 49% of total biomass.

For the same clearing size, scenario 1 has a 240m edge length, scenario 2 a 300m, scenario 3 a 380m, and scenario 4 a 660m edge length. The edge length is not proportional to the loss of biomass.

Consequently scenario 1 is better than the other scenarios because with the same clearing size, the edge length is minimal and so the impact on the forest.

The “offshore inland” colonization is tied to gas or oil plant. There are no roads to the site; everything that enters or leaves, including gas or oil, people or material, is carried either by plane, boat or underground pipeline (Tollefson, 2011). According to Finer et al. (2015) the universal adoption of the “offshore inland” development model is one of the most important actions to minimize future ecological impacts of oil and gas extraction in tropical forest.

As an exemple of “offshore inland” facility, there is in the Brazilian Amazon the site Urucu, developed and operated by Petrobras. A roadless pipeline export natural gas to Manaus and workers are transferred to and from an onsite air strip in 14 days shifts. The site has internal roads, but no over land access from outside as reported by the foundation Blue Moon Fund (2015).

Historically, roads have paved the way for uncontrolled development throughout the forest (Tollefson, 2011). Indeed, once the road is constructed, the access to other forest areas is easier, and increased rates of hunting, poaching, animal capture, as well as higher levels of legal and illegal logging are then observed (Skole and Tucker, 1993). And even when tree harvest is selective, and much of the forest remains, it has been found that the roads themselves have numerous adverse side-effects (NASA, 2012). According to Compton Tucker, a biologist and tropical forest expert (NASA, 2012), roads cut deep into the rainforest and then spread outwards, that’s why there's a much greater loss of

habitat and species than if there were a single area of deforestation, because the amount of edge is critical for biodiversity.

It is primordial to consider these different deforestation patterns when modeling landscape dynamics to evaluate the deforestation impacts on the landscape attributes and the biodiversity.

In conclusion, as urban areas, rivers and roads act as vectors of human occupation, favoring deforestation in its surrounding areas, road planning must be carefully considered in the BAF, since this biome is characterized as a conflict zone for road construction (Laurance et al., 2014).

4.3. Regeneration under different scenarios

Now that we saw the impact of different deforestation patterns on biomass and number of trees of the BAF, the regeneration of the forest under different scenarios will be studied.

With the reduction of forested areas, regeneration of damaged ecosystems is a growing activity (Vieira and Gandolfi, 2006).

The cycle of tropical deforestation generally starts with excessive logging leading to the reduction of the original forest to a noncommercial resource (Shono et al., 2007) Then, new deforested areas are used for agricultural purposes, and when the land has lost productivity, fields are used for cattle ranching (Kangasniemi, 1993). Afterwards unproductive farmlands are abandoned and because of intensive anthropogenic effects (soil degradation, disturbances, and distance from intact forests), natural recovery is very slow and it takes a very long time for the forest to regenerate itself (Shono et al., 2007). In such case, according to Shono et al.(2007), shade intolerant grasses can appear and reach a new equilibrium state, blocking natural forest regeneration for decades or even centuries.

Recovery depends on the land use histories. Soil can become poor and infertile, or animal-dispersed species can disappear. Recovery depends on the matrix around and, in the case of a forested matrix, on the successional stage of the forest (Liebsch et al., 2008).

An ideal case is simulated here. The forest is not fragmented, the matrix is a 200 years forest, the soil is not degraded and it is assumed that animal-dispersed species are still present.

It will be seen how long it takes for the forest to recover after a clear out, and what is the impact of external seed input playing during the regeneration.

The simulation is made using the model described in chapter 3, and with the following assumptions:

- ✓ At t=0, there is no tree in the forest.
- ✓ Patch size is set to 4 ha in periodic boundary conditions.
- ✓ Simulation time is set to 1000 years, to let the forest reach climax again after the alteration.
- ✓ There is no edge effect from t=0 to t=200.
- ✓ At t=200 a logging following one of the three patterns described in figure 37 are implemented.
- ✓ From t=200 to 250 years an edge effect is applied around the clearing as described in section 3.2.7. The assumption is that after 50 years some trees are big enough to cancel the edge effect.
- ✓ There are no variations in the external environmental conditions such as solar radiation or number of hour of sun per day.
- ✓ The mathematical equations representing the natural processes of the growing trees remain unchanged during the simulation (trees do not develop new strategy throughout simulation time).

The mathematical model was simulated using MATLAB 2010.

4.3.1. Different clearing and seed dispersal scenarios

Three clearing sizes of an “offshore inland” pattern clearing are considered.

In figure 37, the tree different clearing sizes considered in our study are presented.

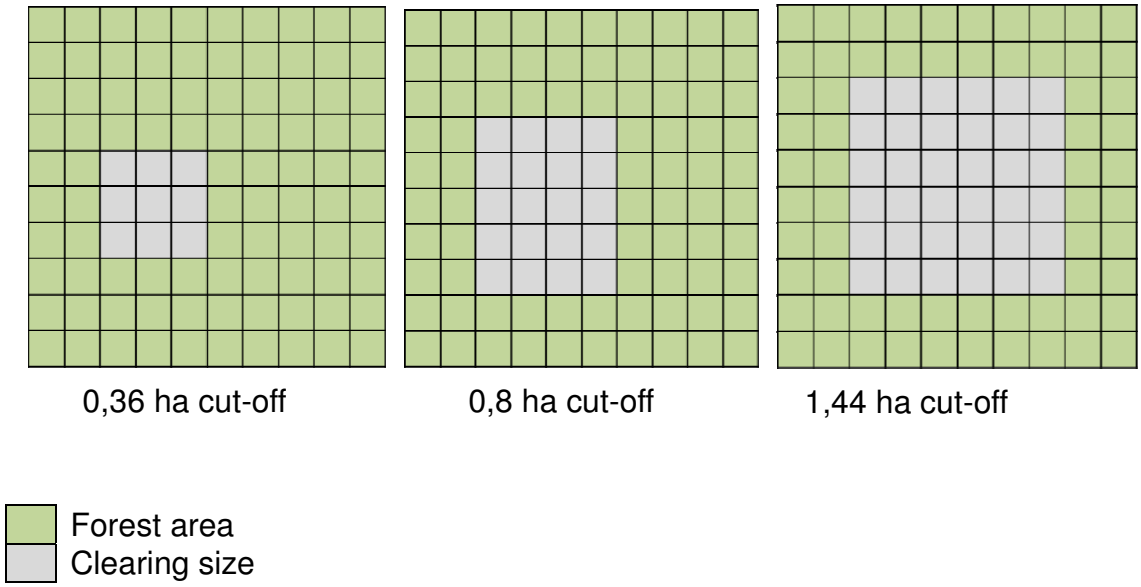

Figure 37: The different "offshore inland" pattern clearings

For the three clearing size cases, the forest dynamics will be analyzed with or without external seed rain. In other words, in one case, it is considered that the regeneration is only due to the seed dispersion of trees around the clearing, and in the second case, it is considered that the regeneration is due to both seed dispersion of the trees around and an additional external seed rain.

In figure 38 the different simulation scenarios considered in this section are presented.

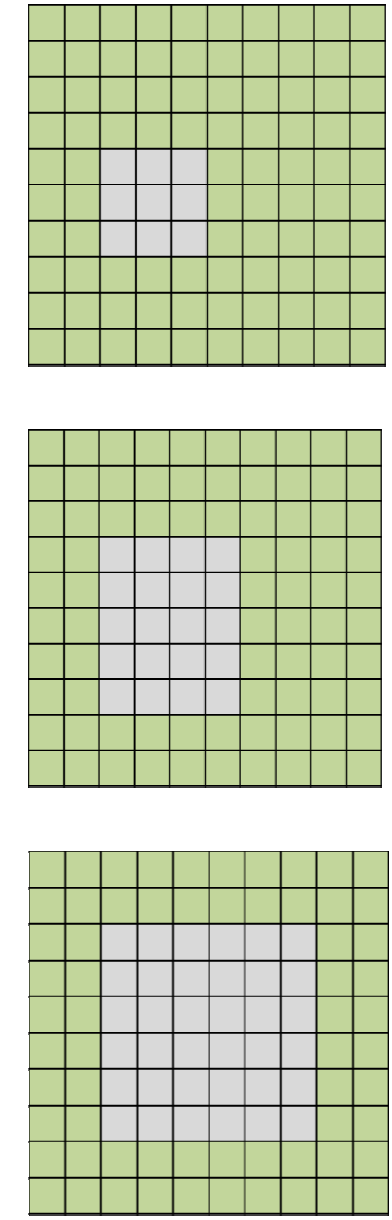

Figure 38: Presentation of the regeneration scenarios

4.3.2. General impacts on clearing regeneration

It can be observed in figure 39 for PFT9 trees that the clearing size impacts on the regeneration time; as expected the bigger the clearing, the longer the regeneration.

Without external seed rain, in none of the scenarios, the number of trees reached the control case climax. A new climax is reached. This situation may be explained by the fact that these scenarios are unrealistic because in the nature a lot of seeds are transported by wind, water or animals. According to (Tabarelli and Peres, 2002) vertebrate seed dispersal mode prevailed in the BAF, and ranged from 52,9% to 98,7% depending on the age of the forest. The proportion animal versus abiotic seed dispersal varies according to plantation age, with an augmentation of animal seed dispersal with forest age (Viani et al., 2015).

On the other hand, with external seed rain, it can be seen in figure 40, that the number of trees of PFT9 of all scenarios reached the control climax values.

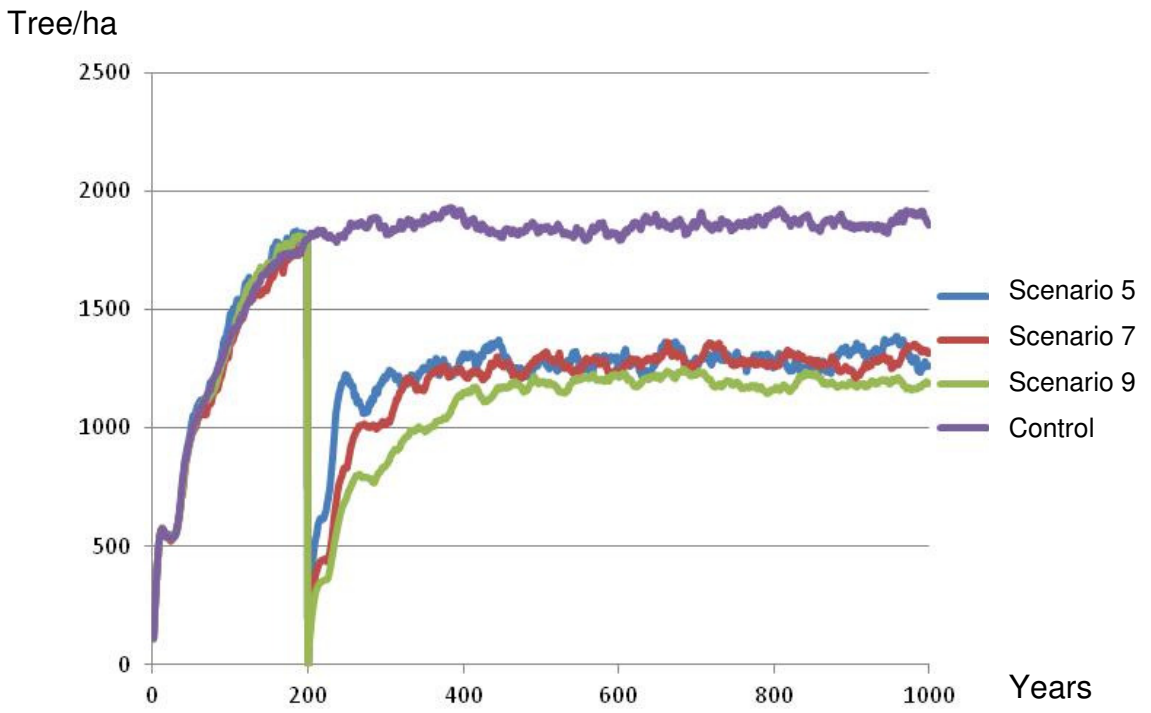

Figure 39: Number of PFT9 trees without external seed rain

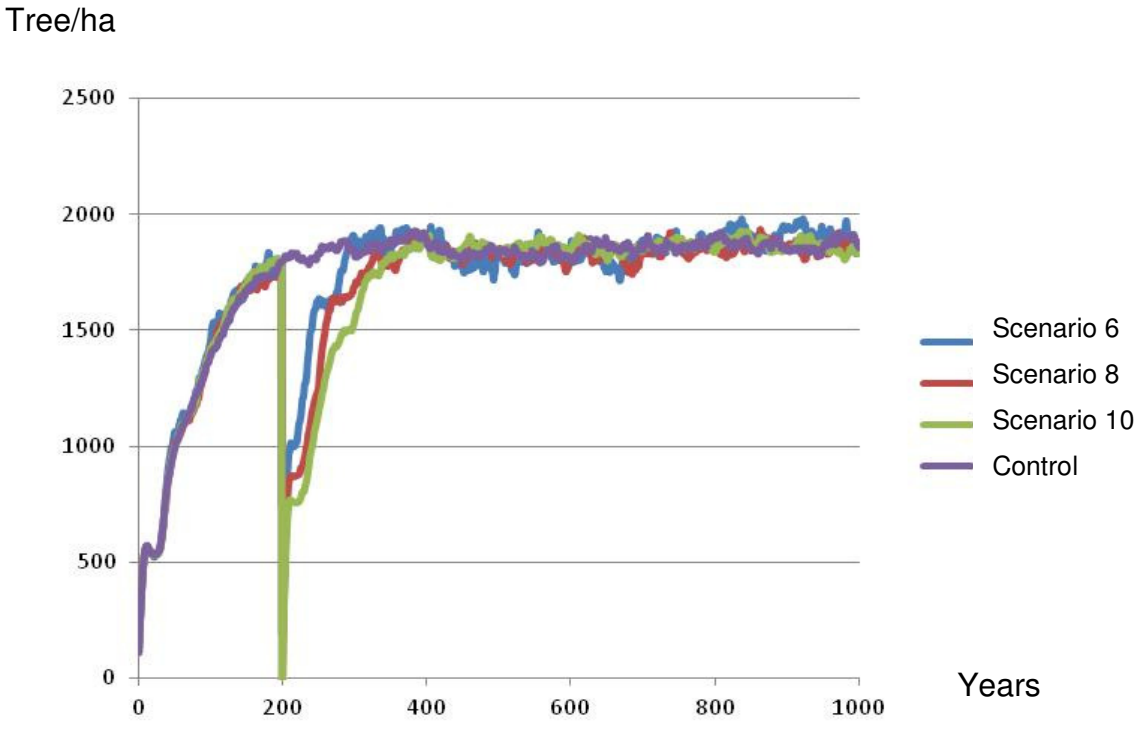

Figure 40: Number of PFT9 trees with external seed rain

4.3.3. Detailed impacts without external seed rain

Without external seed rain, the climax has a different composition, some PFT are more represented than others, when compared to the control case. This new repartition of tree impacts directly the biomass of each PFT and consequently the total biomass of the forest.

To estimate the new climax biomass of each PFT, the average biomass values (in t_{ODM}/ha) of the last 500 years of the simulation (time: t=500 to t=1000 years) are calculated.

As PFT1, PFT2 and PFT3 biomass are negligible at climax (below 0,6% of the total biomass), as a consequence the climax biomass values for these PFTs won't be calculated.

From table 13 the following observations can be made:

- ✓ Without external seed rain, the composition of the forest is different from the control case.
- ✓ The size of the clearing also impacts on the forest composition.

Table 13: Variation of the number of trees at climax state
Percentage relative to the control case.

	PFT 4	PFT 5	PFT 6	PFT 7	PFT 8	PFT 9
Scenario 5	- 40%	+15%	- 53%	-20%	0%	- 29 %
Scenario 7	- 40%	+24%	- 57%	-20%	0%	- 30%
Scenario 9	- 41%	+26%	- 61%	-11%	0%	- 36%

It is interesting to see that the PFT groups are impacted in different ways. For some PFT, such as PFT6, there is a huge decrease of the quantity of trees and for other, such as PFT8, there is no difference, and this is true for all the scenarios. Only for PFT5 an increase of number of trees is noticeable.

It appears that there are not enough seeds for PFT 9 and PFT 6 trees to reach control case climax values. As there is less 32m maximum height trees, PFT8 and PFT5 trees, with both a maximum of 25m height, take advantage of the space. In consequence, as the new conditions are better for these groups, more PFT5 and PT8 trees attain their maximum height and hence these trees have more biomass as seen in table 14.

Scenario 9 clearing is 4 times larger than scenario 5 clearing and 1,8 times larger than in scenario 7 clearing. For its part, scenario 7 clearing is 2,2 times larger than scenario 5 clearing. Looking at table 13 values, the variation of the number of trees at climax is not proportional to clearing size. As a matter of fact, augmentation of clearing size and changes in forest composition are not related by use of a constant multiplier.

Table 14 shows the changes of biomass per hectare in function of the scenario. Comparing table 13 and table 14, it can be said that at climax, the composition of the forest is different than in base case.

For example, there are 29 to 36% less PFT9 trees but 9 to 14 % of PFT9 biomass less. Actually, as there are less trees, there is less space competition, so less mortality due to crowding and more trees are able to reach their maximum height leading to a larger biomass per tree than in base case.

PFT8 and PFT7 trees take advantage of the reduction of PFT9 quantity of trees. More of these trees reach their maximum height than in base case, consequently the biomass of these groups increase.

To conclude, this study seems to show that there are not enough seeds of 32m maximum height trees to reach control case climax value. With more space, trees with a maximum height at 25m are favored in these new conditions.

Table 14: Changes of the biomass at climax state
Percentage relative to the control case

	PFT 4	PFT 5	PFT 6	PFT 7	PFT 8	PFT 9
Scenario 5	- 30%	+20%	- 37%	+3%	+30%	- 9 %
Scenario 7	- 30%	+23%	- 45%	+7%	+31%	- 11%
Scenario 9	- 30%	+29%	- 48%	+8%	+31%	- 14%

4.3.4. Detailed impacts with external seed rain

With external seed rain, the forest under scenarios 6, 8 and 10 reach biomass control climax values as presented in figure 41 for PFT9 and climax number of trees values as shown in figure 40 for PFT9

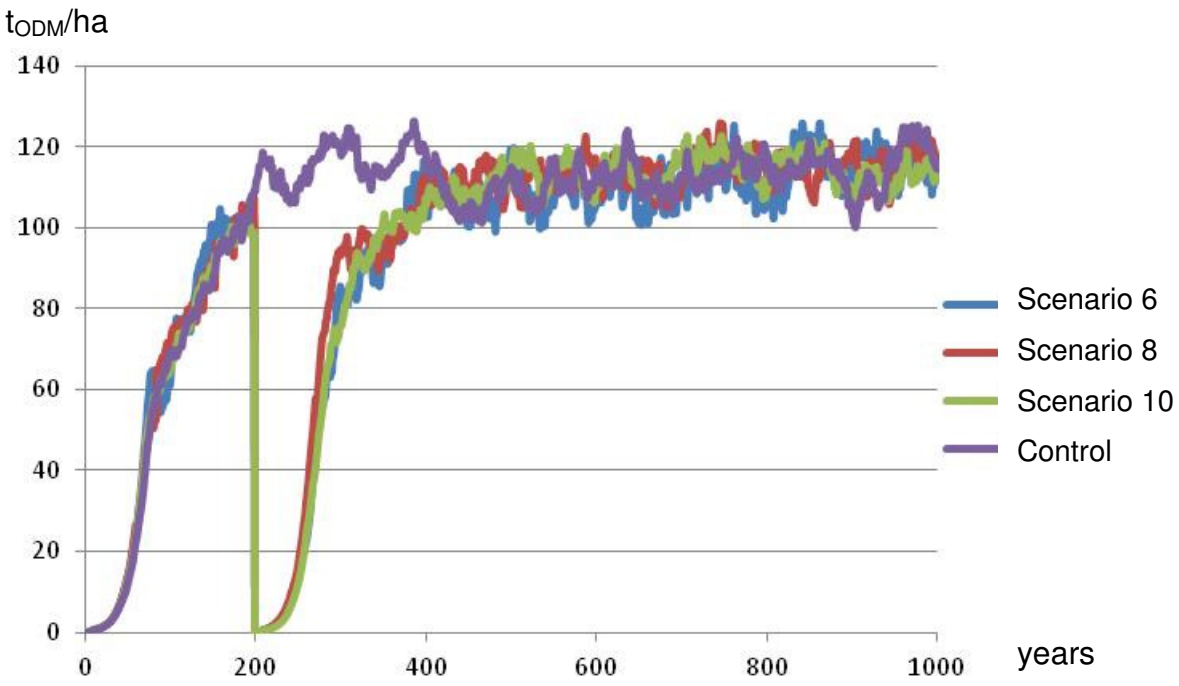

Figure 41: PFT9 biomass under different regeneration scenarios

It can be observed on figure 40 (see page 101) that the delay to reach back the climax depends on the clearing size.

The biomass values were used to estimate when the forest reaches the climax back, but the use of the number of trees per hectare gives very similar results.

To determine when the forest comes back to climax, we focus on the data from t=200 to 800 years of all PFTs for all scenarios. The curves are approximated with a 6^{th} order polynomial trendline. A good approximation of the time to reach climax is then the intersection point between the trendline and the control case biomass value at climax.

Table 15 shows the equations, the R^2 and the time for PFT4 to 9 to reach climax. The time to reach climax for the pioneer species was not calculated as they is only 3% of pioneers at climax state. The coefficient of determination R^2

indicates how well a model fits fit data. With values from 0,776 and 0,9817 the polynomial trendlines approximate satisfactorily the simulation data points.

Table 15: Trendline equations of biomass of different regenaration scenarios after clear-cutting

	Scenario 6	
PFT4	$y = 1E^{-14}x^6 - 2E^{-11}x^5 + 2E^{-08}x^4 - 7E^{-06}x^3 + 0{,}0015x^2 - 0{,}155x + 14{,}28$	$R^2=0{,}8091$
PFT5	$y = 7E^{-14}x^6 - 1E^{-10}x^5 + 1E\text{-}07x^4 - 5E^{-05}x^3 + 0{,}0101x^2 - 1{,}085x + 88{,}8$	$R^2=0{,}8966$
PFT6	$y = -3E^{-14}x^6 + 5E^{-11}x^5 - 3E^{-08}x^4 + 7E^{-06}x^3 + 0{,}0005x^2 - 0{,}35x + 66{,}13$	$R^2=0{,}8510$
PFT7	$y = -9E^{-15}x^6 + 2E\text{-}11x^5 - 1E\text{-}08x^4 + 6E\text{-}06x^3 - 0{,}0013x^2 + 0{,}14x + 4{,}53$	$R^2=0{,}8870$
PFT8	$y = -2E^{-13}x^6 + 3E^{-10}x^5 - 2E\text{-}07x^4 + 8E^{-05}x^3 - 0{,}0143x^2 + 1{,}262x + 7{,}31$	$R^2=0{,}8721$
PFT9	$y = -2E^{-13}x^6 + 3E^{-10}x^5 - 2E^{-07}x^4 + 9E^{-05}x^3 - 0{,}0186x^2 + 2{,}155x - 1{,}50$	$R^2=0{,}9549$

	Scenario 8	
PFT4	$y = 3E^{-15}x^6 - 5E^{-12}x^5 + 4E^{-09}x^4 - 2E^{-06}x^3 + 0{,}0005x^2 - 0{,}0819x + 12{,}93$	$R^2=0{,}7760$
PFT5	$y = -5E^{-14}x^6 + 8E^{-11}x^5 - 4E^{-08}x^4 + 7E^{-06}x^3 + 0{,}0011x^2 - 0{,}433x + 75{,}154$	$R^2=0{,}8832$
PFT6	$y = -8E^{-14}x^6 + 1E^{-10}x^5 - 1E^{-07}x^4 + 3E^{-05}x^3 - 0{,}0035x^2 + 0{,}006x + 56{,}21$	$R^2=0{,}8587$
PFT7	$y = 7E^{-15}x^6 - 1E^{-11}x^5 + 6E^{-09}x^4 - 7E^{-07}x^3 - 0{,}0003x^2 + 0{,}08x + 4{,}8677$	$R^2=0{,}9167$
PFT8	$y = y = -8E^{-14}x^6 + 2E^{-10}x^5 - 1E^{-07}x^4 + 5E^{-05}x^3 - 0{,}01x^2 + 1{,}038x + 7{,}241$	$R^2=0{,}9224$
PFT9	$y = -3E^{-13}x^6 + 6E^{-10}x^5 - 4E^{-07}x^4 + 0{,}0002x^3 - 0{,}0289x^2 + 2{,}705x + 0{,}69$	$R^2=0{,}9540$

	Scenario 10	
PFT4	$y = 6E^{-15}x^6 - 1E^{-11}x^5 + 1E^{-08}x^4 - 5E^{-06}x^3 + 0,0011x^2 - 0,1474x + 15,80$	$R^2=0,9627$
PFT5	$y = -5E^{-14}x^6 + 8E^{-11}x^5 - 4E^{-08}x^4 + 6E^{-06}x^3 + 0,0013x^2 - 0,473x + 80,22$	$R^2=0,9368$
PFT6	$y = -1E^{-13}x^6 + 2E^{-10}x^5 - 1E^{-07}x^4 + 4E^{-05}x^3 - 0,0042x^2 - 0,102x + 69,98$	$R^2=0,9387$
PFT7	$y = 3E^{-15}x^6 - 6E^{-12}x^5 + 3E^{-09}x^4 + 2E^{-07}x^3 - 0,0004x^2 + 0,095x + 4,016$	$R^2=0,9503$
PFT8	$y = 3E^{-14}x^6 - 4E^{-11}x^5 + 7E^{-09}x^4 + 8E^{-06}x^3 - 0,0046x^2 + 0,799x + 4,595$	$R^2=0,9718$
PFT9	$y = -3E^{-13}x^6 + 5E^{-10}x^5 - 3E^{-07}x^4 + 0,0001x^3 - 0,023x^2 + 2,448x - 6,819$	$R^2=0,9817$

Table 16 presents the delays after clear-cutting to reach back climax. It can be observed that the intermediate shade tolerant trees (PFT4 to 6) reach the climax before the shade tolerant trees. Among intermediate shade tolerant trees, smaller maximum height trees reach climax before higher ones. The same occurs with shade tolerant trees.

The delays to reach climax with the scenarios 6, 8 and 10 are different from the control case. It can be explained by the fact that, in these scenarios, the clearing is surrounded by a matrix of adult trees producing seeds, whereas in base case, the forest starts growing from a clear forested land.

Table 16: Time to reach climax (in years)

	PFT 4	PFT 5	PFT 6	PFT 7	PFT 8	PFT 9
Scenario 6	180	180	210	210	240	230
Scenario 8	210	220	250	250	300	290
Scenario 10	240	250	350	360	360	350
Control	210	230	220	220	240	230

4.3.1. Conclusion

Regeneration cannot be explained in the PESM without external seed rain.

Considering only seed dispersion from trees around the clearing, a new climax is reached, different in composition and in biomass quantity from control case.

The time to recover depends on the matrix and on the clearing size. As expected, the larger is the clearcut, the longer the forest will recover after the disturbance.

This study shows an ideal case with a mature forest matrix and a non altered soil, but it would be interesting to study the regeneration of very altered deforested areas. It is possible that these succession times would be slower, or incomplete, due to the severe depletion of forest vegetation (Liebsch et al., 2008). Also composition of the matrix or the distance to forest fragments is an important factor when it comes to regeneration (Baider et al., 2001; Laurance et al., 2014). Finally anthropogenic regeneration would be interesting to examine in the context of our study.

According to Rezende et al. (2015) in the BAF spontaneous regeneration is disfavored near urban areas and this effect tended to stabilize at a distance of 5km. The same pattern is observed to the distance of all roads, which tended to stabilize at the distances of 700 m. This study was conducted in the State of Rio de Janeiro, Southeastern Brazil, and in the future it would be interesting to verify if these values are the same in the PESM.

5. CONCLUSIONS AND DIRECTIONS FOR FUTURE WORKS

Forest growth models have become a very important tool to understand forest dynamic. Nevertheless, it's always a challenge to build a model with an adequate balance between the real forest complexity and the need for model simplicity (Evans et al., 2013; Grimm et al., 2005).

In the first part of the thesis, a forest growth model adapted to the Atlantic forest is addressed. A process based approach is chosen to build a gap individual based model. Data from the PESM were implemented in the model when available, if not, data from other tropical forests were used.

The second part of the work presents the model validation. Compared to other studies, the results obtained here are satisfactory. The results show an extra 2% of biomass and an extra 5% of number of trees than in Alves et al. (2010) study, an extra 34% of number of trees but a 3,4% less of biomass than in Putz et al. (2011) model, and an extra 10% of biomass than in Vieira et al. (2008) study.

Compared to other studies, it can be said that the present work may slightly overestimate the quantity of biomass in the forest. Indeed the model represents an "ideal case" without soil nutrient or water limitation, climate impact or competition with the preceding land use vegetation. On the other hand this model does not take in consideration non-woody components such as lianas, palm, bamboo and epiphytes. According to Vieira et al. (2008) this group can represent more than 10% of the total biomass in the BAF. Although all the simplifications, satisfactory results are obtained.

From a no tree field, this work suggests that about 240 years are needed for the BAF to reach climax state.

To test the numerical stability of the model, two time steps were used: one year and half a year. The dynamics of the forest shows no difference. As the value of the LAI_{max} was a discussed issue, it was tested with other values from other studies. It appears that with this model the value 4 represents better the dynamic of the BAF.

The third part was addressed to the impact of different patterns of non forested areas on the forest growth. Four different clearing shapes with the same area were selected. Forest composition and quantity of biomass changed due to the edge effect of the clearings. The proposed model shows that an “offshore inland” clearing, with a minimal edge length, is optimal. This scenario has less impact on the forest, such as diminution of biomass per hectare, than other clearing shapes. As a result, human occupations and road constructions must be carefully planned in order to preserve as much as possible the BAF.

Finally, regeneration scenarios are addressed with different sizes of clearing and with or without external seed rain. The first observation was that without external seed rain the forest reaches a new climax with a new tree composition and with less biomass per hectare. In these new environmental conditions some PFT, different from base case, are favored.

The model shows that regeneration cannot be explained in the PESM without external seed rain. The time to recover depends on the matrix and on the clearing size. The larger is the clearcut, the longer the forest will recover after the disturbance.

The model developed in this thesis can be improved, for example by trying to increase the number of PFT to represent better the interspecific competition and extinction processes (Fischer et al., 2016), or on this idea, by investigating the suitable quantity of PFT needed to describe the BAF dynamic.

At any time, it would be interesting to use future field studies to improve the species grouping and the parameterization of the model

An interesting thing for comparison would be the relief issue. The relief is not taken into account in this present work, the area is considered a flat landscape. With a steep terrain, emergent tree crowns generally do not touch. How this issue would affect light attenuation and therefore the model outputs? What about light incidence angle and how would this issue affect carbon sequestration? It is expected less strong light attenuation in more steep slopes, due to lateral light entrance through the canopy, but it would be interesting to verify this assertion adjusting the model presented here.

Due to computer improvements, there are still many interesting things to assess using a forest growth model, such as exploring these questions related to forest biomass stocks and climate change. This model does not include the effects of changing CO_2 concentrations on forest growth. How increased CO_2 concentrations might influence species interactions? What about conditions or limits to convert forests from carbon sinks to carbon emissaries? Is there a balance between PFTs that can maximize carbon storage?

The relentless march of technology, new data collection, and new forest knowledge means there is always something new.

6. REFERENCES

Aber, J. D., 1982, FORTNITE: a computer model of organic matter and nitrogen dynamics in forest ecosystems: Research bulletin, Research Division of the College of Agricultural and Life Sciences, University of Wisconsin.

Ahmed, S. E., C. M. Souza, J. Riberio, and R. M. Ewers, 2013, Temporal patterns of road network development in the Brazilian Amazon: Regional Environmental Change, v. 13, p. 927-937.

Alder, D., 1995, Growth Modelling for Mixed Tropical Forests: Tropical Forestry Papers 30, 231 p.

Alves, L. F., S. A. Vieira, M. A. Scaranello, P. B. Camargo, F. A. M. Santos, C. A. Joly, and L. A. Martinelli, 2010, Forest structure and live aboveground biomass variation along an elevational gradient of tropical Atlantic moist forest (Brazil): Forest Ecology and Management, v. 260, p. 679-691.

Babbitt, B., 2015, The benefits of drilling inland as if it were offshore, Inter-American Development Bank.

Baider, C., M. Tabarelli, and W. Mantovani, 2001, The soil seed bank during Atlantic Forest regeneration in Southeast Brazil: Revista Brasileira de Biologia, v. 61, p. 35-44.

Barbour, I. G., 1974, Myths, models, and paradigms: a comparative study in science and religion, Harper & Row, 198 p.

Baudry, O., C. Charmetant, C. Collet, and Q. Ponette, 2014, Estimating light climate in forest with the convex densiometer: operator effect, geometry and relation to diffuse light: European Journal of Forest Research, v. 133, p. 101-110.

Blue moon fund, 2015, Offshore-inland: Advanced oil and gas technology to save tropical forests and indigenous cultures from destruction, Charlottesville, VA, United States of America, Blue moon fund, p. 12.

Bossel, H., and H. Krieger, 1991, Simulation model of natural tropical forest dynamics: Ecological Modelling, v. 59, p. 37-71.

Bossel, H., and H. Krieger, 1994, Simulation of multi-species tropical forest dynamics using a vertically and horizontally structured model: Forest Ecology and Management, v. 69, p. 123-144.

Botkin, D. B., 1993, Forest Dynamics: An Ecological Model, Oxford University Press.

Botkin, D. B., J. F. Janak, and J. R. Wallis, 1972, Some Ecological Consequences of a Computer Model of Forest Growth: Journal of Ecology, v. 60, p. 849-872.

Bourgeron, P. S., 1983, Spatial aspects of vegetation structure, Tropical rain forest ecosystems structure and function: Ecosystems of the World 14A: Amsterdam, Elsevier Scientific Publishing Company, p. 29-47.

Boyle, M., 2014, Biological corredor, Ecology Theory, The encyclopedia of earth.

Brandão, A. O., and C. M. Souza, 2006, Mapping unofficial roads with Landsat images: a new tool to improve the monitoring of the Brazilian Amazon rainforest: International Journal of Remote Sensing, v. 27, p. 177-189.

Bugmann, H., 2001, A Review of Forest Gap Models: Climatic Change, v. 51, p. 259-305.

Bunnell, F. L., 1989, Alchemy and uncertainty: what good are models?, General technical report PNW, U.S. Dept. of Agriculture, Forest Service, Pacific Northwest Research Station.

Byl, J., 2003, Mathematical Models and reality, Langley, BC, Canada, Proceedings of the 2003 Conference of the Association for Christians in the Mathematical Sciences, p. 16.

Carlotti, F., J. Giske, and F. Werner, 2000, 12 - Modeling zooplankton dynamics, *in* R. H. W. L. R. S. Huntley, ed., ICES Zooplankton Methodology Manual: London, Academic Press, p. 571-667.

Chambers, J. Q., J. Dos Santos, R. J. Ribeiro, and N. Higuchi, 2001, Tree damage, allometric relationships, and above-ground net primary production in central Amazon forest, Kidlington, United Kingdom, Elsevier.

Chave, J., C. Andalo, S. Brown, M. A. Cairns, J. Q. Chambers, D. Eamus, H. Fölster, F. Fromard, N. Higuchi, T. Kira, J. P. Lescure, B. W. Nelson, H. Ogawa, H. Puig, B. Riéra, and T. Yamakura, 2005, Tree allometry and improved estimation of carbon stocks and balance in tropical forests: Oecologia, v. 145, p. 87-99.

Clark, D. A., and D. B. Clark, 1999, Assessing the growth of tropical rain forest trees: issues for forest modeling and management: Ecological Applications, v. 9, p. 981-997.

Dale, V. H., M. A. Hemstrom, and S. Pacific Northwest Forest and Range Experiment, 1984, CLIMACS: A Computer Model of Forest Stand Development for Western Oregon and Washington: Research paper PNW, U.S. Department of Agriculture, Forest Service, Pacific Northwest Forest and Range Experiment Station.

Department of Ecological Modelling of the Helmholtz Centre for Environmental Research – UFZ, 2014, FORMIND Handbook, Leipzig, Germany, Helmholtz Centre for Environmental Research – UFZ, p. 59.

Ditzer, T., R. Glauner, M. Förster, P. Köhler, and A. Huth, 2000, The process-based stand growth model Formix 3-Q applied in a GIS environment for growth and yield analysis in a tropical rain forest: Tree Physiology, v. 20, p. 367-381.

Doyle, T., 1981, The Role of Disturbance in the Gap Dynamics of a Montane Rain Forest: An Application of a Tropical Forest Succession Model, *in* D. West, H. Shugart, and D. Botkin, eds., Forest Succession: Springer Advanced Texts in Life Sciences, Springer New York, p. 56-73.

Duz, S. R., A. Siminski, M. Santos, and M. T. S. Paulilo, 2004, Crescimento inicial de três espécies arbóreas da Floresta Atlântica em resposta à variação na quantidade de luz: Brazilian Journal of Botany, v. 27, p. 587-596.

Evans, M. R., V. Grimm, K. Johst, T. Knuuttila, R. de Langhe, C. M. Lessells, M. Merz, M. A. O'Malley, S. H. Orzack, M. Weisberg, D. J. Wilkinson, O. Wolkenhauer, and T. G. Benton, 2013, Do simple models lead to generality in ecology?: Trends in Ecology & Evolution, v. 28, p. 578-583.

FAO, 2001, Mean annual volume increment of selected industrial forest plantation species, Forest Plantations Thematic Paper, Rome (Italy), p. 27.

FAO, 2010, Global Forest Ressources Assessment 2010, Global Forest Ressources, Rome, Italy, Food and Agriculture Organization of the United Nations, p. 378.

FAO, 2012, State of the world's forest 2012: Rome, Food and agriculture organization of the United Nations, 60 p.

Finer, M., B. Babbitt, S. Novoa, F. Ferrarese, S. E. Pappalardo, M. De Marchi, M. Saucedo, and K. Anjali, 2015, Future of oil and gas development in the western Amazon: Environmental Research Letters, v. 10, p. 024003.

Fischer, R., F. Bohn, M. Dantas de Paula, C. Dislich, J. Groeneveld, A. G. Gutiérrez, M. Kazmierczak, N. Knapp, S. Lehmann, S. Paulick, S. Pütz, E. Rödig, F. Taubert, P. Köhler, and A. Huth, 2016, Lessons learned from applying a forest gap model to understand ecosystem and carbon dynamics of complex tropical forests: Ecological Modelling.

Fischer, R., F. Bohn, M. Dantas de Paula, C. Dislich, J. Groeneveld, M. Kazmierczak, N. Knapp, S. Lehmann, S. Paulick, E. Rödig, F. Taubert, P. Köhler, and A. Huth, 2015, FORMIND Handbook, Leipzig, Germany, Helmholtz Centre for Environmental Research – UFZ, p. 65.

Gobron, N., 2008, Terrestrial essential climate variables for climate change assessment, mitigarion and adaptation, Leaf Area Index (LAI), Rome, Italy, Food and Agriculture Organization of the United Nations, p. 44.

Gommers, C. M. M., E. J. W. Visser, K. R. S. Onge, L. A. C. J. Voesenek, and R. Pierik, 2013, Shade tolerance: when growing tall is not an option: Trends in Plant Science, v. 18, p. 65-71.

Grimm, V., 1999, Ten years of individual-based modelling in ecology: what have we learned and what could we learn in the future?: Ecological Modelling, v. 115, p. 129-148.

Grimm, V., E. Revilla, U. Berger, F. Jeltsch, W. M. Mooij, S. F. Railsback, H.-H. Thulke, J. Weiner, T. Wiegand, and D. L. DeAngelis, 2005, Pattern-Oriented Modeling of Agent-Based Complex Systems: Lessons from Ecology: Science, v. 310, p. 987-991.

Groeneveld, J., L. F. Alves, L. C. Bernacci, E. L. M. Catharino, C. Knogge, J. P. Metzger, S. Pütz, and A. Huth, 2009, The impact of fragmentation and density regulation on forest succession in the Atlantic rain forest: Ecological Modelling, v. 220, p. 2450-2459.

Hamilton, W., 2002, Ecological succession, The Pennsylvania State University.

Hilbert, D. W., and C. Messier, 1996, Physical simulation of trees to study the effects of forest light environment, branch type and branch spacing on

light interception and transmission, Functional Ecology, British Ecological Society, p. pp. 777-783.

Huston, M., D. DeAngelis, and W. Post, 1988, New Computer Models Unify Ecological Theory: BioScience, v. 38, p. 682-691.

Instituto Brasileiro de Geografia e Estatística, I., 2012, Manual Técnico da Vegetação Brasileira: Manuais Técnicos em Geociências: Rio de Janeiro, Brasil, Instituto Brasileiro de Geografia e Estatística - IBGE, 271 p.

Instituto Florestal do estado de São Paulo, 2008, Parque Estadual da Serra do Mar - Plano de manejo, p. 485.

Kangasniemi, J., 1993, Sustainable Agriculture and the Environment in the Humid Tropics: Culture & Agriculture, v. 13, p. 24-25.

Keane, R. E., S. F. Arno, J. K. Brown, and D. F. Tomback, 1990, Modelling stand dynamics in whitebark pine (Pinus albicaulis) forests: Ecological Modelling, v. 51, p. 73-95.

Kercher, J. R., and M. C. Axelrod, 1984, A Process Model of Fire Ecology and Succession in a Mixed-Conifer Forest: Ecology, v. 65, p. 1725-1742.

Kienast, F., 1985, FORECE – A Forest Succession Model for Southern Central Europe, Oak Ridge, Tennessee, USA, Environmental Sciences Divisions of the Oak Ridge National Laboratory, p. 88.

King, D. A., S. J. Davies, S. Tan, and N. S. M. Noor, 2006, The role of wood density and stem support costs in the growth and mortality of tropical trees: Journal of Ecology, v. 94, p. 670-680.

Kira, T., 1978, Community architecture and organic matter dynamics in tropical lowland rain forests of southeast Asia with special reference to Pasoh Forest, west Malaysia, *in* C. University, ed., Tropical Trees As Living Systems, p. 561-589.

Koike, T., M. Kitao, Y. Maruyama, S. Mori, and T. T. Lei, 2001, Leaf morphology and photosynthetic adjustments among deciduous broad-leaved trees within the vertical canopy profile: Tree Physiology, v. 21, p. 951-958.

Köhler, P., 2000, Modelling anthropogenic impacts on the growth of tropical rain forests, University of Kassel, Kassel, Deutschland, 214 p.

Köhler, P., T. Ditzer, R. C. Ong, and A. Huth, 2001, Comparison of measured and modelled growth on permanent plots in Sabahs rain forests: Forest Ecology and Management, v. 144, p. 101-111.

Köhler, P., and A. Huth, 1998, The effects of tree species grouping in tropical rainforest modelling: Simulations with the individual-based model Formind: Ecological Modelling, v. 109, p. 301-321.

Laurance, W. F., G. R. Clements, S. Sloan, C. S. O'Connell, N. D. Mueller, M. Goosem, O. Venter, D. P. Edwards, B. Phalan, A. Balmford, R. Van Der Ree, and I. B. Arrea, 2014, A global strategy for road building: Nature, v. 513, p. 229-232.

Lee, K., and P. A. Fishwick, 1996, A methodology for dynamic model abstraction, San Diego, CA, USA, Transactions of the Society for Computer Simulation International - Special issue on model abstraction, p. 217 - 229.

Leemans, R., and I. C. Prentice, 1989, FORSKA, a General Forest Succession Model: Meddelanden från Växtbiologiska Institutionen, Uppsala, Växtbiologiska inst.

Lieberman, M., D. Lieberman, R. Peralta, and G. S. Hartshorn, 1995, Canopy Closure and the Distribuition of Tropical Forest Tree Species at La Selva, Costa Rica, Journal of Tropical Ecology, p. pp. 161-177.

Liebsch, D., M. C. M. Marques, and R. Goldenberg, 2008, How long does the Atlantic Rain Forest take to recover after a disturbance? Changes in species composition and ecological features during secondary succession: Biological Conservation, v. 141, p. 1717-1725.

Liu, J., and P. S. Ashton, 1995, Individual-based simulation models for forest succession and management: Forest Ecology and Management, v. 73, p. 157-175.

Marshall, D., 2005, Modeling Douglas-fir Growth & Yield in the PNW, Managing Stand Density: The Science Behind the Art, Seven Feathers Convention center, Canyonville, Oregon.

Martin, J., and T. Gower, 1996a, Forest Succession: Forestry Facts, v. 78, p. 4.

Martin, J., and T. Gower, 1996b, Tolerance of Tree Species, Madison, WI, USA, Department of forest ecology and management - University of Wisconsin-Madison, p. 2.

Morellato, L. P. C., and C. F. B. Haddad, 2000, Introduction: The Brazilian Atlantic Forest1: Biotropica, v. 32, p. 786-792.

Murcia, C., 1995, Edge effects in fragmented forests: implications for conservation: Trends in Ecology & Evolution, v. 10, p. 58-62.

Myers, N., R. A. Mittermeier, C. G. Mittermeier, G. A. B. da Fonseca, and J. Kent, 2000, Biodiversity hotspots for conservation priorities: Nature, v. 403.

NASA, 2012, Landsat Top 10: International Deforestation Patterns in Tropical Rainforests, Landsat news, NASA.

Nascimento, H. E. M., and W. F. Laurance, 2004, Biomass dynamics in amazonian forest fragments: Ecological Applications, v. 14, p. 127-138.

Natural Sciences and Engineering Research Council of Canada, N., 2003, Qu'est-ce qu'un modèle?, Laval, Canada, Alcan pour les femmes en sciences et génie au Québec.

Nowak, D. J., M. Kuroda, and D. E. Crane, 2004, Tree mortality rates and tree population projections in Baltimore, Maryland, USA: Urban Forestry & Urban Greening, v. 2, p. 139-147.

Okuda, T., N. Manokaran, Y. Matsumoto, K. Niiyama, S. C. Thomas, and P. S. Ashton, 2013, Pasoh: Ecology of a Lowland Rain Forest in Southeast Asia, Springer Japan.

Olivas, P. C., S. F. Oberbauer, D. B. Clark, D. A. Clark, M. G. Ryan, J. J. O'Brien, and H. Ordonez, 2013, Comparison of direct and indirect methods for assessing leaf area index across a tropical rain forest landscape, Agricultural and Forest Meteorology, p. 177.

Pastor, J., and W. M. Post, 1985, Development of a Linked Forest Productivity-Soil Process Model, Oak Ridge, Tennessee, USA, Environmental Sciences Division of the Oak Ridge National Laboratory, p. 176.

Perz, S. G., M. M. Caldas, E. Arima, and R. J. Walker, 2007, Unofficial Road Building in the Amazon: Socioeconomic and Biophysical Explanations: Development and Change, v. 38, p. 529-551.

Phillips, P. D., I. Yasman, T. E. Brash, and P. R. van Gardingen, 2002, Grouping tree species for analysis of forest data in Kalimantan (Indonesian Borneo): Forest Ecology and Management, v. 157, p. 205-216.

Pimenta Veloso, H., F. Rangel, Antonio Lourenço Rosa, and J. C. Alves Lima, 1991, Classificação da vegetação brasileira, adaptada a um sistema universal, Rio de Janeiro, Brasil, Fundação Instituto Brasileiro de Geografia e Estatistica, p. 124p.

Poorter, L., 1999, Growth reponses of 15 rain-forest tree species to a light gradient: the relative importance of morphologiecal and physiological traits, British Ecological Society, p. 396-410.

Poorter, L., 2009, Leaf traits show different relationships with shade tolerance in moist versus dry tropical forests: New Phytologist, v. 181, p. 890-900.

Porté, A., and H. H. Bartelink, 2002, Modelling mixed forest growth: a review of models for forest management: Ecological Modelling, v. 150, p. 141-188.

Pretzsch, H., 2009, Forest Dynamics, Growth and Yield: Berlin, Germany, Sringer, 664 p.

Pütz, S., J. Groeneveld, L. F. Alves, J. P. Metzger, and A. Huth, 2011, Fragmentation drives tropical forest fragments to early successional states: A modelling study for Brazilian Atlantic forests: Ecological Modelling, v. 222, p. 1986-1997.

Reich, P. B., C. Buschena, M. G. Tjoelker, K. Wrage, J. Knops, D. Tilman, and J. L. Machado, 2003, Variation in growth rate and ecophysiology among 34 grassland and savanna species under contrasting N supply: a test of functional group differences: New Phytologist, v. 157, p. 617-631.

Reynolds, C. W., 1987, Flocks Herds and Schools: A Distributed Behavioral, Los Angeles, California, Computer Graphics, p. 25-34.

Rezende, C. L., A. Uezu, F. R. Scarano, and D. S. D. Araujo, 2015, Atlantic Forest spontaneous regeneration at landscape scale: Biodiversity and Conservation, v. 24, p. 2255-2272.

Rigueira, D. M. G., A. L. M. Molinari, D. L. S. Mariano, R. M. Reis, A. B. Portugal, N. d. S. Santana, and R. A. d. Santos, 2012, Influência da distância da borda e do adensamento foliar sobre a abundância de plantas pioneiras em um fragmento de floresta tropical submontana na Estação Ecológica de Wenceslau Guimarães (Bahia, Brasil): Acta Botanica Brasilica, v. 26, p. 197-202.

Scaranello, M. A. d. S., L. F. Alves, S. A. Vieira, P. B. d. Camargo, C. A. Joly, and L. A. Martinelli, 2012, Height-diameter relationships of tropical

Atlantic moist forest trees in southeastern Brazil: Scientia Agricola, v. 69, p. 26-37.

Scatena, F. N., W. Silver, T. Siccama, A. Johnson, and M. J. Sanchez, 1993, Biomass and Nutrient Content of the Bisley Experimental Watersheds, Luquillo Experimental Forest, Puerto Rico, Before and After Hurricane Hugo, 1989, Biotropica.

Scurlock, J., G. Asner, and S. Gower, 2001, Worldwide Historical Estimates and Bibliography of Leaf Area Index, Oak Ridge, Tennessee, U.S.A, Oak Ridge National Laboratory.

Seo, J. H., 2005, Modeling Applications for Optimizing Forest Development, Cuvillier.

Shono, K., E. A. Cadaweng, and P. B. Durst, 2007, Application of Assisted Natural Regeneration to Restore Degraded Tropical Forestlands, Washington, D.C, USA, Restoration Ecology.

Shugart, H. H., and I. R. Noble, 1981, A computer model of succession and fire response of the high-altitude Eucalyptus forest of the Brindabella Range, Australian Capital Territory: Australian Journal of Ecology, v. 6, p. 149-164.

Shugart, H. H., and D. C. West, 1977, Development of an Appalachian deciduous forest succession model and its application to assessment of the impact of the chestnut blight: J. Environ, Manage., v. 5, p. 161-179.

Skole, D., and C. Tucker, 1993, Tropical deforestation and habitat fragmentation in the Amazon: Satellite data from 1978 to 1988, *Science*.

Snyder, M., 2010, What is Shade Tolerance and Why is it so Important? , Corinth, VT, USA, Northen Woodlands, p. 75.

Souza, G. M., A. M. Sato, R. V. Ribeiro, and C. H. B. A. Prado, 2010, Photosynthetic responses of four tropical tree species grown under gap and understorey conditions in a semi-deciduous forest: Brazilian Journal of Botany, v. 33, p. 529-538.

Swaine, M. D., and T. C. Whitmore, 1988, On the definition of ecological species groups in tropical rain forests: Vegetatio, v. 75, p. 81-86.

Tabarelli, M., A. V. Aguiar, M. C. Ribeiro, J. P. Metzger, and C. A. Peres, 2010, Prospects for biodiversity conservation in the Atlantic Forest: Lessons

from aging human-modified landscapes: Biological Conservation, v. 143, p. 2328-2340.

Tabarelli, M., A. V. Lopes, and C. A. Peres, 2008, Edge-effects Drive Tropical Forest Fragments Towards an Early-Successional System: Biotropica, v. 40, p. 657-661.

Tabarelli, M., and C. A. Peres, 2002, Abiotic and vertebrate seed dispersal in the Brazilian Atlantic forest: implications for forest regeneration: Biological Conservation, v. 106, p. 165-176.

Tiepolo, G., M. Calmon, and A. Ferreti, 2002, Measuring and Monitoring Carbon Stocks at the Guaraqueçaba Climate Action Project, Paraná, Brazil, International Symposium on Forest Carbon Sequestration and Monitoring, Curitiba, Brazil, p. 98-115.

Tollefson, J., 2011, Fighting for the forest: The roadless warrior, Nature Publishing Group, p. 22-24.

Van der Pluijm, B., 2010, Global changes: the sustainability challenge, *in* E. E. Sciences, ed., Ann Arbor, Michigan, USA, University of Michigan.

Vanclay, J. K., 1994, Modelling forest growth and yield: applications to mixed tropical forests: Modelling forest growth and yield: applications to mixed tropical forests, CAB International, Wallingford, 312 p.

Vanclay, J. K., 1995, Growth models for tropical forests: a synthesis of models and methods, Forest Science, p. 4-42.

Viani, R. A. G., N. B. Vidas, M. M. Pardi, D. C. V. Castro, E. Gusson, and P. H. S. Brancalion, 2015, Animal-dispersed pioneer trees enhance the early regeneration in Atlantic Forest restoration plantations: Natureza & Conservação, v. 13, p. 41-46.

Vieira, D. C. M., and S. Gandolfi, 2006, Chuva de sementes e regeneração natural sob três espécies arbóreas em uma floresta em processo de restauração: Brazilian Journal of Botany, v. 29, p. 541-554.

Vieira, S. A., L. F. Alves, M. Aidar, L. S. Araújo, T. Baker, J. L. F. Batista, M. C. Campos, P. B. Camargo, J. Chave, W. B. C. Delitti, N. Higuchi, E. Honorio, C. A. Joly, M. Keller, L. A. Martinelli, E. A. d. Mattos, T. Metzker, O. Phillips, F. A. M. d. Santos, M. T. Shimabukuro, M. Silveira, and S. E. Trumbore, 2008, Estimation of biomass and carbon stocks: the case of the Atlantic Forest: Biota Neotropica, v. 8, p. 0-0.

Weiskittel, A., 2012, Lessons Learned: Writing a Book on Forest Growth and Yield Modeling, p. 27.

Weiskittel, A. R., D. W. Hann, J. A. J. Kershaw, and J. K. Vanclay, 2011, Forest Growth and Yield Modeling: Chicester, UK, Wiley-Blackwell, 430 p.

Whitmore, T. C., 1998, An Introduction to Tropical Rain Forests, Oxford Oxford University Press, p. 296.

Zipperer, W. C., 1993, Deforestation patterns and their effects on forest patches, Syracuse, NY, USA, Landscape Ecology p. 177-184.

7. APPENDIX A - Seed dispersal function

```
% Seed dispersal function

function repart_graines=seed_dispersal(dist,CD,Nseed,n)

repart_graines=zeros(n,n);

 for i=1:Nseed,

       r=wblrnd(dist+CD/2,2);

    Dir=360*rand();

    xseed=round(round(n/2)+r/20*sin(2*pi*Dir*360));

    yseed=round(round(n/2)+r/20*cos(2*pi*Dir*360));

    if xseed<1 | xseed>n |yseed<1 |yseed>n

          else  repart_graines(xseed,yseed)=repart_graines(xseed,yseed)+1;

    end

end

end
```

```
% Matrix of seed dispersal probability


CD=[2.47 2.47 4 2.47 2.47 4 2.47 2.47 4]; % Mother tree crown diameter

dist=[100 100 100 75 75 75 50 50 50]; % Maximum distance to mother tree

Nb_PFT=9; % Number of PFT

 prob_seed=zeros(5,5,Nb_PFT);
```

```
for i=1:Nb_PFT,
   prob_seed(:,:,i)=seed_dispersal(dist(i),CD(i),10000,5)/10000;
   end
```